Hadronic D and D_s Meson Decays

Anders Ryd*

Laboratory of Elementary-Particle Physics, Cornell University, Ithaca, NY 14853 USA

Alexey A Petrov†

Department of Physics and Astronomy, Wayne State University, Detroit, MI 48201 and Michigan Center for Theoretical Physics, University of Michigan, Ann Arbor, MI 48109

We provide a comprehensive review of hadronic decays of D and D_s mesons. We discuss current theoretical and experimental challenges and successes in understanding of hadronic transitions of those mesons. A brief overview of the theoretical and experimental tools are given before discussing the absolute branching fractions for D and D_s mesons. Cabibbo suppressed and rare hadronic decays are discussed and compared with theory before discussing our understanding of hadronic multibody decays.

Contents

I. INTRODUCTION

The discovery of charmed meson states in 1974 signaled a new era in particle physics. The arrival of the first heavy quark has solidified the evidence that the Standard Model (SM) provides a correct low-energy description of particle physics. Three decades later, the charm quark still plays an important role in studies of strong and weak interactions. It also serves as an important tool for exploring physics beyond the Standard Model, indirectly

*Electronic address: `Anders.Ryd@cornell.edu`

†Electronic address: `apetrov@wayne.edu`

probing energy scales well above several TeV, which will be directly probed by the Large Hadron Collider (LHC). In some cases, charm transitions provide possibilities for almost background-free studies of low-energy signals of new physics. For example, signals of CP violation in the charm system predicted within the Standard Model are very small, so any observation of CP violation in the current round of experiments would rather unambiguously signal presence of new physics. Charm is also rather unique in that it is the only up-type quark that can have flavor oscillations.

A distinctive feature of all charmed hadrons is that their masses, $\mathcal{O}(2\text{ GeV})$, place them in the middle of the region where non-perturbative hadronic physics is operative. While this fact does not markedly affect theoretical description of leptonic and semileptonic decays of charmed hadrons, it poses significant challenges in the analyses of their hadronic transitions. There is a great deal of optimism, however, that abundant experimental data would provide some hints on the structure of charm hadronic decays, so those problems will eventually be overcome.

The data on charm transitions originate from several different types of experiments. Experiments at e^+e^- machines operating at the $\psi(3770)$ and $\psi(4140)$ resonances, such as CLEO-c and BES III, have several important advantages. First, the final state is extremely simple, being essentially just a $D\bar{D}$ pair. Second, the cross-section for charm production is relatively high, $\sigma(D^0\bar{D}^0) = 3.66\pm0.03\pm0.06$ nb and $\sigma(D^+D^-) = 2.91\pm0.03\pm0.05$ nb at the $\psi(3770)$. In conjunction with low multiplicity of the final state, this allows for measurements of absolute branching fractions for several reference modes. We refer to these as reference modes as they are used to normalize other decay channels. Finally, in those experiments, the $D\bar{D}$ pairs are produced in a quantum-coherent state, which allows for unique probes of the structure of decay amplitudes and phases, as well as novel measurements of mixing and CP violation.

The B factory e^+e^- experiments BABAR and Belle, operating at the $\Upsilon(4S)$ center-of-mass energy, produce significant amount of charm data. In fact, at the resonance center-of-mass energy, $\sigma(b\bar{b}) \sim 1.1$ nb, while $\sigma(c\bar{c}) \sim 1.3$ nb. The very large integrated luminosities of these experiments have produced large samples of reconstructed charm. The higher operating energy makes possible the production of charmed baryons.

Experiments at hadron machines, such as CDF and DØ at the Tevatron, and fixed target facilities are plagued by even higher backgrounds. However, much higher production cross-section, combined with a relatively long lifetime of charmed hadrons, provides a possibility to trigger on charm decay events with displaced vertices. This technique allowed for hadron machines to be major players in charm physics. New results from the Large Hadron Collider (LHC) experiments LHCb, ATLAS, and CMS will continue to supply us with new data.

This paper provides a comprehensive review of hadronic decays of D and D_s mesons. In this review we adopt the averages performed by the Particle Data Group (Amsler *et al.*, 2008). Only if there are newer measurements that are not included in the review by the Particle Data Group we will do our own averaging.

This review is organized as follows. Section II contains a brief discussion of the discovery of open charm followed in Section III by a discussion of the experimental techniques used for studying charm decays. This includes a brief discussion of the main experiments that have contributed to our understanding of D decays and the production mechanisms employed in these studies. Final-state radiation is discussed in this section as it is an important effect in many of the precision measurements discussed in this review. In Section IV the theoretical description of hadronic D decays is provided. This includes discussion of $\mathrm{SU(3)_F}$ flavor symmetry, the flavor-flow-diagram approach, and factorization. These are common tools used to analyze and interpret hadronic D decay data. Sections V and VI discuss the determination of the absolute branching fractions for for D and D_s decays. Rare and suppressed modes are discussed in Section VII. Multibody decays and Dalitz plot studies are discussed in Section IX. This review concludes in Section X with a summary and outlook.

II. DISCOVERY OF OPEN CHARM

The arrival of the quark model in 1964 (Gell-Mann, 1964; Zweig, 1964) greatly simplified the description of elementary particles. The idea that all observed particles are made of the three quarks, u, d, and s, was gaining acceptance. By the early 1970's, the proton structure was probed and the quarks were found to be real particles. Further development of perturbative Quantum Chromodynamics and the concept of asymptotic freedom allowed consistent explanation of those experiments in terms of those three quark flavors. The possible existence of a fourth quark had been theoretically discussed in the 60's (Björken and Glashow, 1964), however it was not required.

Hints of the incompleteness of the current picture came after experimental observation of rare, electroweak, decays of kaons. The observed rate for $K_L^0 \to \mu^+\mu^-$ turned out to be smaller than predicted. Similarly, the K_S^0–K_L^0 mass difference did not agree with predictions based on only having the u, d, and s quarks. To solve those problems, Glashow, Iliopoulos, and Maiani (GIM) proposed an elegant mechanism (Glashow *et al.*, 1970), which involved adding the forth quark, c. The resulting mechanism not only established the absence of the tree-level flavor-changing neutral currents in the Standard Model, but also provided for reduced rates for $K_L^0 \to \mu^+\mu^-$ decays by requiring cancellations with additional diagrams involving intermediate charm quarks. Using the observed rate for $K_L^0 \to \mu^+\mu^-$ and K_S^0–K_L^0 mass difference, it was

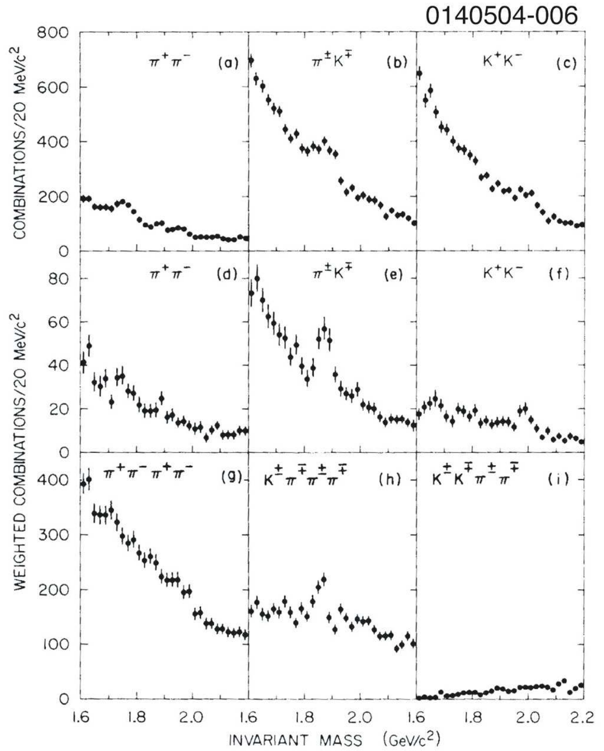

FIG. 1 The invariant mass distributions observed by the SLAC-LBL experiment for two and four hadrons in the final state. (a) $\pi^+\pi^-$ assigning pion mass to all tracks, (b) $K^{\mp}\pi^{\pm}$ assigning kaon and pion masses to all tracks, (c) K^+K^- assigning kaon mass to all tracks, (d) $\pi^+\pi^-$ weighted by $\pi\pi$ time of flight probability, (e) $K^{\mp}\pi^{\pm}$ weighted by $K\pi$ time of flight, (f) K^+K^- weighted by KK time of flight, (g) $\pi^+\pi^-\pi^+\pi^-$ weighted by 4π time of flight probability (h) $K^{\pm}\pi^{\mp}\pi^+\pi^-$ weighted by $K3\pi$ time of flight probability (i) $K^{\pm}K^{\mp}\pi^+\pi^-$ weighted by $KK\pi\pi$ time of flight probability. From Goldhaber *et al.* (1976).

estimated that the charm quark would have a mass in the range 1 to 3 GeV (Gaillard and Lee, 1974; Gaillard *et al.*, 1975). The existence of the new quark implied that it would form bound states with its own anti-quark, as well as with the lighter quarks, which could be observable experimentally.

These bound states were experimentally discovered in November 1974 by two independent research groups at SLAC (Aubert *et al.*, 1974) and BNL (Augustin *et al.*, 1974). The mass of the observed J/ψ resonance of about 3.1 GeV was in the range where a $c\bar{c}$ bound state was expected. In addition, the very small width, of about 93 keV, was very different from other high mass resonances observed. The interpretation of the J/ψ as a $c\bar{c}$ bound state was confirmed when "open charm" states were discovered a little later, first the D^0 (Goldhaber *et al.*, 1976) and then the D^+ (Peruzzi *et al.*, 1976). The first observation of the D^0 was made in the final states $K^-\pi^+$ and $K^-\pi^+\pi^-\pi^+$. The observed invariant mass distributions are shown in Fig. 1.

Another source of information about open-charm mesons was neutrino scattering experiments, such as HPWF (Benvenuti *et al.*, 1975a,b). That experiment reported observation of two opposite-sign muons in a reaction $\nu_\mu + N \to \mu^+\mu^- + X$, which was interpreted as evidence for production of a new heavy hadron with the mass around 2 GeV/c^2. Those D-mesons were produced in charged current interactions of neutrinos with d and s quarks. It is also interesting to note that there were hints of the existence of open charm states in photoemulsion experiments even before the J/ψ had been discovered (Hoshino *et al.*, 1975; Niu *et al.*, 1971).

After the observation of the D^0 and D^+ mesons it took a little longer to establish the D_s^+. There were several false sightings before the D_s^+, originally called the F meson, was observed by CLEO (Chen *et al.*, 1983). These observations firmly established the charm quark as the fourth quark in the family of strongly-interacting particles.

III. GENERAL REMARKS ON EXPERIMENTAL FACILITIES AND TECHNIQUES

Charm has been studied in a large number of different experiments. In e^+e^- collisions charm decays have been studied from threshold to the Z pole. There have also been a number of fixed target experiments, either using hadroproduction or photoproduction. The e^+e^- and fixed target experiments dominate the literature on charm meson decays. In addition, there are also studies using proton–anti-proton collisions.

In this section we review some of the basic properties of the different types of production mechanisms and the experiments used to collect the data. First, e^+e^- experiments are discussed and then fixed target. For e^+e^- experiments, where typically triggering is very open and most of the produced events are recorded, we compare the luminosity and the produced number of $c\bar{c}$ events. A summary of e^+e^- experiments is given in Table I. For fixed target experiments a similar comparison is made in Table II for the number of exclusively reconstructed D mesons. At threshold the final state charm mesons are produced without any additional hadrons. The CLEO-c experiment is described in more detail as it is the experiment operating near threshold with the largest data samples to date. At higher e^+e^- center-of-mass energy the charm hadrons are produced either in fragmentation of charm jets or in decays of heavier particles such as hadrons containing b-quarks. A series of fixed target experiments has been performed to study charm, and are discussed next. Fixed target experiments can be categorized as photoproduction or hadroproduction experiments based on the particle type incident on the target. Last, final-state radiation is discussed. The precision on many measurements of hadronic charm decays has reached the level where radiative corrections can not be ignored.

TABLE I Summary of charm samples produced in e^+e^- colliding beam experiments.

Experiment	Year	$\sqrt{s}$	$\int \mathcal{L}$	Produced Charm
Mark III	1982-1988	3.77 GeV	9 pb^{-1}	28,000 $D^0\bar{D}^0$
				20,000 D^+D^-
		4.14 GeV	6.3 pb^{-1}	
BES-I	1992-1993	4.03 GeV	22.3 pb^{-1}	
		4.14 GeV	1.8 pb^{-1}	
BES-II	2001-2003	3.77 GeV	17.3 pb^{-1}	
CLEO-c	2003-2008	3.77 GeV	818 pb^{-1}	3.0×10^6 $D^0\bar{D}^0$
				2.4×10^6 D^+D^-
		4.17 GeV	589 pb^{-1}	0.58×10^6 $D_s^\pm D_s^{*\mp}$
BES-III[a]	2009-	3.77 GeV	>500 pb^{-1}	
CLEO	1979-1988	10.5 GeV	314 pb^{-1}	0.41×10^6 $c\bar{c}$
CLEO II	1989-1994	10.5 GeV	4.7 fb^{-1}	6.1×10^6 $c\bar{c}$
CLEO II.V	1995-1999	10.5 GeV	9.1 fb^{-1}	12×10^6 $c\bar{c}$
CLEO III	2000-2003	10.5 GeV	15 fb^{-1}	19×10^6 $c\bar{c}$
ARGUS	1982-1992	10.5 GeV	514 pb^{-1}	0.67×10^6 $c\bar{c}$
BABAR	1999-2008	10.5 GeV	531 fb^{-1}	0.69×10^9 $c\bar{c}$
Belle[b]	1999-	10.5 GeV	1040 fb^{-1}	1.35×10^9 $c\bar{c}$
HRS	1982-1986	29 GeV	300 pb^{-1}	52,000 $c\bar{c}$
LEP	1989-1996	91 GeV	4.2×10^6 $Z's$	220,000 $c\bar{c}$
			per experiment	per experiment

[a]As of May 1, 2010
[b]As of June 30, 2010

TABLE II The number of reconstructed charm mesons for different fixed target experiments.

Experiment	Year	Events Recorded (10^6)	Reconstructed Charm Decays
Photoproduction:			
E691	1985	100	10,000
E687	1992	500	100,000
FOCUS (E831)	1996	7,000	1.2×10^6
Hadroproduction:			
WA75	1984	2	350
NA32	1986	17	1,300
WA82	1989	10	3,000
E653	1988	10	1,000
E769	1988	500	4,000
E791	1992	20,000	200,000

A. Experiments using e^+e^- annihilation near threshold

At threshold D meson pairs are produced without any additional hadrons. This provides the experiments operating at threshold with a very clean environment for studying charm decays. As will be discussed in Section III.A.3 the initial electron or positron may radiate low energy photons, initial state radiation (ISR), such that the total energy of the produced charm hadrons is less than the center-of-mass energy in the e^+e^- initial state.

Experiments that studied charm decays at threshold include the Mark I, II, and III experiments (Abrams *et al.*, 1979a; Augustin *et al.*, 1975; Bernstein *et al.*, 1984) at SPEAR; BES I, BES II, BES III (Bai *et al.*, 1994, 2001; Collaboration, 2009) at BEPC, and CLEO-c (Artuso *et al.*, 2003; Kubota *et al.*, 1992; Peterson *et al.*, 2002) at CESR-c. The physics programs of CLEO-c and BES-III are described in details in Briere *et al.* (2001) and Asner *et al.* (2008). For studies of D^0 and D^+ decays experiments have run at the $\psi(3770)$. The total hadronic cross-section at the $\psi(3770)$ resonance has been measured by CLEO-c (Besson *et al.*, 2006)

$$\sigma(e^+e^- \to \text{hadrons}) = (6.38 \pm 0.08^{+0.41}_{-0.30}) \text{ nb}. \quad (1)$$

The cross-sections for $D^0\bar{D}^0$ and D^+D^- production has been measured by CLEO-c (Dobbs *et al.*, 2007)

$$\sigma(e^+e^- \to D^0\bar{D}^0) = (3.66 \pm 0.03 \pm 0.06) \text{ nb}, \quad (2)$$
$$\sigma(e^+e^- \to D^+D^-) = (2.91 \pm 0.03 \pm 0.05) \text{ nb}. \quad (3)$$

Adding these two measurements, CLEO-c obtains the total cross-section for $D\bar{D}$ production at the $\psi(3770)$ to be $\sigma(e^+e^- \to D\bar{D}) = (6.57 \pm 0.04 \pm 0.10)$ nb. This is larger than, but consistent with, the inclusive hadronic cross-section discussed above. These results indicates that the majority of the $\psi(3770)$ decays to $D\bar{D}$. CLEO-c (Adam *et al.*, 2005) and BES II (Bai *et al.*, 2005) have observed some non-$D\bar{D}$ decays of the $\psi(3770)$. The largest of these decays is the radiative transition $\psi(3770) \to \gamma\chi_{c0}$ with a branching fraction of $(0.73 \pm 0.09)\%$. Summing the observed branching fractions for non-$D\bar{D}$ decays we obtain

$(1.4 \pm 0.1)\%$, consistent with the cross-section measurements above. BES II (Ablikim *et al.*, 2006a,b, 2007, 2008) has performed indirect measurements of the cross-section for $\psi(3770) \to$ non$-D\bar{D}^0$ final states as well as measurements of the $D\bar{D}$ cross-sections. The PDG (Amsler *et al.*, 2008) average these measurements and finds that $(14.7 \pm 3.2)\%$ of $\psi(3770)$ resonances decays to non-$D\bar{D}$ final states. This result is inconsistent with the CLEO-c results at the 2σ level.

Different e^+e^- center-of-mass energies have been used for studies of D_s mesons. The cross-sections for producing $D_{(s)}$, or $D^*_{(s)}$ mesons, as measured by CLEO-c (Cronin-Hennessy *et al.*, 2009), are shown in Fig. 2. BES collected data at 4.03 GeV. At this energy $D_s^+ D_s^-$ mesons pairs are produced. CLEO-c on the other hand ran at a higher energy, about 4.17 GeV. At this energy pairs of $D_s^{\pm} D_s^{*\mp}$ mesons are produced. The D_s^* meson decays to either $D_s\gamma$ or $D_s\pi^0$, with branching fractions of $(94.2 \pm 0.7)\%$ and $(5.8 \pm 0.7)\%$, respectively (Amsler *et al.*, 2008; Aubert *et al.*, 2005d). The advantage of the higher energy is the larger cross-section. CLEO-c reports (Cronin-Hennessy *et al.*, 2009) a cross-section of (0.27 ± 0.03) nb at 4.03 GeV for $D_s^+ D_s^-$ production and (0.92 ± 0.05) nb at 4.17 GeV for $D_s^{*\pm} D_s^{\mp}$ production. For most analyses the larger cross-section outweighs the complication of the additional particles in the final state.

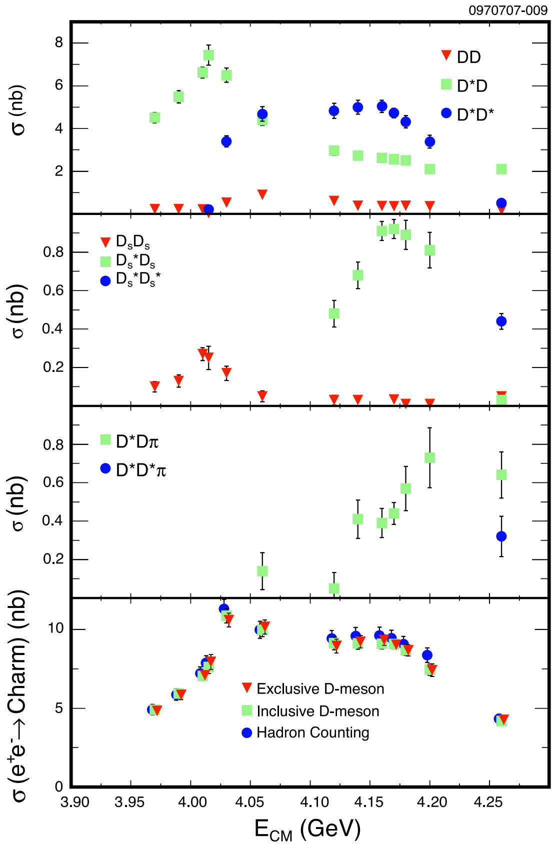

FIG. 2 The measured cross-sections for different $D\bar{D}$ final states. From Cronin-Hennessy *et al.* (2009).

1. Quantum coherence

Threshold production of $D\overline{D}$ pairs can be explored to understand the phase structure of hadronic decay amplitudes of D^0 mesons. Here one can use the fact that neutral charm mesons D^0 and $\bar{D}^0$ mix. $D^0 - \bar{D}^0$ mixing arises from electroweak or new physics $|\Delta C| = 2$ interactions that generate off-diagonal terms in the neutral D mass matrix (see, e.g. Artuso *et al.* (2008); Bergmann *et al.* (2000) for more information)

$$\left[\mathbf{M} - i\frac{\mathbf{\Gamma}}{2}\right] = \begin{pmatrix} A & p^2 \\ q^2 & A \end{pmatrix}, \tag{4}$$

where A parameterizes masses and lifetimes of D^0 and $\bar{D}^0$ states and the complex parameters p^2 and q^2 parameterize contributions from $|\Delta C| = 2$ interactions. The non-diagonal structure of the mixing matrix of Eq. (4) leads to the (physical) mass eigenstates of a Hamiltonian of Eq. (4) D_1 and D_2 becoming superpositions of the flavor eigenstates D^0 and $\bar{D}^0$,

$$|D_{\frac{1}{2}}\rangle = p\,|D^0\rangle \;\pm\; q\,|\bar{D}^0\rangle\ , \tag{5}$$

where $|p|^2 + |q|^2 = 1$. A simplified assumption can be made that in the studies of strong phases described below CP violation may be neglected. This can be justified in the Standard Model by noting that CP-violating contributions are always suppressed by small values of the third-generation Cabibbo-Kobayashi-Maskawa (CKM) matrix elements (Artuso *et al.*, 2008). In such case $p = q$, so mass eigenstates also become eigenstates of CP,

$$|D_{\pm}\rangle = \frac{1}{\sqrt{2}}\left[|D^0\rangle \pm |\bar{D}^0\rangle\right]. \tag{6}$$

It follows then that these CP eigenstates $|D_{\pm}\rangle$ do not evolve with time. Their mass and lifetime differences can be observed,

$$x = \frac{\Delta M_D}{\Gamma}, \quad y = \frac{\Delta\Gamma_D}{2\Gamma}, \tag{7}$$

where $\Gamma = (\Gamma_+ + \Gamma_-)/2$ is the average lifetime of mass and CP eigenstates.

At threshold e^+e^- experiments, such as BES and CLEO-c, $D^0\bar{D}^0$ pairs are produced through resonances of specific charge conjugation. The $D^0\bar{D}^0$ will therefore be in an entangled state with the same quantum numbers as the parent resonance. In particular, since both mesons are pseudoscalars, charge conjugation reads $C = (-1)^L$, if the produced resonance has angular momentum L. This implies that the quantum mechanical state at the time of $D^0\bar{D}^0$ production is

$$\Psi = \frac{1}{\sqrt{2}}\left\{|D^0(\mathbf{k_1})\bar{D}^0(\mathbf{k_2})\rangle + C|D^0(\mathbf{k_2})\bar{D}^0(\mathbf{k_1})\rangle\right\} \tag{8}$$

where $\mathbf{k_1}$ and $\mathbf{k_2}$ are the momenta of the mesons. Rewriting this in terms of the CP basis we arrive at

$$\begin{aligned}\Psi_{C=+1} &= \frac{1}{\sqrt{2}}\left\{|D_+(\mathbf{k_1})D_+(\mathbf{k_2})\rangle - |D_-(\mathbf{k_1})D_-(\mathbf{k_2})\rangle\right\},\\ \Psi_{C=-1} &= \frac{1}{\sqrt{2}}\left\{|D_-(\mathbf{k_1})D_+(\mathbf{k_2})\rangle + |D_+(\mathbf{k_1})D_-(\mathbf{k_2})\rangle\right\}.\end{aligned} \tag{9}$$

Thus in the L = odd; $C = -1$ case, which would apply to the experimentally important $\psi(3770)$ resonance, the CP eigenstates of the D mesons are anti-correlated while if L = even; $C = +1$ the eigenstates are correlated. This can happen when $D^0\bar{D}^0$ pair is produced in the decays $\psi(4140) \to D\overline{D}\gamma$ of the more massive charmonium state $\psi(4140)$. In either case the CP conservation implies that correlation between the eigenstates is independent of when they decay. In this way, if $D(\mathbf{k_1})$ decays to the final state which is also a CP-eigenstate, then the CP eigenvalue of the meson $D(\mathbf{k_2})$ is therefore *determined*: it is either the same as $D(\mathbf{k_1})$ for $C = +1$ or opposite, as in the case of $C = -1$. The use of this eigenstate correlation as a tool to investigate CP violation has been earlier suggested in K-physics (Bernabeu *et al.*, 1988; Dunietz *et al.*, 1987; Lipkin, 1968), and in B-physics (Atwood and Soni, 2002; Falk and Petrov, 2000). In charm physics this method of *CP-tagging* can be used to study relative strong phases of D^0-meson amplitudes. Such measurements are needed for studies of $D^0\bar{D}^0$-mixing.

To illustrate the method, the amplitude for the CP-tagged eigenstate decaying to, say, $K\pi$ final state can be written as

$$\sqrt{2}\mathcal{A}(D_\pm \to K^-\pi^+) = \mathcal{A}(D^0 \to K^-\pi^+) \pm \mathcal{A}(\bar{D}^0 \to K^-\pi^+) \tag{10}$$

which follows from Eq. (6). This relation implies that

$$1 \pm 2\cos\delta_{K\pi}\sqrt{R_{K\pi}} \equiv 1 \pm z_{K\pi}\sqrt{R_{K\pi}} = 2\frac{\mathcal{B}(D_\pm \to K^-\pi^+)}{\mathcal{B}(D^0 \to K^-\pi^+)}, \tag{11}$$

where R_f is the small ratio of doubly-Cabibbo suppressed (DCS) decay rate to Cabibbo favored (CF) one (see Section IV), and δ_f is the strong phase difference between those amplitudes, $\mathcal{A}(\bar{D}^0 \to K^-\pi^+)/\mathcal{A}(D^0 \to K^-\pi^+) = -\sqrt{R_{K\pi}}e^{-i\delta_{K\pi}}$. Eq. (11) can be used to extract $\delta_{K\pi}$ if the CP-tagged branching ratio is measured (Atwood and Petrov, 2005; Gronau *et al.*, 2001).

The method of quantum correlations can be used to study the multitude of parameters of D^0 decay and mixing (Asner and Sun, 2006; Atwood and Petrov, 2005). In particular, correlated decays of D-mesons into CP-mixed final states (such as $K^-\pi^+$), CP-specific final states $S_\pm$ (such as $S_+ = K^+K^-$ or $S_- = K_S\pi^0$), or a flavor specific semi-leptonic decay $L^\pm$ into a state containing $\ell^\pm$ can probe various combinations of mixing and decay parameters (see Table III). We defined the $D^0 - \bar{D}^0$ mixing rate $R_m = (x^2+y^2)/2$ and the "wrong-sign" rate for the final state f as $R_{\rm ws,f} = R_f + \sqrt{R_f}\,(y\cos\delta_f - x\sin\delta_f) + R_m$.

TABLE III Correlated branching ratios for various processes. Correlated results are presented for $C = 1$ and normalized to the product of the uncorrelated branching fractions. CP violation is neglected.

Decay modes	Correlated branching fractions
$K^-\pi^+$ vs. $K^-\pi^+$	$R_{\rm m}$
$K^-\pi^+$ vs. $K^+\pi^-$	$(1 + R_{{\rm ws},K\pi})^2 - 4r_{\delta,K\pi}(r_{\delta,K\pi} + y)$
$K^-\pi^+$ vs. $S_\pm$	$1 + R_{{\rm ws},K\pi} \pm 2r_{\delta,K\pi} \pm y$
$K^-\pi^+$ vs. $L^\pm$	$1 - \sqrt{R_{K\pi}}(y\cos\delta_{K\pi} + x\sin\delta_{K\pi})$
$S_\pm$ vs. $S_\pm$	0
$S_\pm$ vs. $S_\mp$	4
$S_\pm$ vs. $L^\pm$	$1 \pm y$

Also, $r_{\delta,f} = \sqrt{R_f}\cos\delta_f \equiv \sqrt{R_f}z_f/2$. The quantum-correlated rates are clearly different from the singly-tagged (ST) rates, i.e. when only one of the D^0 mesons is reconstructed. For example, the ST rate for the wrong-sign (*e.g.* $D^0 \to K^+\pi^-$) decay is given by $R_{{\rm ws},K\pi}$.

Besides the discussed studies of the phases of hadronic decay amplitudes, the results summarized in Table III can be used to extract $D^0 - \overline{D}^0$-mixing parameters. The discussion of the current status of charm mixing goes beyond the scope of this review. For the most recent reviews see Gedalia and Perez (2010), Artuso *et al.* (2008), or Bianco *et al.* (2003).

2. Experiments at threshold

The CLEO-c experiment plays a unique role here as it has a very large data sample collected at threshold. The CLEO-c detector is an evolution of the CLEO III detector where the silicon-strip vertex detector has been replaced with a low-mass inner six-layer drift chamber (Artuso *et al.*, 2003; Kubota *et al.*, 1992; Peterson *et al.*, 2002). The CLEO-c experiment is shown schematically in Fig. 3. The wires in the inner drift chamber are at a small stereo angle with respect to the drift chamber axis. This allows determining the z position of charged particles. The charged particle tracking system in CLEO-c also includes the 47-layer main drift chamber, operating in a 1.0 T magnetic field along the drift chamber axis. The CLEO-c tracking system provides a momentum resolution of about 0.6% for tracks with a momentum of 1 GeV that traverses all layers of the drift chamber. CLEO-c has excellent electromagnetic calorimetry from the approximately 7800 CsI(Tl) crystal calorimeter. For energies of 1 GeV the calorimeter has an energy resolution of about 2%. For energies of 100 MeV the resolution is about 5%. The excellent energy resolution and coverage allow CLEO-c to efficiently reconstruct π^0 and η mesons in the $\gamma\gamma$ final state. The π^0 mass resolution obtained is about 6 MeV. Charged hadrons are identified by a combination of specific ionization, dE/dx, in the drift chamber for particles with momenta below about 700 MeV. For

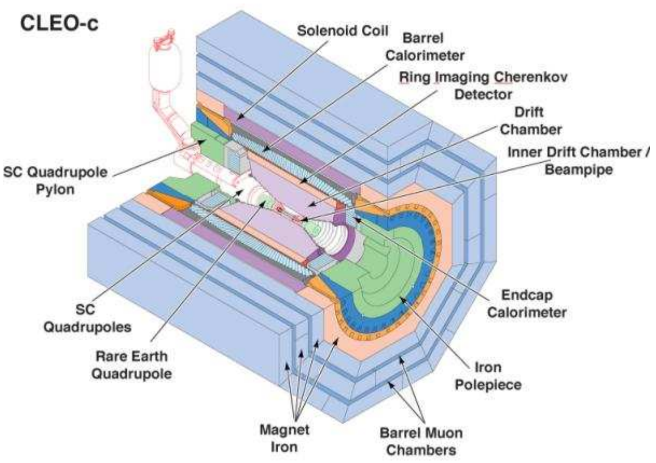

FIG. 3 The CLEO-c detector. The charged particle tracking system consists of an inner drift chamber near the interaction point and the main drift chamber for the momentum measurement. Radially outside the main drift chamber is the RICH detector for charged hadron identification followed by the CsI electromagnetic calorimeter. The instrumented flux return for muon detection is outside the super conducting solenoid coil.

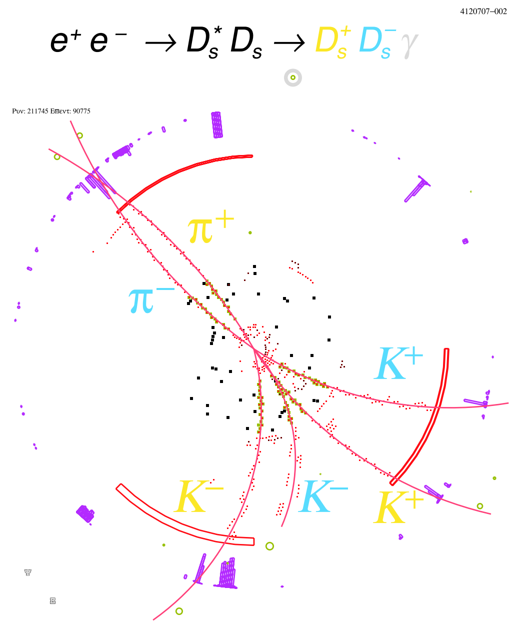

FIG. 4 Event display from CLEO-c showing a candidate $D_s^{*+}D_s^-$ event with $D_s^{*+} \to D_s^+\gamma$ and both $D_s^\pm$ candidates decaying to $K^+K^-\pi^\pm$. The charged particle trajectories, as determined from fits to the hits in the CLEO-c drift chambers, are shown as the curved lines.

higher momenta, where dE/dx is less powerful, CLEO-c uses the RICH detector to separate kaons from pions.

The BES III (Collaboration, 2009) detector constitutes a substantial upgrade of the earlier BES II detector. Among the new features are a 1 T magnetic field generate by a superconducting coil, a new drift chamber, and a CsI(Tl) doped electromagnetic calorimeter. The time-of-flight system provides π-K separation at 0.9 GeV with a 2σ separation. The operation with the BES III detector started in 2009 with a run which collected about 100×10^6 $\psi(2S)$ and 200×10^6 J/ψ events. In 2010 running at the $\psi(3770)$ started and as of August 2010 a sample of about 900 pb^{-1} has been recorded.

3. Experimental features at threshold

At threshold D mesons are produced in pairs. A very powerful analysis technique involves reconstructing one D meson exclusively. This allows experiments to infer the existence of another $\bar{D}$ mesons in the event. This "tagging" technique, or "double tag" technique, was first used by MARK III (Adler *et al.*, 1988; Baltrusaitis *et al.*, 1986), but due to their relatively small sample of tags the technique was of limited use. With much larger samples, and a more modern detector, the CLEO-c experiment has made great use of this tagging technique. The event environment at threshold is very clean. The $D\bar{D}$ signal is produced with no additional hadrons. An example from CLEO-c of a fully reconstructed $D_s^{*\pm}D_s^\mp$ is shown in Fig. 4.

Many analyses make use of fully reconstructed D candidates. The D candidates are built from charged kaons and pions, neutral pions, η and K_S^0 mesons. CLEO-c typically require that kaon and pion candidates are consistent with charged hadron particle identification based on energy loss in the drift chamber and Cherenkov radiation in the RICH detector. The K_S^0 candidates are reconstructed in the $\pi^+\pi^-$ final state. For the $\pi^+\pi^-$ pairs used to form K_S^0 candidates the usual track quality criteria are relaxed and no particle identification criteria are applied.

To extract the signal in fully reconstructed hadronic D decays it is typically required that the reconstructed D candidate energy is consistent with the beam energy, as each D in the final state will carry half of the center-of-mass energy. Specifically,

$$\Delta E \equiv E_{\rm cand} - E_{\rm beam}, \tag{12}$$

where

$$E_{\rm cand} = \sum_i \sqrt{\mathbf{p}_i^2 + m_i^2} \tag{13}$$

is the energy of the D candidate. For correctly reconstructed D candidates the ΔE distribution peak at zero. The resolution on ΔE is mode dependent and the actual criteria applied vary between different analyses depending on the backgrounds and cleanliness of the signal that is desired.

After applying a mode dependent ΔE selection criteria

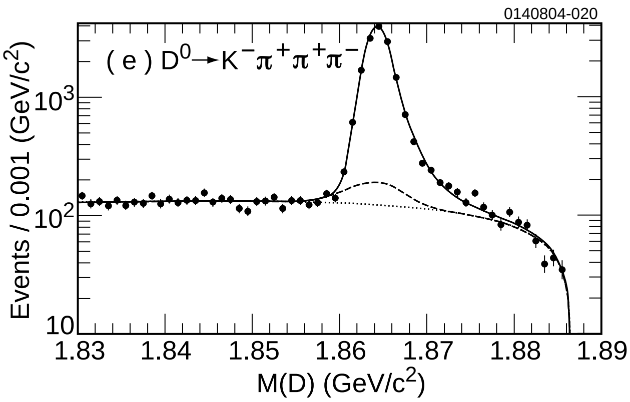

FIG. 5 The $M_{\rm BC}$ distribution. The dotted line shows the contribution from the ARGUS function that describes the combinatorial background. The solid and the dashed lines show the contributions to the signal shape for two different detector resolution functions. The tail on the high side for the signal shape is due to initial state radiation that lowers the energy of the produced D mesons.

the beam constrained mass is formed

$$M_{\rm BC} \equiv \sqrt{E_{\rm beam}^2 - (\sum_i \mathbf{p}_i)^2}. \tag{14}$$

Here the candidate energy has been replaced by the beam energy which typically is much better known.

A typical plot of the $M_{\rm BC}$ distribution is shown in Fig. 5. The signal yield is determined by fitting the $M_{\rm BC}$ distribution to a background shape plus a signal shape. The background shape is due to combinatorial backgrounds either from other D decays or from continuum. The background is typically fit using an "ARGUS" function (Albrecht *et al.*, 1990)

$$a(M_{\rm BC}; m_0, \xi, \rho) = A\, M_{\rm BC}\left(1 - \frac{M_{\rm BC}^2}{m_0^2}\right)^{\rho} e^{\xi\left(1-\frac{M_{\rm BC}^2}{m_0^2}\right)}. \tag{15}$$

This function describes the phase space distribution expected near the threshold at m_0 for $\rho = 1/2$ and $\xi = 0$. By allowing ρ and ξ to take on different values a more general function which can describe the data better is obtained.

For the signal shape several different parameterizations have been used. The most detailed description is that used for example in Dobbs *et al.* (2007). This form incorporates the effects of detector resolution, beam energy distribution, initial state radiation, and the line shape of the $\psi(3770)$. The beam energy distribution, initial state radiation, and the $\psi(3770)$ lineshape control the energy of the produced D-mesons. The effect of ISR is to produce the $\psi(3770)$ with an energy below the nominal e^+e^- center-of-mass energy. This produces a tail on the high side of the $M_{\rm BC}$ distribution as seen in Fig. 5. The detector resolution effects lead to a smearing of the measured momentum.

4. Systematic uncertainties

Many of the analyses discussed in this review are limited by systematic uncertainties. This applies in particular to the determination of the Cabibbo favored D^0 and D^+ absolute branching fractions that are discussed in Sect. V. A substantial effort has been put into understanding the systematic uncertainties associated with track finding, K_S^0 reconstruction, particle identification, and π^0 reconstruction. At the $\psi(3770)$ resonance many of these uncertainties can be evaluated using hadronic decays in an event environment very similar to the channels studied. This gives confidence in the sometimes small systematic uncertainties obtained in these studies. The most detailed systematic studies carried out by CLEO-c are described in Dobbs *et al.* (2007). As the results of these studies are important for many results discussed in this review, some of these studies are discussed below.

Track finding has been studied in CLEO-c using a missing mass technique where all particles in an event are reconstructed except for one particle which they are interested in studying. As an example consider the use of the kaon in $D^0 \to K^-\pi^+$ to measure the kaon tracking efficiency. In this case the opposite $\bar{D}^0$ in the event is fully reconstructed in some channel and the π^+ from D^0 decay looked for. Given the $\bar{D}^0$ and π^+ candidates the missing mass in the event can be calculated

$$M_{\rm miss}^2 = (p_{\rm tot} - p_{\bar{D}} - p_{\rm other})^2, \tag{16}$$

where $p_{\bar{D}}$ is the four-momentum of the reconstructed $\bar{D}$, $p_{\rm other}$ is the four-momentum of the other particles that were combined with the tag $\bar{D}$, in this example the π^+, and $p_{\rm tot}$ is the four-momentum of the initial e^+e^- pair. In the missing mass squared calculation, the $\bar{D}$ momentum is rescaled to the momentum magnitude expected from the beam energy, but its direction is left unchanged. This constraint improves the $M_{\rm miss}^2$ resolution.

The missing mass candidates are separated into two samples; the sample where the missing particle was found and the remaining events where the missing particle was not found. An example is shown in Fig. 6. The case where the missing particle is found corresponds to a fully reconstructed $\psi(3770)$ event and is very clean. The events in this sample are fit to a signal shape using a sum of two Gaussians. A small background component is also included in the fit. For the sample where the missing particle is not found a clear peak can be seen corresponding to the events where there was an inefficiency. In addition to this peak there are also substantial backgrounds. These backgrounds include semileptonic decays as well as higher multiplicity hadronic D decays. These backgrounds are parameterized using Monte Carlo simulated events.

As described in detail in Dobbs *et al.* (2007) CLEO-c measures the tracking efficiency for both kaons and pions in three momentum ranges ($0.2 < p < 0.5$ GeV, $0.5 < p < 0.7$ GeV, and $p > 0.7$ GeV). CLEO-c evaluates the tracking efficiency and find agreement between data and the Monte Carlo simulation and assigns a per track systematic uncertainty of $\pm 0.3\%$ for pions. For kaons an additional, uncorrelated with respect to the $\pm 0.3\%$, uncertainty of $\pm 0.6\%$ is added due to evidence for a tracking efficiency difference between K^+ and K^-.

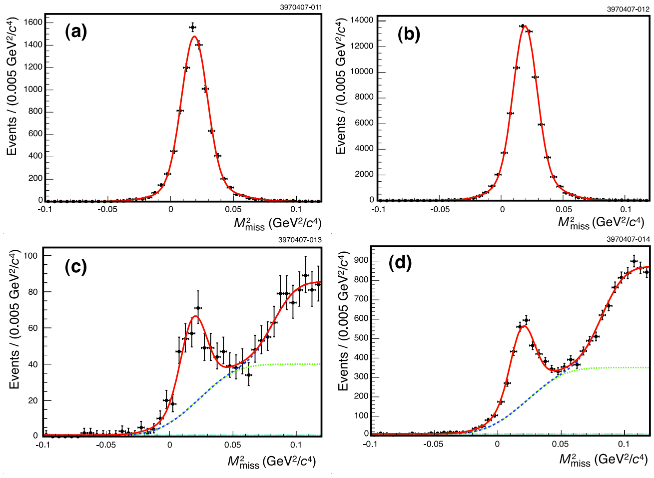

FIG. 6 Histograms of and fits to $M^2_{\rm miss}$ distributions from $D^+ \to K^-\pi^+\pi^+$ decays to determine the charged pion efficiency for $p_{\pi^+} > 0.2$ GeV. Figures (a) and (c) are from events in data, and (b) and (d) are from events in Monte Carlo simulation. Figures (a) and (b) are from decays in which the pion was found, while (c) and (d) are from decays in which the pion was not found. The solid curves are fits to the data or Monte Carlo sample; the dashed curves in (c) and (d) are background contributions. From Dobbs *et al.* (2007).

The $K^0_S \to \pi^+\pi^-$ reconstruction efficiency is studied in D^0 and $\bar{D}^0$ decays to $K^0_S\pi^+\pi^-$ decays using a technique similar to what was used for the tracking efficiencies. One tag D is fully reconstructed and two charged pions are required to be found. To factor out the track finding efficiency and also to reject $K^0_L\pi^+\pi^-$ and $K^0_S \to \pi^0\pi^0$ decays it is required that two additional tracks are found in the event. These tracks are required to satisfy loose consistency requirements with coming from a K^0_S decay. The invariant mass of the two tracks are required to be in the range from 0.2 to 0.7 GeV. In addition, the difference between the missing momentum vector and the momentum vector of the sum of the two charged tracks is required to be less than 60 MeV. Events that satisfy these requirements are searched for a K^0_S candidate using the standard K^0_S vertex finder. Similar to the tracking studies the candidates are separated into two categories; where the K^0_S was found and where it was not found. Compared to the tracking systematics study described above the K^0_S study is more complicated because there are fake K^0_S candidates from wrong $\pi^+\pi^-$ tracks in either $K^0_S\pi^+\pi^-$ or $\pi^+\pi^-\pi^+\pi^-$ events. This gives rise to a "hole" in the events where the K^0_S candidate was not found because combinatorial background got promoted to signal. This is illustrated in Fig. 7. Using this technique CLEO-c assigns a systematic uncertainty of $\pm 1.8\%$

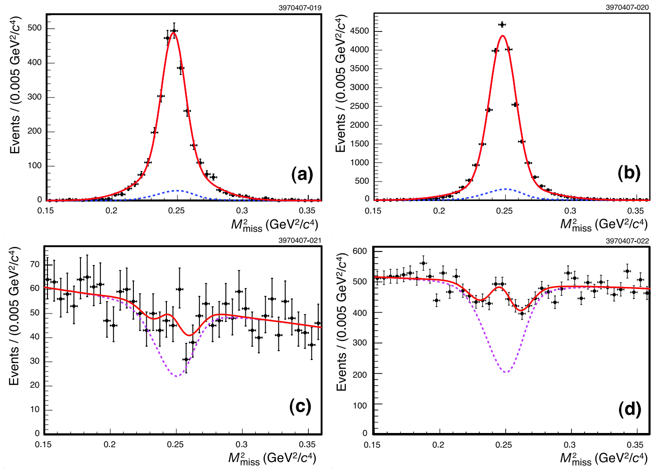

FIG. 7 Histograms of and fits to $M^2_{\rm miss}$ distributions to determine the K^0_S efficiency. Figures (a) and (c) are from events in data, and (b) and (d) are from events in Monte Carlo simulation. Figures (a) and (b) are from decays in which the K^0_S was found, while (c) and (d) are from decays in which the K^0_S was not found. The background peak and deficit are determined by searching for K^0_S candidates in high and low sidebands of the K^0_S mass. In Figs. (a) and (b), the dashed curves are the contributions from fake K^0_S candidates. In Figs. (c) and (d), the dashed curve is the background — a linear function with a deficit due to events in which a fake K^0_S candidate was found — and the solid curve is the total fit function including the signal peak. The area between the curves is proportional to the number of K^0_S mesons not found. From Dobbs *et al.* (2007).

for the K^0_S finding efficiency.

The efficiency for $\pi^0 \to \gamma\gamma$ reconstruction has been studied using a missing mass technique in $\psi(2S) \to J/\psi\pi^0\pi^0$ events recorded at $E_{\rm CM} = m_{\psi(2S)}$. CLEO-c assigns a $\pm 2.0\%$ uncertainty to the π^0 reconstruction efficiency.

B. $c\bar{c}$ production in e^+e^- above threshold

At energies above charm threshold, charm hadrons are produced in fragmentation of charm jets and are part of a jet, or are produced as secondary particles in decays of b-hadrons. The largest charm samples are those produced at the B factories at e^+e^- center-of-mass energies near 10.58 GeV corresponding to the $\Upsilon(4S)$ resonance. The large cross-section, about 1.3 nb, combined with the large integrated luminosities recorded by CLEO, BABAR, and Belle experiments have produced very large charm samples.

At even higher energy, the LEP operated near the Z resonance and produced over 4 million Z bosons per experiment. The jet nature of the events here is more clear than at the $\Upsilon(4S)$.

Many studies of D^0 decays above charm threshold makes use of a D^* tagging technique. In this technique a D^{*+} is reconstructed using the decay $D^{*+} \to D^0\pi^+$. Due to the small energy release in this decay, $M_{D^{*+}} - M_{D^0} - M_{\pi^+}$ is approximately 5.8 MeV, the reconstructed mass difference $M_{D^{*+}} - M_{D^0}$ provides a powerful tool to tag the presence of a D^0, and also determine the flavor at the time of production.

The CLEO, BABAR, and Belle experiments were designed to study B meson decays but they are also well suited for studying charm. These experiments all have excellent charged particle tracking capabilities and vertex detectors capable of detecting the separated vertices from the relatively long lived charm and beauty hadrons. All three experiments have CsI(Tl) electromagnetic calorimeters with excellent photon detection capabilities and electron identification using E/p. Detection of muons in all three experiments is done using an instrumented flux return. Also key for these experiments is the identification of charged hadrons, particularly K–π separation. The three experiments chose different technologies here. BABAR used a DIRC (Detector of Internally Reflected Cherenkov light), CLEO-III used a RICH (Ring Imaging Cherenkov Detector), and Belle uses aerogel Cherenkov counters complemented by a time-of-flight system. All three different types of charged hadron particle identification detectors have worked well.

The BABAR and Belle experiments were built for an energy asymmetric collision to allow resolving the time evolution of the produced B mesons, as discussed in the BABAR Physics Book (Harrison and Quinn, 1998). The energy asymmetric collisions are reflected in the design of the detector; the interaction point is offset to optimize the acceptance due to the boost of the collision center-of-mass.

C. Fixed target experiments

Charm mesons are sufficiently light that they can be produced efficiently in fixed target experiments. The main experimental challenge is to separate charm production from the large non-charm rate. The development of silicon based tracking detectors enabled experiments to effectively identify the long lived charmed hadrons. The pioneering Fermilab photoproduction experiment E691 was the first experiment to produced large samples of reconstructed charm hadrons. In this experiment a beam of photons with an average energy around 180 GeV was incident on a Beryllium target. The cross-section for charm production was measured to be about 0.5 μb. This is about 0.5% of the 100 μb total hadronic cross-section. The E791 experiment was a pioneering experiment for hadroproduction of charm - 200,000 hadronic charm decays were reconstructed. The most powerful tool for identifying the charm signal is to make use of the relatively long charm-hadron lifetimes, from (410.1 ± 1.5) fs for the D^0 to (1040 ± 7) fs for the D^+. Using silicon vertex detectors it is possible to separate the long lived charm-hadrons from the prompt backgrounds. A series of fixed target experiments for charm physics are summarized in Table II. The latest of these experiments at Fermilab, FOCUS or E831, reconstructed over 1.2 million exclusive charm decays. The FOCUS spectrometer is shown in Fig. 8. The FOCUS experiment and experimental techniques are described in Link *et al.* (2002a), Link *et al.* (2002d), and Link *et al.* (2004c). Measurements (Link *et al.*, 2002c, 2005a) from FOCUS dominate the world average for the lifetimes of charmed mesons.

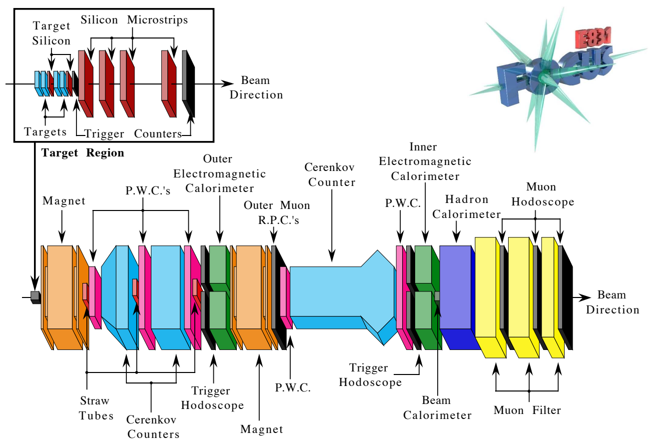

FIG. 8 The FOCUS (E831) spectrometer.

D. Proton–anti-proton Experiments

The Tevatron collider, colliding proton and anti-proton at a center of mass energy of 1.96 TeV, has produced a very large number of charmed mesons. Each of the two experiments at the Tevatron, CDF and DØ, has collect over 6 fb^{-1}. With a D^0 cross-section of 13 μb^{-1} for $\eta < 1.0$ and $p_{\rm T} > 5.5$ GeV this corresponds to over 10^{10} produced D^0 mesons. However, at a hadron collider the challenge is to trigger on these events. At CDF the use of a separated vertex trigger (Ashmanskas *et al.*, 2004) designed for B-physics allow also triggering on tracks from charmed hadrons. CDF has competitive results on a number of Cabibbo-suppressed charm meson branching fractions as discussed in Section VII.B.1.

E. Final-state radiation

The treatment of final-state radiation (FSR) is common to many analyses and will be discussed here. In many earlier measurements the effects of final-state radiation was often omitted, but as the measurements have become increasingly more precise this has become an important effect that can not be ignored. In the latest measurements of the branching fraction for $D^0 \to K^-\pi^+$ the size of the radiative correction is larger than the combined statistical and systematic uncertainties.

Any reaction involving charged particles will also radiate photons (Bloch and Nordsieck, 1937). In fact, an arbitrarily large number of photons will be produced, though most of these are very soft. In general, when we discuss a branching fraction for a process, like for example $\mathcal{B}(D^0 \to K^-\pi^+)$, this includes final states with additional (soft) photons. Experimentally, if photons are emitted with an energy that is smaller than the experimental resolution these events are automatically included in the measurement. However, sometimes the photon energies are larger, and the energy carried away by the photon will make the event fail the selection criteria. In order to account for this, and provide a measurement of a physically meaningful quantity, experiments simulate the effect of final-state radiation in their Monte Carlo simulations. This has been a common practice for semileptonic decays, in particular with electrons in the final state, for quite some time. For hadronic final states this is not yet universally done. In D decays the first experiment that considered FSR corrections was CLEO (Akerib *et al.*, 1993). Today most measurements of hadronic D decays include FSR corrections.

For simulation of final-state radiation in hadronic decays the most commonly used tool is the PHOTOS package (Barberio and Was, 1994). In the measurement of the $D^0 \to K^-\pi^+$ branching fraction CLEO-c uses version 2.15 with interference enabled. The effect of interference, here referring to interference between photons radiated from different charged particles in the final state, is important. For the final state $D^0 \to K^-\pi^+$ the effect of including interference changes the fraction of events that radiate more than 30 MeV from 2.0% to 2.8%. Earlier versions of PHOTOS were only able to simulate the interference for decays to final state with a particle—anti-particle pair. PHOTOS has been compared with calculations to higher order in α and found to reproduce the amount of energy radiated very well in semileptonic decays of B mesons and decays of τ leptons (Richter-Was, 1993). However, for hadronic final states there is an additional uncertainty introduced by the fact that the final-state particles, kaons and pions, are not point like. This uncertainty affects in particular higher energy photons that probe the structure of the final-state particles. Higher energy photons could also be radiated directly from the quarks; this effect is not included in the simulation. CLEO-c includes a 30% systematic uncertainty on the correction to the branching fraction due to including final-state radiation. Given the excellent agreement between exact calculations and next order calculations in α this systematic uncertainty is probably conservative.

For many earlier measurements it is not always clear what was done to correct for the FSR effects. If the effects due to FSR are not included in the analysis it is hard to correct for it after-the-fact as the signal efficiency loss due to FSR depends on the selection criteria used and the experimental resolution.

IV. THEORETICAL DESCRIPTION OF D DECAYS

Hadronic decays of D mesons involve transitions of the initial-state D meson into several final-state mesons or baryons. Thus, they are described by an effective Hamiltonian containing four-quark operators. The theoretical description of hadronic decays of charmed mesons is significantly more complicated than leptonic or semileptonic ones, although relevant effective Hamiltonians look similar.

Charmed hadronic decays are usually classified by the degree of Cabibbo-Kobayashi-Maskawa (CKM) matrix element suppression. Least suppressed, where the quark level transitions are $c \to s u \bar{d}$ are labeled "Cabibbo favored" (CF) decays and governed by

$$\mathcal{H}_{CF} = \frac{G_F}{\sqrt{2}} V_{ud} V_{cs}^* \left[C_1(\mu) \mathcal{O}_1 + C_2(\mu) \mathcal{O}_2 \right] + \text{h.c}, \tag{17}$$

$$\mathcal{O}_1 = \left(\overline{s}_i \Gamma_\mu c_i \right) \left(\overline{u}_k \Gamma^\mu d_k \right), \tag{18}$$

$$\mathcal{O}_2 = \left(\overline{s}_i \Gamma_\mu c_k \right) \left(\overline{u}_k \Gamma^\mu d_i \right), \tag{19}$$

where $C_n(\mu)$ are the Wilson coefficients obtained by perturbative QCD running from M_W scale to the scale μ relevant for hadronic decay, and the Latin indices denote quark color. G_F is a Fermi constant, and $\Gamma_\mu = \gamma_\mu (1 - \gamma_5)$.

The "Cabibbo suppressed" (CS) or singly Cabibbo suppressed (SCS) transitions are driven by $c \to d u \bar{d}$ or $c \to s u \bar{s}$ quark processes. Due to the presence of quark-antiquark pair of the same flavor in the final state, the effective Hamiltonian takes much more elaborate form,

$$\begin{aligned} \mathcal{H}_{CS} &= \frac{G_F}{\sqrt{2}} \sum_{q=s,d} V_{uq} V_{cq}^* \left[C_1(\mu) \mathcal{O}_1^q + C_2(\mu) \mathcal{O}_2^q \right] \\ &- \frac{G_F}{\sqrt{2}} V_{ub} V_{cb}^* \sum_{n=3}^{6} C_n(\mu) \mathcal{O} + \text{h.c}, \end{aligned} \tag{20}$$

$$\mathcal{O}_1 = \left(\overline{q}_i \Gamma_\mu c_i \right) \left(\overline{u}_k \Gamma^\mu q_k \right), \tag{21}$$

$$\mathcal{O}_2 = \left(\overline{q}_i \Gamma_\mu c_k \right) \left(\overline{u}_k \Gamma^\mu q_i \right), \tag{22}$$

where $q = d,\ s$, and $\mathcal{O}_{3-6}$ are the so-called "penguin" operators of the type $(\overline{u}c)_{V-A} \sum_q (\overline{q}q)_{V \pm A}$ (see, *e.g.* Buccella *et al.* (1995, 1996)). It is often easy to denote the degree of suppression by powers of the Wolfenstein parameter $\lambda = \sin\theta_C = V_{us} \simeq 0.22$, there θ_C is a Cabibbo angle.

The doubly-Cabibbo suppressed decay is the one in which $c \to d u \bar{s}$ quark transition drives the decay. The effective Hamiltonian for DCS decay can be obtained from Eq. (17) by interchanging $s \leftrightarrow d$.

Calculations of hadronic decay rates governed by these transitions are quite complicated and model-dependent. Most often, simplified assumptions, such as factorization (Bauer *et al.*, 1987; Buras *et al.*, 1986) are used to estimate the needed branching ratios. Some dynamical approaches, such as QCD sum rules, have been used to justify those assumptions (Blok and Shifman, 1993). The main problem with reliable calculations of charmed meson decays is that they populate the energy range where non-perturbative quark dynamics is active. This leads to resonance effects that affect the phases of hadronic decay amplitudes (Falk *et al.*, 1999), which makes predictions based on factorization quite unreliable.

It remains a difficult exercise in QCD to calculate non-factorizable corrections to hadronic decay amplitudes. QCD sum rules provided the first systematic way to include those (Blok and Shifman, 1993), albeit in the $SU(3)$ flavor symmetry limit. Large N_c limit provided another interesting insight into this problem (Buras *et al.*, 1986), however, calculation of (supposedly large) $1/N_c$ corrections are not possible at the moment. It was also shown (Gao, 2007) that application of the QCD factorization approach developed for B-decays (Beneke *et al.*, 1999) does not provide a reliable method of calculation for charm hadronic transitions. The methods developed in those references represented fascinating exercises in using QCD-based approaches to calculate hadronic decay amplitudes. The discussion of those methods goes beyond the scope of this review, but we encourage the interested reader to examine those papers.

Instead of predicting an absolute decay rate, it is often useful to obtain relations among several decay rates. These relations are helpful when some decay rates in a relation are measured, and some are unknown. This allows for a relation to be used to predict the unknown transition rate(s). The relations can be built based on some symmetries, such as standard flavor $SU(3)$ (Savage, 1991), or on overcomplete set of universal quark-level amplitudes (Gronau *et al.*, 1994; Rosner, 1999). We shall discuss those methods below.

The partial width for a specific two-body decay of a charmed meson depends on both the invariant amplitude $\mathcal{A}$ and a phase space factor. For a specific two-body decay into a PP final state,

$$\Gamma(D \to PP) = \frac{\mid \mathbf{p} \mid}{8\pi M_D^2} \left|\mathcal{A}(D \to PP)\right|^2 , \qquad (23)$$

where $|\mathbf{p}|$ is a center-of-mass 3-momentum of each final-state particle. For a decay into a PV final state,

$$\Gamma(D \to PV) = \frac{\mid \mathbf{p} \mid^3}{8\pi M_D^2} \left|\mathcal{A}(D \to PV)\right|^2 . \qquad (24)$$

Note that in the case of PP final state the final-state mesons are in the S-wave, while in the case of PV final state they are in a P-wave. This is why $|\mathcal{A}(D \to PP)|$ has dimension of energy, while $|\mathcal{A}(D \to PV)|$ is dimensionless.

A. $SU(3)_F$ flavor symmetries

One popular approach that was adopted for studies of hadronic charm decays involves application of approximate flavor symmetries, such as flavor $SU(3)_F$. This approach is based on the fact that the QCD Lagrangian acquires that symmetry in the limit where masses of all light quarks are the same. The $SU(3)_F$ analysis of decay amplitudes cannot predict their absolute values. However, at least in the symmetry limit, this approach can relate transition amplitudes for different decays, which could prove quite useful for an experimental analysis. One potential difficulty with this approach is related to the fact that available experimental data show that flavor $SU(3)_F$ symmetry is broken in charm transitions, so symmetry-breaking corrections should be taken into account (Hinchliffe and Kaeding, 1996; Savage, 1991).

In the flavor-symmetry approach all particles are denoted by their $SU(3)_F$ representations. Charm quark transforms as singlet under flavor $SU(3)$. The fundamental representation of $SU(3)_F$ is a triplet, $\mathbf{3}$, so the light quarks u, d, and s belong to this representation with $(1,2,3) = (u,d,s)$. The operator D_i that creates a $\overline{D}$-meson is of the form $\bar{c}u$, so it also transforms in the fundamental representation of $SU(3)$. In the hadronic decay of a charm meson the final-state mesons are made of u, d, and s quarks, so they either form an octet $\mathbf{8}$ representation of $SU(3)_F$ (pseudoscalars $\pi^\pm$, π^0, $K^\pm$, K^0, $\overline{K}^0$, η_8 and vectors $\rho^\pm$, ρ^0, $K^{*\pm}$, K^{*0}, $\overline{K}^{*0}$, ω_8), e.g.

$$P_i^k = \begin{pmatrix} \frac{1}{\sqrt{6}}\eta_8 + \frac{1}{\sqrt{2}}\pi^0 & \pi^+ & K^+ \\ \pi^- & \frac{1}{\sqrt{6}}\eta_8 - \frac{1}{\sqrt{2}}\pi^0 & K^0 \\ K^- & \overline{K}^0 & -\sqrt{\frac{2}{3}}\eta_8 \end{pmatrix}, \qquad (25)$$

or an $SU(3)_F$ singlet (η_1 and ω_1). The physical states η, η', ϕ, and ω are linear combinations of $\eta_{1,8}$ and $\omega_{1,8}$ states respectively.

The $\Delta C = -1$ part of the weak Hamiltonian has the flavor structure $(\bar{q}_i c)(\bar{q}_j q_k)$ (see Eq. (17)), so its matrix representation is written with a fundamental index and two antifundamentals, H_k^{ij}. This operator is a sum of irreducible representations contained in the product $3 \times \overline{3} \times \overline{3} = \overline{15} + 6 + \overline{3} + \overline{3}$. In the limit in which the third generation is neglected, H_k^{ij} is traceless, so only the $\overline{15}$ (symmetric on i and j) and 6 (antisymmetric on i and j) representations appear. That is, the $\Delta C = -1$ part of $\mathcal{H}_w$ may be decomposed as $\frac{1}{2}(\mathcal{O}_{\overline{15}} + \mathcal{O}_6)$, where

$$\begin{aligned} \mathcal{O}_{\overline{15}} &= (\bar{s}c)(\bar{u}d) + (\bar{u}c)(\bar{s}d) + s_1(\bar{d}c)(\bar{u}d) \\ &\quad + s_1(\bar{u}c)(\bar{d}d) - s_1(\bar{s}c)(\bar{u}s) - s_1(\bar{u}c)(\bar{s}s) \\ &\quad - s_1^2(\bar{d}c)(\bar{u}s) - s_1^2(\bar{u}c)(\bar{d}s) , \qquad (26) \\ \mathcal{O}_6 &= (\bar{s}c)(\bar{u}d) - (\bar{u}c)(\bar{s}d) + s_1(\bar{d}c)(\bar{u}d) \\ &\quad - s_1(\bar{u}c)(\bar{d}d) - s_1(\bar{s}c)(\bar{u}s) + s_1(\bar{u}c)(\bar{s}s) \\ &\quad - s_1^2(\bar{d}c)(\bar{u}s) + s_1^2(\bar{u}c)(\bar{d}s) , \qquad (27) \end{aligned}$$

and $s_1 = \sin\theta_C \approx 0.22$. The matrix representations

$H(\overline{15})^{ij}_k$ and $H(6)^{ij}_k$ have non-zero elements

$$
\begin{aligned}
H(\overline{15})^{ij}_k: \quad & H^{13}_2 = H^{31}_2 = 1\,, && H^{12}_2 = H^{21}_2 = s_1\,,\\
& H^{13}_3 = H^{31}_3 = -s_1\,, && H^{12}_3 = H^{21}_3 = -s_1^2\,,\\
H(6)^{ij}_k: \quad & H^{13}_2 = -H^{31}_2 = 1\,, && H^{12}_2 = -H^{21}_2 = s_1\,,\\
& H^{13}_3 = -H^{31}_3 = -s_1\,, && H^{12}_3 = -H^{21}_3 = -s_1^2\,.
\end{aligned} \tag{28}
$$

In the $SU(3)_F$ limit the effective Hamiltonian for the hadronic decays to two pseudoscalars $D \to PP$ can be written as

$$
\begin{aligned}
\mathcal{H}_{\mathrm{eff}\ SU(3)} &= a_{\overline{15}} D_i H(15)^{ij}_k P^l_j P^k_l + b_{\overline{15}} D_i P^i_l H(15)^{lj}_k P^k_j \\
&+ c_6 D_i H(6)^{ij}_k P^l_j P^k_l
\end{aligned} \tag{29}
$$

There are a number of amplitude relations that can be obtained from Eq. (29). In particular, it can be seen that it implies that $|A_{D^0\to K^+K^-}| = |A_{D^0\to\pi^+\pi^-}|$. In practice, the corresponding branching fractions differ by a factor of three (see Table XVI below). Clearly, $SU(3)_F$ symmetry is broken in D decays.

A consistent approach should then include $SU(3)_F$-breaking corrections, which could consistently be included in the analysis. For example, one could assume that $SU(3)_F$ breaking is proportional to light quark masses. In this case, it can be included in the analysis as a perturbation that transforms as $\mathbf{8} + \mathbf{1}$, as the quark mass operator belongs to the matrix representation $M^i_j = \mathrm{diag}(m_u, m_d, m_s)$, which is an $\mathbf{8}$. Note that the $SU(3)_F$ breaking term that transforms as a triplet $\mathbf{3}$ also breaks isospin, so it is usually neglected in all analyses. A complete analysis with broken $SU(3)_F$ is possible (Hinchliffe and Kaeding, 1996; Savage, 1991), although is not quite useful due to a large number of unknown amplitudes.

In some cases one does not need to employ the full formalism of $SU(3)_F$, but only rely on its subgroups. An example of such subgroup is isospin. Isospin relations among decay amplitudes are much more robust, as isospin breaking is believed to be quite small in charm decays. For example, the di-pion modes, $D^+ \to \pi^+\pi^0$, $D^0 \to \pi^+\pi^-$ and $D^0 \to \pi^0\pi^0$ are related by two isospin amplitudes A_0 and A_2 corresponding, respectively, to the S-wave di-pion isospin $I = 0$ and $I = 2$ states produced

$$
\begin{aligned}
A^{+0} &= \sqrt{\frac{3}{2}} A_2, \qquad A^{+-} = \sqrt{\frac{2}{3}} A_0 + \sqrt{\frac{1}{3}} A_2 \\
A^{00} &= \sqrt{\frac{1}{3}} A_0 - \sqrt{\frac{2}{3}} A_2.
\end{aligned} \tag{30}
$$

Some conclusions about strong interaction dynamics in D meson decays can be reached by extracting these amplitudes from experimental information. The phases of amplitudes in Eq. (30) give an indication of the size of strong interactions among decay products in those decays. Following the procedure outlined in (Selen *et al.*, 1993), CLEO obtains (Rubin *et al.*, 2006) from their results $|A_2/A_0| = 0.420 \pm 0.014 \pm 0.016$ and $\arg(A_2/A_0) = (86.4 \pm 2.8 \pm 3.3)^\circ$. As one can see, the phase is rather large. It is thus clear that final-state interactions play an important role in D decays.

Other subgroups of the $SU(3)_F$ also offer useful predictions. For example, the U-spin, a symmetry of the Lagrangian with respect to $s \to d$ quark interchange, can be employed to obtain several useful relations. For example, for the decays of D^0 mesons into final states containing $M^0 = \pi^0$, η, and η', one can obtain

$$
\frac{\mathcal{A}(D^0 \to K^0 M^0)}{\mathcal{A}(D^0 \to \overline{K}^0 M^0)} = -\tan^2\theta_C. \tag{31}
$$

Equation (31) derives from the following argument. The initial state, D^0 contains c and $\bar{u}$ quarks, and so is a U-spin singlet. The CF transition $c \to s u \bar{d}$ and DCS transition $c \to d u \bar{s}$ produce $U = 1$ finals states with opposite third component $U_3 = \pm 1$ in the decays of D^0 meson. The final-state meson M^0 form a linear combination of U-spin singlet and triplet states, while neutral kaons are $U = 1$, $U_3 = \pm 1$ states. Thus, U-spin triplet part of M^0 cannot be produced, as it leads to the $U = 2$ final state. Thus, only the singlet part of M^0 can contribute to the transition, which leads to Eq. (31).

B. Flavor-flow (topological) diagram approach

Another useful approach to tackle hadronic decays of charmed mesons, equivalent to the $SU(3)_F$ amplitude method described above, is the flavor-flow (or topological $SU(3)$ approach), which involves an overcomplete set of quark diagrams (Gronau *et al.*, 1994; Rosner, 1999). The application of this method to D decays can even prove advantageous compared to flavor $SU(3)$ approach, as the number of unknown amplitudes grows rapidly if $SU(3)_F$-breaking is taken into account.

In the topological flavor-flow approach each decay amplitude is parametrized according to the topology of Feynman diagrams (see Fig. 9): a color-favored tree amplitude (usually denoted by T), a color-suppressed tree amplitude (C), an exchange amplitude (E), and an annihilation amplitude (A). This set of amplitudes is sufficient for description of CF and DCS decays. For SCS decays other amplitudes must be added (Chiang *et al.*, 2003).

In order to describe charm meson decays in terms of these amplitudes, it is convenient to decompose initial and final states according to their isospin structure. For instance, in the notation of (Rosner, 1999), the following phase conventions are used:

1. Charmed mesons: $D^0 = -c\overline{u}$, $D^+ = c\overline{d}$, and $D_s = c\overline{s}$.
2. Pseudoscalar mesons: $\pi^+ = u\overline{d}$, $\pi^0 = \left(u\overline{u} - d\overline{d}\right)/\sqrt{2}$, $\pi^- = -d\overline{u}$, $K^+ = u\overline{s}$, $K^0 = d\overline{s}$, $\overline{K}^0 = s\overline{d}$, $K^- = -s\overline{u}$, $\eta = \left(s\overline{s} - u\overline{u} - d\overline{d}\right)/\sqrt{3}$, and $\eta' = \left(u\overline{u} + d\overline{d} - 2s\overline{s}\right)/\sqrt{6}$.

3. Vector mesons: $\rho^+ = u\bar{d}$, $\rho^0 = \left(u\bar{u} - d\bar{d}\right)/\sqrt{2}$, $\rho^- = -d\bar{u}$, $\omega^0 = \left(u\bar{u} + d\bar{d}\right)/\sqrt{2}$, $K^{*+} = u\bar{s}$, $K^{*0} = d\bar{s}$, $\overline{K}^{*0} = s\bar{d}$, $K^{*-} = -s\bar{u}$, and $\phi = s\bar{s}$.

As with the $SU(3)_F$ approach, this method does not provide absolute predictions for the branching fractions in D-meson decays. However, it provides relations among several decay amplitudes by matching the quark-level "flavor topology" graphs with the final states defined above. For example, a DCS transition $D^0 \to K^+\pi^-$ can proceed via a tree-level amplitude $T(c \to u\bar{s}d)$ and an exchange amplitude $E(c\bar{u} \to \bar{s}d)$. Matching those with the initial state meson $D^0 = -c\bar{u}$ and final-state mesons $K^+ = u\bar{s}$ and $\pi^- = -d\bar{u}$, one obtains the following amplitude relation,

$$A(D^0 \to K^+\pi^-) = T + E \equiv \frac{G_F}{\sqrt{2}} V_{ud} V_{cs}^* \left(\mathcal{T} + \mathcal{E}\right), \quad (32)$$

where we use calligraphic notation for the amplitudes with $G_F/\sqrt{2}$ and CKM-factors removed. Similarly, for other transitions one obtains

$$\begin{aligned}
A(D^0 \to K^0\pi^0) &= \frac{1}{\sqrt{2}}(C - E) \\
&= \frac{1}{\sqrt{2}} \frac{G_F}{\sqrt{2}} V_{us} V_{cd}^* \left(\mathcal{C}'' - \mathcal{E}''\right), && (33) \\
A(D^0 \to \overline{K}^0\pi^0) &= \frac{1}{\sqrt{2}}(C - E) \\
&= \frac{1}{\sqrt{2}} \frac{G_F}{\sqrt{2}} V_{ud} V_{cs}^* \left(\mathcal{C} - \mathcal{E}\right), && (34) \\
A(D^+ \to K^0\pi^+) &= C + A = \frac{G_F}{\sqrt{2}} V_{us} V_{cd}^* \left(\mathcal{C}'' + \mathcal{A}''\right), && (35) \\
A(D^+ \to \overline{K}^0\pi^+) &= T + C = \frac{G_F}{\sqrt{2}} V_{ud} V_{cs}^* \left(\mathcal{T} + \mathcal{C}\right), && (36) \\
A(D^0 \to K^0\eta) &= \frac{1}{\sqrt{3}} C = \frac{1}{\sqrt{3}} \frac{G_F}{\sqrt{2}} V_{us} V_{cd}^* \, \mathcal{C}'', && (37)
\end{aligned}$$

and so on. Note that in Eq. (33) we denoted DCS amplitudes with double primes. Singly-Cabibbo-suppressed amplitudes are conventionally denoted by a single prime. CF amplitudes can be related to SCS and DCS amplitudes by proper scaling with $\tan\theta_C$. We shall give particular examples below.

The employed phase convention makes it easy to build $SU(3)_F$-required sum rules. For example, for transitions $D^+ \to K^+\pi^0$, $D^+ \to K^+\eta$, and $D^+ \to K^+\eta'$, a sum rule

$$3\sqrt{2}A(K^+\pi^0) + 4\sqrt{3}A(K^+\eta) + \sqrt{6}A(K^+\eta') = 0 \quad (38)$$

can be written. With the flavor-flow parameterization,

$$\begin{aligned}
A(D^+ \to \overline{K}^+\pi^0) &= \frac{1}{\sqrt{2}}\left(T - A\right), && (39) \\
A(D^+ \to \overline{K}^+\eta) &= -\frac{1}{\sqrt{3}}\, T && (40) \\
A(D^+ \to \overline{K}^+\eta') &= \frac{1}{\sqrt{6}}\left(T + 3A\right) && (41)
\end{aligned}$$

the above sum rule gives $3(T - A) - 4T + (T + 3A) = 0$.

Thus, provided that a sufficient number of decay modes is measured, one can predict both branching fractions and amplitude phases for a number of transitions. Still, no prediction for absolute branching ratios are possible in this approach.

C. Factorization ansatz

The simplest way to estimate an absolute decay rate of a charmed meson is to employ a factorization ansatz. This ansatz implies that the amplitude for the hadronic transition can be written as a product of known form-factors. Schematically,

$$\begin{aligned}
\mathcal{A}(D_q \to M_1 M_2) &= \langle M_1, M_2 | \mathcal{H} | D_q \rangle && (42) \\
&\sim \langle M_1 | \left(\overline{u}_k \Gamma^\mu q_k\right) | 0 \rangle \times \langle M_2 | \left(\overline{q}_i \Gamma_\mu c_i\right) | D_q \rangle
\end{aligned}$$

This is a clear simplification, as the first non-perturbative parameter $\langle M_1 | \left(\overline{u}_k \Gamma^\mu q_k\right) | 0 \rangle$ can be written in terms of a meson decay constant f_{M_1},

$$\langle M_1 | \bar{u} \gamma^\mu \gamma_5 q | 0 \rangle = i f_{M_1} p_{M_1}^\mu, \quad (43)$$

which parameterizes the amplitude of probability for quarks to "find each other" in a light mesons and can be measured in leptonic decays of M_1,

$$\Gamma(M_1 \to \ell\nu) = \frac{G_F^2}{8\pi} f_{M_1}^2 m_\ell^2 m_{M_1} \left(1 - \frac{m_\ell^2}{m_{M_1}^2}\right)^2 |V_{uq}|^2 \quad , \quad (44)$$

where m_{M_1} is the M_1 mass, m_ℓ is the mass of the final-state lepton, and $|V_{uq}|$ is the CKM matrix element associated with the $q \to u$ transition. The decay constants can also be computed in lattice gauge theories or using other non-perturbative approaches (see Artuso *et al.* (2008) for a recent review).

The second non-perturbative parameter, $\langle M_2 | \left(\overline{q}_i \Gamma_\mu c_i\right) | D_q \rangle$, is related to form-factors that can be extracted from semileptonic D_q decays,

$$\frac{d\Gamma(D \to M_2 e \nu_e)}{dq^2} = \frac{G_F^2 |V_{cq}|^2}{24\pi^3} \left|\mathbf{p}_{M_2}\right|^3 |f_+(q^2)|^2 \quad (45)$$

where $\mathbf{p}_{M_2}$ is the hadron 3-momentum in the D rest frame. Note that, in principle, Eq. (45) depends on two form factors (see below). We dropped the contribution from $f_-(q^2)$ because it is multiplied by m_e^2.

Theoretical parameterizations of semileptonic decays involve two non-perturbative quantities parameterizing the matrix element of a single hadronic current. Traditionally, the hadronic matrix elements for transitions to pseudoscalar hadrons are described in terms of two form factors, $f_+(q^2)$ and $f_-(q^2)$,

$$\langle M_2 | \bar{q} \Gamma^\mu c | D \rangle = f_+^{D \to M_2}(q^2) P^\mu + f_-^{D \to M_2}(q^2) q^\mu, \quad (46)$$

where $P = p_D + p_{M_2}$ and $q = p_D - p_{M_2}$. An alternative parameterization is often used,

$$\begin{aligned}\langle M_2|\bar{q}\Gamma^\mu c|D\rangle &= \left(P^\mu - \frac{m_D^2 - m_{M_2}^2}{q^2} q^\mu\right) f_+^{D\to M_2}(q^2) \\ &+ \frac{m_D^2 - m_{M_2}^2}{q^2} q^\mu f_0^{D\to M_2}(q^2), \qquad (47)\end{aligned}$$

with $f_0^{D\to M_2}(q^2) = f_+^{D\to M_2}(q^2) + f_-^{D\to M_2}(q^2) q^2/(m_D^2 - m_{M_2}^2)$. Form factors have been evaluated at specific q^2 points in a variety of phenomenological models, where the shape is typically assumed from some model arguments.

Clearly, naive factorization of Eq. (42), while convenient, cannot be correct, as it assumes that scale and scheme dependence of a product of quark bilinears is the same as that of a four-fermion operator, which it is not. The situation can in principle be corrected, at least in the heavy-quark limit. In B decays, a QCD factorization formula has been written that takes into account perturbative QCD corrections (Beneke *et al.*, 1999). It is however not clear that this approach is applicable to charm decays, as charm quark might be too light for this approach to be applicable. Nevertheless, even naive factorization provides a convenient way to estimate D-meson decay rates.

Besides decay amplitudes for D-mesons, which can be computed using the factorization arguments above, both flavor-flow and $SU(3)_F$ amplitudes can also be estimated. For example, contrary to the relation Eq. (31), the corresponding relation for charged D-meson decays,

$$\frac{\mathcal{A}(D^+ \to K^0\pi^+)}{\mathcal{A}(D^+ \to \overline{K}^0\pi^+)} = -\tan^2\theta_C \frac{\mathcal{C}'' + \mathcal{A}''}{\mathcal{C} + \mathcal{T}} = \frac{\mathcal{C} + (C_2/C_1)\,\mathcal{E}}{\mathcal{C} + \mathcal{T}}, \qquad (48)$$

cannot be fixed by symmetry arguments alone. However, the factorization approach can be used to estimate this ratio. In particular,

$$\begin{aligned}\mathcal{T} &= f_\pi \left(m_D^2 - m_K^2\right) f_+^{D\to K}(m_\pi^2)\; a_1, &(49)\\ \mathcal{C} &= f_K \left(m_D^2 - m_\pi^2\right) f_+^{D\to \pi}(m_\pi^2)\; a_2, &(50)\\ \mathcal{T}'' &= f_K \left(m_D^2 - m_\pi^2\right) f_+^{D\to \pi}(m_K^2)\; a_1, &(51)\\ \mathcal{C}'' &= f_\pi \left(m_D^2 - m_K^2\right) f_+^{D\to K}(m_\pi^2)\; a_2 &(52)\end{aligned}$$

where $a_{1,2} = C_{1,2} + C_{2,1}/N_c$. Note that some analyses employ $a_{1,2} \to a_{1,2}^{eff}$, which are fitted from the data and treated as universal fit parameters. This way of calculating charm hadronic decay matrix elements is sometimes called "modified factorization" approach. The argument for doing this is an attempt to include unknown non-perturbative corrections to Eq. (49). While this approach defines a convenient model to deal with hadronic decays, there is no reason to believe that soft contributions are universal in all transitions.

Calculations of $\mathcal{E}$ and $\mathcal{A}$ amplitudes in factorization are much more complicated. It has been argued (Gao, 2007) that they can be estimated using methods similar

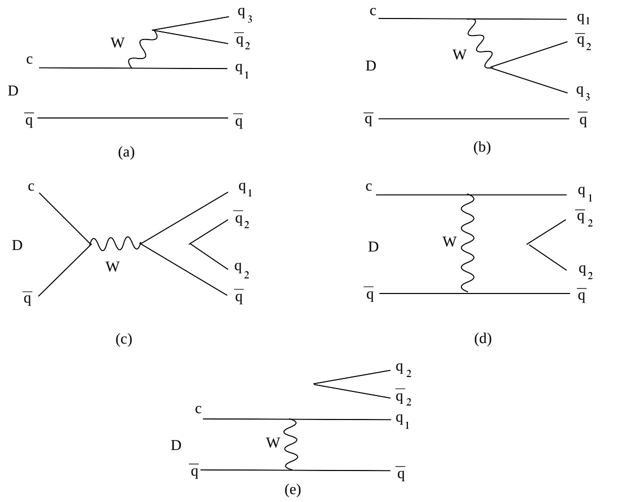

FIG. 9 Basic topological amplitudes for D-meson decays. Top row: tree $T^{(\prime)}$ (a) and color-suppressed $C^{(\prime)}$ (b), middle row: weak annihilation $A^{(\prime)}$ (c) and weak exchange $E^{(\prime)}$ (d), bottom row: singlet weak exchange SE' (e). CSC amplitudes are usually denoted by primes.

to those employed in B decays (Beneke *et al.*, 1999). Numerically, the calculation of the ratio of Eq. (48) amounts to

$$\frac{\mathcal{A}(D^+ \to K^0\pi^+)}{\mathcal{A}(D^+ \to \overline{K}^0\pi^+)} = -\tan^2\theta_C r_s e^{i\phi_s}, \qquad (53)$$

with $r_s \approx 1.521$ and $\phi_s \approx 103^o$ for $C_2/C_1 \approx -0.5$. This ratio will be used to estimate decay asymmetries with kaons later in this paper.

V. CABIBBO FAVORED D^0 AND D^+ DECAYS

The absolute branching fractions for decays of the ground state charmed mesons are important as they are used to normalize many B and D meson decays. For example, the determination of $|V_{cb}|$ from $B \to D^*\ell\nu$ (Richman and Burchat, 1995) depends directly on the determination of the D branching fractions used to reconstruct the final state.

To measure the absolute branching fractions we need to have a mechanism to determine the number of D mesons produced. As the cross-sections for producing D mesons are not directly calculable we have to count the D mesons in the data sample. Broadly speaking there are two methods employed for this D counting. At threshold MARK III and CLEO-c have used a tagging technique described in Sect. III.A, where one D meson is fully reconstructed and tag the existence of another $\bar{D}$ in the event. At higher energies the presence of a D^{*+} meson can be tagged using the "slow pion" in the $D^{*+} \to D^0\pi^+$ decay. The slow pion in this decay is often denoted π_s. This slow pion tagging technique has been used by several experiments including CLEO and ALEPH to count the number of $D^{*+} \to D^0\pi^+$ decays in charm jets produced in e^+e^- collisions. A variation of this idea has been used by ARGUS, CLEO, and BABAR where D^* mesons produced in semileptonic B decays, $\bar{B}^0 \to D^{*+}\ell^-\bar{\nu}$, are tagged by the presence of a slow pion and a lepton. These different techniques are discussed in this Section.

Before the CLEO-c measurement of the $D^+ \to K^-\pi^+\pi^+$ branching fraction using tagging as described in Sect. V.C there was a statistics limited study by MARK III (Adler *et al.*, 1988) and model-dependent analyses. CLEO (Balest *et al.*, 1994) reconstructed the two decay chains $D^{*+} \to D^0\pi^+$, $D^0 \to K^-\pi^+$ and $D^{*+} \to D^+\pi^0$, $D^+ \to K^-\pi^+\pi^+$. This allowed CLEO to measure the ratio of produced $K^-\pi^+\pi^+$ to $K^-\pi^+$ final states, which can be expressed as

$$\frac{N_{K\pi\pi}}{N_{K\pi}} = \frac{\mathcal{B}(D^{*+} \to D^+\pi^0)\mathcal{B}(D^+ \to K^-\pi^+\pi^+)\epsilon(K\pi\pi)}{\mathcal{B}(D^{*+} \to D^0\pi^+)\mathcal{B}(D^0 \to K^-\pi^+)\epsilon(K\pi)}, \tag{54}$$

where $\epsilon(K\pi\pi)$ and $\epsilon(K\pi)$ are the efficiencies for reconstructing the $D^+ \to K^-\pi^+\pi^+$ and $D^0 \to K^-\pi^+$ final states, respectively, including the D^{*+}. To extract the $D^+ \to K^-\pi^+\pi^+$ branching fraction CLEO used the measured $D^0 \to K^-\pi^+$ branching fraction and the ratio

$$\frac{\mathcal{B}(D^{*+} \to D^+\pi^0)}{\mathcal{B}(D^{*+} \to D^0\pi^+)}. \tag{55}$$

The determination of this ratio is discussed by Butler *et al.* (1992) and Bartelt *et al.* (1998); it ultimately relies on isospin conservation. Though the errors are expected to be small they are hard to quantify.

A. Absolute D^0 branching fractions using slow pion tagging

The method of tagging $D^{*+} \to D^0\pi^+$ decays in jets produced in $e^+e^- \to c\bar{c}$ interactions by the presence of a slow pion from the D^* decay is sometimes referred to as the HRS technique after the first experiment that used this method. As the Q value of the $D^{*+} \to D^0\pi^+$ decay is only about 5 MeV and the produced pion has a momentum of only 39 MeV in the D^* restframe it can at most contribute this amount to the transverse momentum with respect to the thrust axis. Experimentally, the slow pion from the D^{*+} decay closely follows the original D^* direction. Due to the soft track associated with this decay, the pion tends to bend out from the jet in the magnetic field of the tracking system.

The HRS experiment (Abachi *et al.*, 1988) used 300 pb^{-1} of data collected at $E_{\rm cm} = 29$ GeV. For candidate slow pions the transverse momentum, p_T, is calculated with respect to the thrust axis determined from the particles in the opposite hemisphere with respect to the slow pion candidate under consideration. The choice of using only tracks in the opposite hemisphere for the calculation of the thrust axis is to avoid any possible bias due to the decay of the D meson. In Fig. 10 the p_T^2 distribution is shown in two ranges of the fractional momentum

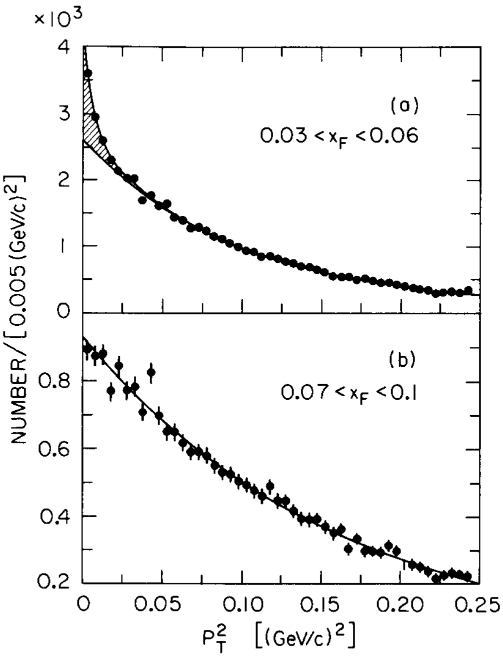

FIG. 10 The p_T^2 distribution for data from the HRS collaboration. In (a) the fractional slow pion momentum in the range $0.03 < x_F < 0.06$ is shown while in (b) the fractional momentum range $0.07 < x_F < 0.1$ is shown. In the low momentum range where we expect slow pions from D^* decays a clear excess at very low p_t^2 is seen. From Abachi *et al.* (1988).

$x_F = 2p_{\|}/E_{\rm cm}$ of the slow pion, where $p_{\|}$ is the component of the slow pion momentum that is parallel to the thrust axis. In the low fractional momentum range ($0.03 < x_F < 0.06$) a clear excess is seen at very low values of the transverse momentum due to slow pions from $D^{*+} \to D^0\pi^+$ decays. This excess is not present in the higher x_F range as slow pions from D^{*+} decays do not populate this range. The HRS collaboration use the excess at low p_t^2 to determine that they had 1584 ± 110 $D^{*+} \to D^0\pi^+$ decays in their sample. Next a D^0 is reconstructed in the $D^0 \to K^-\pi^+$ channel. The D^0 candidate is combined with the slow pion and the mass difference $M_{K\pi\pi_s} - M_{K\pi}$ is required to be in the range 0.143 to 0.148 GeV. The yield was determined by fitting the $M_{K\pi}$ mass distribution. A total of 56 ± 9 events were observed. The efficiency for finding the $K\pi$ pair, given that the π_s is found, is determined to be 79% giving a branching fraction of $\mathcal{B}(D^0 \to K^-\pi^+) = (4.5 \pm 0.8 \pm 0.5)\%$. The largest systematic uncertainty quoted is bias due to event selection criteria. This uncertainty is evaluated by changing the event selection criteria to remove the thrust and collinearity criteria used. The analysis was limited by statistics.

The same technique as pioneered above by the HRS collaboration has been used by ALEPH (Barate *et al.*, 1997; Decamp *et al.*, 1991), CLEO (Akerib *et al.*, 1993), and ARGUS (Albrecht *et al.*, 1994b). ALEPH used a sample of e^+e^- data collected from 1991 to 1994 at LEP near the Z pole. CLEO and ARGUS used samples of 1.79 fb^{-1} and 355 pb^{-1} respectively of e^+e^- data collected near the $\Upsilon(4S)$ resonance.

ALEPH followed the HRS approach closely. They analyzed the data in six ranges of the slow pion momentum, from 1.0 to 4.0 GeV. The transverse momentum squared distributions in the six momentum bins are shown in Fig. 11. A $D^0 \to K^-\pi^+$ candidate is searched for in events with a slow pion, and candidates where $0.1435 < M_{K\pi\pi_s} - M_{K\pi} < 0.1475$ GeV are accepted. In Table IV the yields and branching fractions from the ALEPH analysis are summarized. The results from the different momentum bins are combined, including correlations, to obtain the final result

$$\mathcal{B}(D^0 \to K^-\pi^+) = (3.90 \pm 0.09 \pm 0.12)\%. \quad (56)$$

This result includes corrections (1.9%) due to final-state radiation. The largest systematic uncertainties come from the background shape in extracting the inclusive D^* yield and the modeling of the angle between the D^* and the jet thrust axis.

ARGUS used the same technique to count $D^{*+} \to D^0\pi^+$ decays. To extract the $D^{*+} \to D^0\pi^+$ yield ARGUS plot the distributions of $|\cos\theta|$ where θ is the angle between the slow pion candidate and the thrust axis of the jet in the opposite hemisphere. Figure 12 shows the $|\cos\theta|$ distribution in two ranges of the slow pion momentum. In the momentum range 0.2 to 0.3 GeV a clear excess of events near $|\cos\theta| = 1$ is seen from $D^{*+} \to D^0\pi^+$ decays. In the range 0.4 to 0.5 GeV no excess is seen as this is above the momentum where we have slow pions from D^{*+} decays. From a fit to the $|\cos\theta|$ distribution ARGUS determines a yield of $51,327 \pm 757$ $D^{*+} \to D^0\pi^+$ decays in the sample. The systematic uncertainty on this yield is estimated to be 5.9% by varying the signal shape parameterization. ARGUS reconstructs the D^0 in three channels and determines the following branching fractions

$$\begin{aligned}
\mathcal{B}(D^0 \to K^-\pi^+) &= (3.41 \pm 0.12 \pm 0.28)\%, && (57)\\
\mathcal{B}(D^0 \to K^-\pi^+\pi^-\pi^+) &= (6.80 \pm 0.27 \pm 0.57)\%, && (58)\\
\mathcal{B}(D^0 \to \bar{K^0}\pi^-\pi^+) &= (5.03 \pm 0.39 \pm 0.49)\%. && (59)\\
& && (60)
\end{aligned}$$

The CLEO (Akerib *et al.*, 1993) study is very similar to the ARGUS analysis. CLEO only studied the final state $D^0 \to K^-\pi^+$. They tagged $165,658 \pm 1,149 \pm 2,485$ $D^{*+} \to D^0\pi^+$ decays and measured the branching fraction

$$\mathcal{B}(D^0 \to K^-\pi^+) = 3.95 \pm 0.08 \pm 0.17\%. \quad (61)$$

This includes a correction of about 1% for the effects of final-state radiation. The largest contribution to the systematic uncertainty ($\pm 4.0\%$) comes from the track reconstruction efficiency for the final $K\pi$ system.

These measurements are limited by systematic uncertainties on the determination of the number of $D^{*+} \to D^0\pi^+$ decays in the data sample. The yield is extracted by extrapolating the background into the signal region based on shapes determined from Monte Carlo simulations.

B. Tagging with $\bar{B}^0 \to D^{*+}\ell^-\bar{\nu}$

Tagging semileptonic B decays with the presence of a lepton plus a slow pion was first used by ARGUS (Albrecht *et al.*, 1994a) and has since been used by CLEO (Artuso *et al.*, 1998) and most recently BABAR (Aubert *et al.*, 2008b). The BABAR analysis uses the largest data sample, 210 fb^{-1} of e^+e^- data collected at the $\Upsilon(4S)$.

In the first study that used this technique ARGUS used a sample of 246 pb^{-1} of e^+e^- data collected at the $\Upsilon(4S)$ containing $209,000 \pm 9,500$ $B\bar{B}$ pairs. They obtained the branching fractions

$$\begin{aligned}
\mathcal{B}(D^0 \to K^-\pi^+) &= (4.5 \pm 0.6 \pm 0.4)\%, && (62)\\
\mathcal{B}(D^0 \to K^-\pi^+\pi^+\pi^-) &= (7.9 \pm 1.5 \pm 0.9)\%. && (63)
\end{aligned}$$

This measurement is clearly statistics limited, ARGUS reconstructed a sample of $2,693 \pm 183 \pm 105$ $D^{*+} \to D^0\pi^+$ candidates.

CLEO used a sample of 3.1 fb^{-1} of e^+e^- data collected at the $\Upsilon(4S)$ containing 3.3×10^6 $B\bar{B}$ events. A sample of 1.6 fb^{-1} of data collected below the $\Upsilon(4S)$ resonance was used for continuum subtraction. CLEO reconstructed $44,504 \pm 360$ inclusive events and $1,165 \pm 45$ exclusive $D^0 \to K^-\pi^+$ decays and determined the branching fraction

$$\mathcal{B}(D^0 \to K^-\pi^+) = (3.81 \pm 0.15 \pm 0.16)\%. \quad (64)$$

This branching fraction does not include radiative corrections.

BABAR used 210 fb^{-1} of e^+e^- data collected at the $\Upsilon(4S)$ resonance, corresponding to 230×10^6 $B\bar{B}$ pairs, and 22 fb^{-1} collected 40 MeV below the resonance. The offresonance sample is used to subtract non-$B\bar{B}$ backgrounds. In this analysis the semileptonic B decay, $\bar{B}^0 \to D^{*+}\ell^-\bar{\nu}$ followed by $D^{*+} \to D^0\pi^+$ is used. BABAR use the lepton in the B decay and the slow pion from the D^* to count $\bar{B}^0 \to D^{*+}\ell^-\bar{\nu}$ decays followed by $D^{*+} \to D^0\pi^+$. BABAR used both electrons and muons in the momentum range $1.4 < |\mathbf{p}|_\ell < 2.3$ GeV/c. For the soft pion candidate the momentum is in the range $60 < |\mathbf{p}_{\pi_s}| < 190$ MeV/c. As the energy release in the $D^{*+} \to D^0\pi^+$ decay is very small the reconstructed slow pion direction is used to approximate the direction of the D^{*+}. The momentum magnitude of the D^{*+} is parameterized as a linear function of the slow pion momentum. Using this estimate of the D^{*+} momentum, the missing mass squared of the neutrino is approximated as

$$M_\nu^2 = (E_{\rm beam} - E_{D^*} - E_\ell)^2 - (\mathbf{p}_{D^*} + \mathbf{p}_\ell)^2, \quad (65)$$

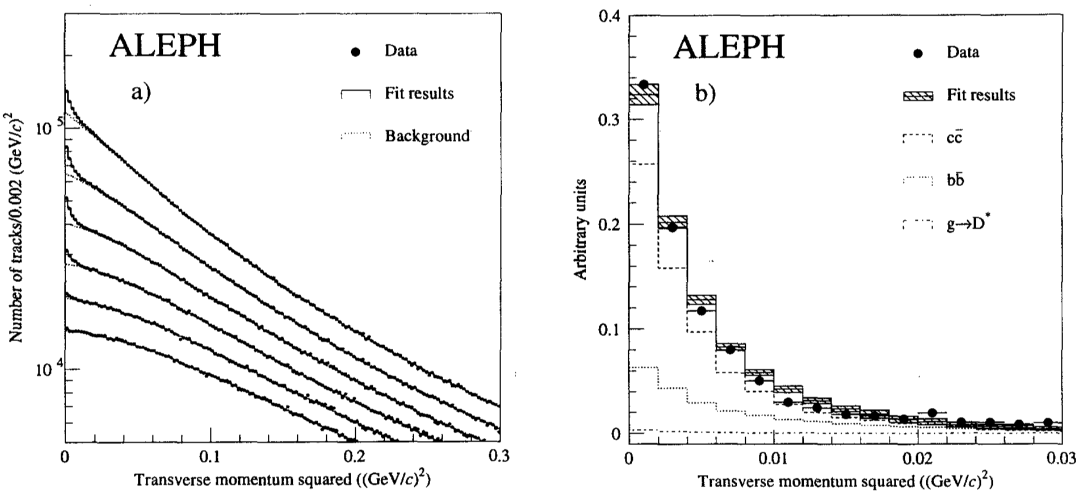

FIG. 11 The p_t^2 distribution for data from the ALEPH experiment. In (a) the transverse slow pion momentum squared in six equal momentum bins from 1.0 to 4.0 GeV. The 1.0 to 1.5 GeV momentum bin is the uppermost and the 3.5 to 4.0 GeV bin is the lowest. The slow pion from $D^{*+} \to D^0\pi^+$ is clearly visible in the lower momentum range. In (b) the transverse momentum distributions from different sources of D^* mesons are shown. From Barate *et al.* (1997).

TABLE IV Event yields and branching fractions for the ALEPH study (Barate *et al.*, 1997) of the $D^0 \to K^-\pi^+$ decay in bins of the slow pion momentum. The first column is the momentum range, the second and third columns show the $D^{*+} \to D^0\pi^+$ yield determined from the slow pion transverse momentum and the $D^0 \to K^-\pi^+$ yields, respectively. The last column shows the $D^0 \to K^-\pi^+$ branching fraction.

Momentum Range (GeV)	$N_{D^{*+}\to D^0\pi^+}$	$N_{D^0\to K^-\pi^+}$	$\mathcal{B}(D^0 \to K^-\pi^+)$ (%)
1.0—1.5	$79,038.2 \pm 2,021.9 \pm 12,018.0$	$2,472.9 \pm 55.5 \pm 11.0$	$4.400 \pm 0.150 \pm 1.041$
1.5—2.0	$56,393.2 \pm 1,140.4 \pm 921.6$	$1,558.3 \pm 41.4 \pm 5.4$	$3.990 \pm 0.133 \pm 0.139$
2.0—2.5	$35,303.4 \pm 855.8 \pm 842.2$	$913.8 \pm 30.9 \pm 2.8$	$3.768 \pm 0.157 \pm 0.150$
2.5—3.0	$12,287.8 \pm 674.7 \pm 535.1$	$321.5 \pm 18.2 \pm 1.3$	$3.758 \pm 0.296 \pm 0.206$
3.0—3.5	$3,497.4 \pm 499.2 \pm 630.4$	$115.7 \pm 10.9 \pm 0.7$	$5.010 \pm 0.857 \pm 1.228$
3.5—4.0	$192.4 \pm 366.8 \pm 401.5$	$9.8 \pm 3.3 \pm 0.4$	$7.44 \pm 14.2 \pm 19.4$

where $E_{\rm beam}$ is half the center-of-mass energy and the momentum of the B is taken to be zero. The energies and momenta in this expression are evaluated in the e^+e^- center-of-mass frame. For signal candidates it is required that the charge of the slow pion and the lepton are opposite. For background studies BABAR considers same-charge candidates. BABAR extracts the number of $\bar{B}^0 \to D^{*+}\ell^-\bar{\nu}$ decays using the missing mass squared, M_ν^2, against the D^* and the lepton. Besides the $\bar{B}^0 \to D^{*+}\ell^-\bar{\nu}$ signal events there are a few additional sources of events that peaks near zero in the missing mass squared. BABAR includes the following events as signal candidates 1) $\bar{B} \to D^{*+}(n\pi)\ell^-\bar{\nu}$ ("D^{**}") where $n \geq 1$; 2) $\bar{B} \to D^{*+}\bar{D}$, $\bar{D} \to \ell^- X$; 3) $\bar{B}^0 \to D^{*+}\tau^-\bar{\nu}$, $\tau^- \to \ell^-\bar{\nu}_\ell\nu_\tau$ ("cascade"); 4) $\bar{B}^0 \to D^{*+}h^-$ ("fake-lepton") , where h^- is a kaon or pion that has been misidentified as a lepton. The M_ν^2 distributions are shown in Fig. 13. A clear signal is observed for $M_\nu^2 > -2.0$ GeV^2. However, there are substantial backgrounds from combinatorics in $B\bar{B}$ events and in continuum production that need to be subtracted. The continuum background is modeled using offresonance data and the $B\bar{B}$ combinatorial background, as well as the signal components, are modeled using Monte Carlo simulations. The signal yields are extracted from fits to the M_ν^2 distributions in the range from -10.0 to 2.5 GeV^2. The data are divided into ten different lepton momentum ranges to reduce sensitivity to the Monte Carlo simulation. In each lepton momentum bin the continuum yields are fixed by scaling the offresonance sample to the luminosity of the on-resonance sample; while the number of events from primary signal, D^{**}, and combinatorial $B\bar{B}$ are independently varied. The contributions from cascades and fake-leptons are fixed from the simulation. These two contributions account for about 3% of the total inclusive signal.

Table V summarizes the event yields for the inclusive $\bar{B}^0 \to D^{*+}\ell^-\bar{\nu}$ reconstruction in the column "Inclusive". BABAR finds $N^{\rm incl} = 2,170,640 \pm 3,040 \pm 18,100$ $\bar{B}^0 \to$

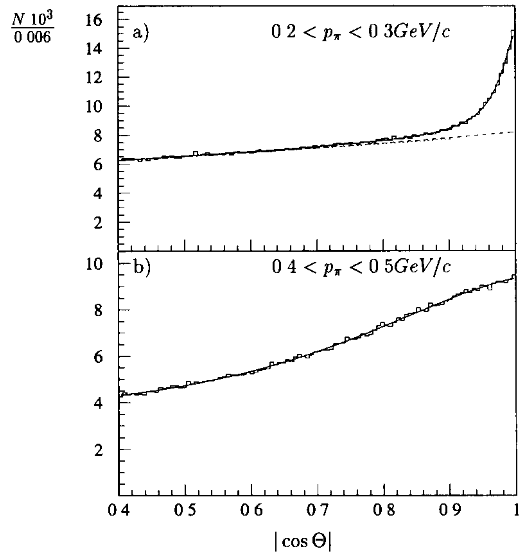

FIG. 12 The $|\cos\theta|$ distribution for data from the ARGUS experiment. In (a) the distribution is shown for the slow pion momentum in the range 0.2 to 0.3 GeV and in (b) for the range 0.4 to 0.5 GeV. From Albrecht *et al.* (1994b).

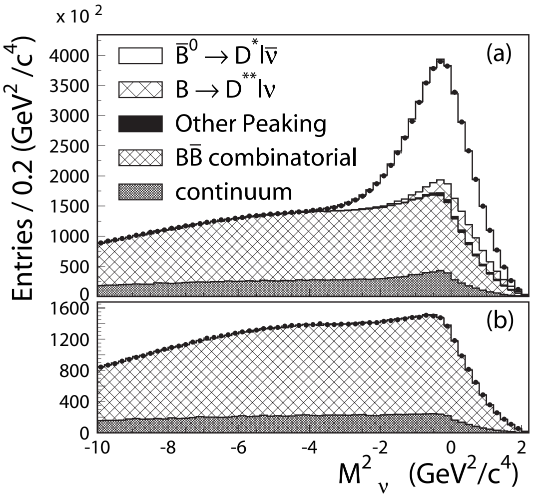

FIG. 13 The distribution of the missing mass squared, M_ν^2 for (a) right sign events and (b) wrong sign events. The wrong sign events show that the simulation of the background shape is good. From Aubert *et al.* (2008b).

$D^{*+}\ell^-\bar{\nu}$ decays followed by $D^{*+} \to D^0\pi^+$ in their data sample.

The next step in this analysis is to reconstruct the $D^0 \to K^-\pi^+$ decay. All reconstructed charged tracks in the event are considered except for the tracks associated with the lepton and slow pion candidates. Pairs of tracks with opposite charge are combined, and the track with the opposite charge with respect to the slow pion candidate is assigned the kaon mass. The kaon candidate is required to satisfy loose kaon identification criteria that retain more than 80% of real kaons while rejecting 95% of pions. The kaon plus pion invariant mass is required to satisfy $1.82 < M_{K\pi} < 1.91$ GeV. Each D^0 candidate is combined with the slow pion and the mass difference $\Delta M = M(K^-\pi^+\pi_s^+) - M(K^-\pi^+)$ is computed. The signal is looked for in the range $142.4 < \Delta M < 149.9$ MeV.

TABLE V Event yields for the inclusive $\bar{B}^0 \to D^{*+}\ell^-\bar{\nu}$ reconstruction and the exclusive analysis where the $D^0 \to K^-\pi^+$ final state is reconstructed in the BABAR analysis (Aubert *et al.*, 2008b) to determine the branching fraction for $D^0 \to K^-\pi^+$ decay. Errors are only statistical.

Source	Inclusive ($\times 10^6$)	Exclusive ($\times 10^4$)
Data	4.4124 ± 0.0021	4.727 ± 0.022
Continuum	0.46 ± 0.0021	0.309 ± 0.017
Combinatorial $B\bar{B}$	1.7817 ± 0.0007	0.819 ± 0.005
Peaking		0.163 ± 0.008
Cabibbo suppressed		0.055 ± 0.001
Signal	2.1706 ± 0.0030	3.381 ± 0.029

Besides the signal events, the exclusive sample contains: continuum, combinatorial $B\bar{B}$, uncorrelated peaking D^{*+}, and Cabibbo suppressed decays. As for the inclusive sample, the continuum background is subtracted using the offresonance sample. The combinatorial $B\bar{B}$ background is determined from simulated $B\bar{B}$ events, normalized in the ΔM sideband $153.5 < \Delta M < 162.5$ MeV. The background from uncorrelated peaking D^{*+} arises from events where the D^{*+} and lepton comes from different B mesons. This background peaks in ΔM but not in M_ν^2. This background is estimated using the sideband in M_ν^2. The backgrounds from Cabibbo suppressed $D^0 \to K^-K^+$ and $D^0 \to \pi^-\pi^+$ decays are subtracted using simulated events.

The mass difference, ΔM, is shown in Fig. 14. The yields for this "exclusive" sample are given in Table V. After background subtraction BABAR finds $N^{\rm excl} = (3.381 \pm 0.029) \times 10^4$ events, where the uncertainty is only statistical. The branching fraction for $D^0 \to K^-\pi^+$ is calculated using

$$\mathcal{B}(D^0 \to K^-\pi^+) = \frac{N^{\rm excl}}{N^{\rm incl}\xi\epsilon_{K\pi}}, \tag{66}$$

where $\epsilon_{K\pi} = (36.96 \pm 0.09)\%$ from simulation and $\xi = 1.033 \pm 0.002$ is the selection bias for the partial reconstruction. The selection bias stems from the fact that the reconstruction efficiency for the slow pion is larger in events where the $D^0 \to K^-\pi^+$ than in generic D decays with more tracks.

BABAR has considered many sources of systematic uncertainties that affects the measured $D^0 \to K^-\pi^+$ branching fraction. The most important uncertainties include: selection bias ($\pm 0.35\%$), non-peaking combi-

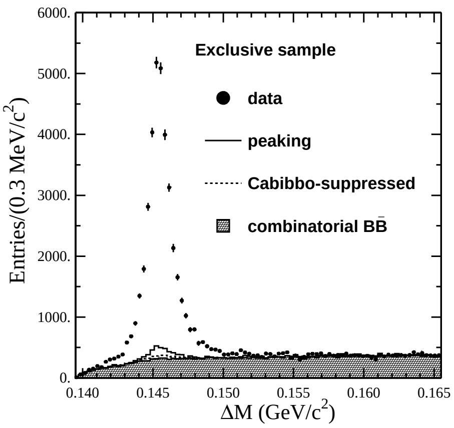

FIG. 14 The ΔM distribution for the reconstructed $D^0 \to K^-\pi^+$ candidates in events with a $\bar{B}^0 \to D^{*+}\ell^-\bar{\nu}$ tag. From Aubert *et al.* (2008b).

natorial background ($\pm 0.89\%$), peaking combinatorial background ($\pm 0.34\%$), tracking efficiency for kaon and pion ($\pm 1.00\%$), K^- identification ($\pm 0.70\%$), D^0 invariant mass selection ($\pm 0.56\%$), and final-state radiation in the $D^0 \to K^-\pi^+$ decay ($\pm 0.50\%$). The total systematic uncertainty is estimated to be $\pm 1.80\%$. BABAR obtains the final result

$$\mathcal{B}(D^0 \to K^-\pi^+) = (4.007 \pm 0.037 \pm 0.072)\%.$$

C. Absolute D hadronic branching fractions using double tags

CLEO-c (Dobbs *et al.*, 2007; He *et al.*, 2005) has used a double tag technique, where by reconstructing one D in the event the presence of an additional $\bar{D}$ in the event is tagged. By determining how often the other D meson can be reconstructed in the event the branching fraction for the D decays can be calculated. This type of analysis was first pioneered by the Mark III collaboration (Adler *et al.*, 1988; Baltrusaitis *et al.*, 1986). The CLEO-c analysis described here uses the same basic idea.

The CLEO-c analysis determines the number of single tags, separately for D and $\bar{D}$ decays,

$$N_i = \epsilon_i \mathcal{B}_i N_{D\bar{D}} \tag{67}$$

and

$$\bar{N}_j = \bar{\epsilon}_j \mathcal{B}_j N_{D\bar{D}} \tag{68}$$

where ϵ_i and $\mathcal{B}_i$ are the efficiencies and branching fractions for mode i and $N_{D\bar{D}}$ is the number of produced $D\bar{D}$ pairs. Though the yields are determined separately for D and $\bar{D}$ decays it is assumed that the branching fractions are the same. Similarly, CLEO-c reconstructs double tags where both D mesons are reconstructed. The number of double tags found is given by

$$N_{ij} = \epsilon_{ij} \mathcal{B}_i \mathcal{B}_j N_{D\bar{D}} \tag{69}$$

where i and j label the D and $\bar{D}$ mode used to reconstruct the event and ϵ_{ij} is the efficiency for reconstructing the final state. Combining the two equations above allow us to solve for $N_{D\bar{D}}$ as

$$N_{D\bar{D}} = \frac{N_i \bar{N}_j}{N_{ij}} \frac{\epsilon_{ij}}{\epsilon_i \bar{\epsilon}_j}. \tag{70}$$

This gives the number of produced $D\bar{D}$ events. Note that many systematic uncertainties cancel in the ratio of efficiencies. This includes for example track finding efficiencies and particle identification that are common to efficiencies in the denominator and numerator. However, systematic uncertainties from, for example, the determination of the yields do not cancel as they are not correlated. In this analysis CLEO-c determines all the single tag and double tag yields in data and the efficiencies from Monte Carlo simulations. The branching fractions and $D\bar{D}$ yields are extracted from a combined fit to all measured data yields and efficiencies.

CLEO-c used three D^0 decay modes ($K^-\pi^+$, $K^-\pi^+\pi^0$, and $K^-\pi^+\pi^-\pi^+$) and six D^+ decay modes ($K^-\pi^+\pi^+$, $K^-\pi^+\pi^+\pi^0$, $K^0_S\pi^+$, $K^0_S\pi^+\pi^0$, $K^0_S\pi^+\pi^-\pi^+$, and $K^-K^+\pi^+$). The π^0 candidates are reconstructed in the $\gamma\gamma$ final state, and the K^0_S candidates are reconstructed in the $\pi^+\pi^-$ final state. Particle identification criteria are applied on kaons and pions (excluding pions in K^0_S candidates). A mode dependent selection criteria on ΔE, the candidate energy minus the beam energy, is applied. To extract the signal yields fits are performed to the $M_{\rm BC}$ distributions for the candidates that pass the selection criteria. The fit is described in Sect. III.A.3. The fit is performed separately for D and $\bar{D}$ candidates in each mode. These fits are shown in Fig. 15 where the D and $\bar{D}$ decays have been combined. Many backgrounds have been considered in this analysis and are discussed in detail in Dobbs *et al.* (2007).

The double tag yields are determined separately for the $45 = 3^2 + 6^2$ double tag modes. The same criteria on ΔE that was applied for the single tags are applied to the double tags. This ensures that the systematic uncertainty from the selection in single and double tag yields cancels in the ratio for the signal mode. To extract the number of double tag candidates a two-dimensional unbinned maximum likelihood fit is performed in the plane of $M_{\rm BC}(D)$ vs. $M_{\rm BC}(\bar{D})$. This is illustrated in Fig. 16. The signal peaks at $M_{\rm BC}(\bar{D}) = M_{\rm BC}(D) = M_D$. Beam energy smearing affects both $M_{\rm BC}(\bar{D})$ and $M_{\rm BC}(D)$ in a correlated fashion to spread the signal along the $M_{\rm BC}(\bar{D})$ vs. $M_{\rm BC}(D)$ diagonal. In addition, the effects of initial state radiation will spread the signal along the same diagonal to larger values of $M_{\rm BC}(\bar{D})$ and $M_{\rm BC}(D)$. If all particles produced in the e^+e^- interaction are used to

TABLE VI Single tag efficiencies, yields from data, and peaking background expectations. The efficiencies include the branching fractions for $\pi^0 \to \gamma\gamma$ and $K^0_S \to \pi^+\pi^-$ decays. The entries in the column labeled "Background" are the number of peaking events in the signal region produced by non-signal events and the associated systematic uncertainty. The quoted yields include these background events. From Dobbs *et al.* (2007).

Single Tag Mode	Efficiency (%)	Data Yield	Background
$D^0 \to K^-\pi^+$	64.18 ± 0.19	$25,760 \pm 165$	96 ± 27
$\bar{D}^0 \to K^+\pi^-$	64.90 ± 0.19	$26,258 \pm 166$	96 ± 27
$D^0 \to K^-\pi^+\pi^0$	33.46 ± 0.12	$50,276 \pm 258$	114 ± 10
$\bar{D}^0 \to K^+\pi^-\pi^0$	33.78 ± 0.12	$50,537 \pm 259$	114 ± 10
$D^0 \to K^-\pi^+\pi^+\pi^-$	45.27 ± 0.16	$39,709 \pm 216$	889 ± 135
$\bar{D}^0 \to K^+\pi^-\pi^-\pi^+$	45.81 ± 0.16	$39,606 \pm 216$	889 ± 135
$D^+ \to K^-\pi^+\pi^+$	54.07 ± 0.18	$40,248 \pm 208$	< 1
$D^- \to K^+\pi^-\pi^-$	54.18 ± 0.18	$40,734 \pm 209$	< 1
$D^+ \to K^-\pi^+\pi^+\pi^0$	26.23 ± 0.18	$12,844 \pm 153$	< 1
$D^- \to K^+\pi^-\pi^-\pi^0$	26.58 ± 0.18	$12,756 \pm 153$	< 1
$D^+ \to K^0_S\pi^+$	45.98 ± 0.18	$5,789 \pm 82$	81 ± 22
$D^- \to K^0_S\pi^-$	46.07 ± 0.18	$5,868 \pm 82$	81 ± 22
$D^+ \to K^0_S\pi^+\pi^0$	23.06 ± 0.19	$13,275 \pm 157$	113 ± 53
$D^- \to K^0_S\pi^-\pi^0$	22.93 ± 0.19	$13,126 \pm 155$	113 ± 53
$D^+ \to K^0_S\pi^+\pi^+\pi^-$	31.70 ± 0.24	$8,275 \pm 134$	173 ± 83
$D^- \to K^0_S\pi^-\pi^-\pi^+$	31.81 ± 0.24	$8,285 \pm 134$	173 ± 83
$D^+ \to K^+K^-\pi^+$	45.86 ± 0.36	$3,519 \pm 73$	< 1
$D^- \to K^-K^+\pi^-$	45.57 ± 0.35	$3,501 \pm 73$	< 1

form the D and $\bar{D}$ candidate, but the particles are either from continuum, or from a $D\bar{D}$ event but not assigned to the right D candidate (mispartitioning) the reconstructed $M_{\rm BC}(\bar{D})$ and $M_{\rm BC}(D)$ will lie on the diagonal. There are also events in which one of the two D candidates are misreconstructed. These events form horizontal and vertical bands in $M_{\rm BC}(\bar{D})$ vs. $M_{\rm BC}(D)$.

The combined double tag data with the sum of the fits are shown in Fig. 17 for the $D^0\bar{D}^0$ and D^+D^- modes. There are a total of $13,591 \pm 119$ $D^0\bar{D}^0$ double tags and $8,870 \pm 96$ D^+D^- double tags. For most of the modes studied in this analysis the statistical uncertainty on the measured branching fraction is limited by the number of double tags. For the D^0 modes this statistical uncertainty is $\pm 0.88\%$ and for the D^+ modes this is $\pm 1.1\%$.

A detailed study of systematic uncertainties has been performed. The signal shape systematic uncertainty for double tags is taken to be $\pm 0.2\%$, while for the single tags a range of systematic uncertainties from $\pm 0.3\%$, for $D^0 \to K^-\pi^+$, to $\pm 1.3\%$, for $D^+ \to K^-\pi^+\pi^+\pi^0$, are assigned. These systematic uncertainties were assigned based on trying alternative signal shape parameterizations in the fit. For the neutral D decays there is an uncertainty due to "double Cabibbo suppressed interference". The source of this uncertainty comes from the interference between signal decays and decays where both the D^0 and the $\bar{D}^0$ decays via doubly Cabibbo suppressed decays. The relative size of this interference is $\Delta \approx 2R_{\rm ws}\cos 2\delta$ where $R_{\rm ws}$ is the ratio of the doubly Cabibbo suppressed rate to the Cabibbo favored rate and δ is the relative strong phase between the doubly Cabibbo suppressed amplitude and the Cabibbo favored amplitude. CLEO-c assigns a systematic uncertainty of $\pm 0.8\%$ for this effect. This covers the range of allowed values of Δ for $R_{\rm ws} = 0.004$ and incorporates the uncertainties in δ.

For the charged track reconstruction CLEO-c assigns $\pm 0.3\%$ uncertainty and for charged kaons an additional $\pm 0.6\%$ added in quadrature. In addition CLEO-c assigns a $\pm 1.8\%$ uncertainty on the K^0_S reconstruction in the $\pi^+\pi^-$ final state and a $\pm 2.0\%$ uncertainty for the π^0 reconstruction in the $\gamma\gamma$ final state. These systematic uncertainties were discussed in Sect. III.A.4. Kaons and pions, except for pions in the reconstruction of $K^0_S \to \pi^+\pi^-$ candidates, are required to satisfy particle identification criteria. Uncertainties of $\pm 0.25\%$ and $\pm 0.3\%$ respectively for pions and kaons are assigned for the particle identification.

Multibody final states suffer from an uncertainty in the simulation of the efficiency due to imperfect modeling of the resonant substructure. The uncertainties associated with the three- or four-body final states were estimated by comparing the kinematic distributions in these decays between data and Monte Carlo simulations. Many three-body final states have been studied using Dalitz plot fits and are well described in the Monte Carlo (Lange, 2001). The Dalitz plot analyses are described in Sect. IX.

Last, final-state radiation, as discussed in Sect. III.E, was considered. CLEO-c compared the signal efficiencies with and without FSR included in the Monte Carlo simulation. A systematic uncertainty of $\pm 30\%$ of the change due to not including final-state radiation was assigned. This gives the largest uncertainty of about 0.9% in the $D^0 \to K^-\pi^+$ mode.

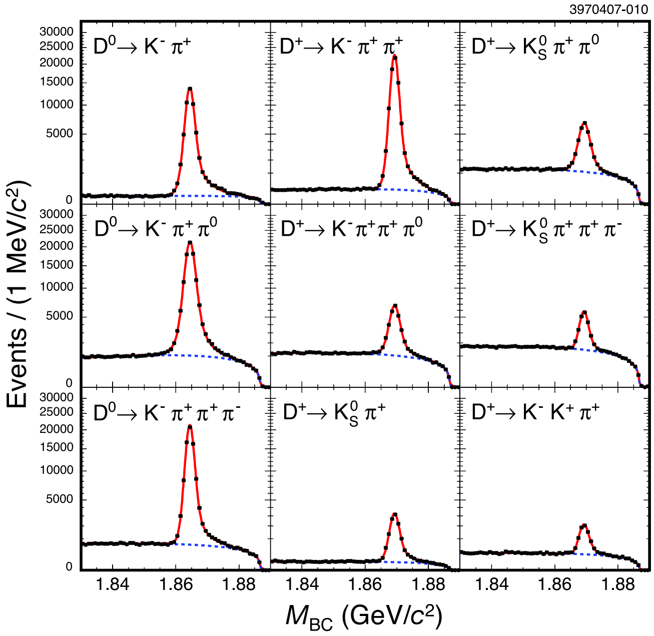

FIG. 15 Distributions of measured $M_{\rm BC}(D)$ and $M_{\rm BC}(\bar{D})$ values for single tag D^0 and D^+ candidates with D and $\bar{D}$ candidates combined in each plot. The points are data and the curves are fits to the data. In each plot, the dashed curve shows the background contributions and the solid curve shows the sum of the background and signal function. The number of events is shown on a square-root scale. From Dobbs *et al.* (2007).

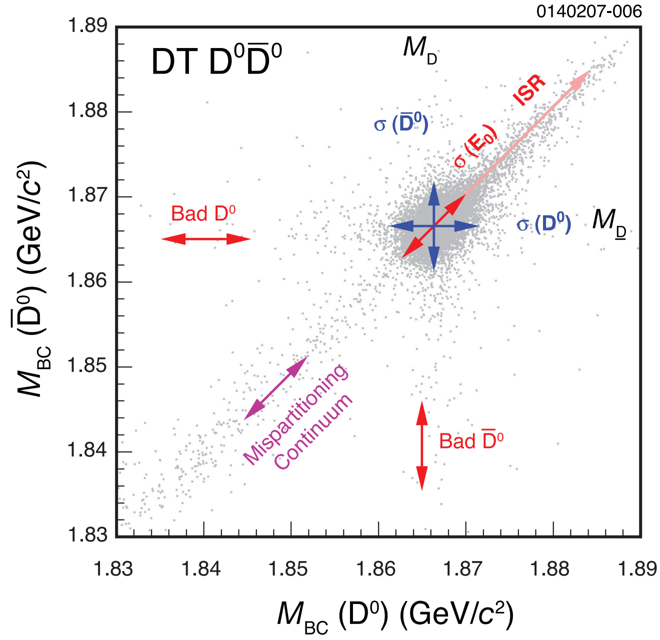

FIG. 16 Scatter plot of $M_{\rm BC}(\bar{D})$ *vs.* $M_{\rm BC}(D)$ for $D^0\bar{D}^0$ double tag candidates. Signal candidates are concentrated at $M_{\rm BC}(\bar{D}) = M_{\rm BC}(D) = M_D$. The signal shape and different background contributions are discussed in the text. From Dobbs *et al.* (2007).

The signal yields for single and double tags and the efficiencies determined from Monte Carlo simulations are combined in a χ^2 fit (Sun, 2006). This fit includes both statistical and systematic uncertainties. The fit extracts the branching fractions for the nine D decay modes studied in this analysis and the produced number of $D^0\bar{D}^0$ and D^+D^- pairs. The result of this fit is shown in Table VII. The χ^2 of the fit is 39.2 for 52 degrees of freedom, corresponding to a confidence level of 98%. The χ^2 includes systematic uncertainties.

The CLEO-c analysis obtains the main branching fraction results

$$\mathcal{B}(D^0 \to K^-\pi^+) = (3.891 \pm 0.035 \pm 0.059 \pm 0.035)\%, \quad (71)$$

$$\mathcal{B}(D^+ \to K^-\pi^+\pi^+) = (9.15 \pm 0.10 \pm 0.16 \pm 0.07)\%, \quad (72)$$

where the errors are statistical, systematic, and from final-state radiation respectively. In addition the $D\bar{D}$ yields determined from this analysis are used to normalize many other CLEO-c measurements. The cross-sections for $D\bar{D}$ production are discussed in Sect. III.A.

D. Summary of $D^0 \to K^-\pi^+$

The absolute branching fraction for $D^0 \to K^-\pi^+$ has been measured by many different experiments, using different techniques as discussed in this Section. The different measurements are summarized in Table VIII. The two most recent, and most precise, measurements are from CLEO-c and BABAR. They use very different techniques but find branching fractions that are in good agreement. We adopt the PDG average

$$\mathcal{B}(D^0 \to K^-\pi^+) = 3.89 \pm 0.05. \quad (73)$$

These measurements are now limited by systematic uncertainties. There are many sources of systematic uncertainties that contribute. Some of these can be improved with additional data. Both CLEO-c and BABAR can increase the data samples used in their analyses.

E. Modes with K^0_L or K^0_S in the final states

It has commonly been assumed that $\Gamma(D \to K^0_S X) = \Gamma(D \to K^0_L X)$. However, as pointed out by Bigi and Yamamoto (Bigi and Yamamoto, 1995) this is not generally true as for many D decays there are contributions from Cabibbo favored and Cabibbo suppressed decays that interfere and produce different rates to final states with K^0_S versus K^0_L. As an example consider $D^0 \to K^0_{S,L}\pi^0$. Contributions to these final states involve the Cabibbo favored decay $D^0 \to \bar{K}^0\pi^0$ as well as the doubly Cabibbo suppressed decay $D^0 \to K^0\pi^0$. However, we don't observe the K^0 and the $\bar{K}^0$ but rather the K^0_S and the K^0_L. As the amplitudes for $D^0 \to \bar{K}^0\pi^0$ and $D^0 \to K^0\pi^0$

TABLE VII Fitted branching fractions and $D\bar{D}$ pair yields. For $N_{D^0\bar{D}^0}$ and $N_{D^+D^-}$, uncertainties are statistical and systematic, respectively. For branching fractions and ratios, the systematic uncertainties are divided into the contribution from FSR (third uncertainty) and all others combined (second uncertainty). The column of fractional systematic errors combines all systematic errors, including FSR. The last column, $\Delta_{\rm FSR}$, is the relative shift in the fit results when FSR is not included in the Monte Carlo simulations used to determine efficiencies. From Dobbs *et al.* (2007).

Parameter	Fitted Value	Fractional Error		$\Delta_{\rm FSR}$
		Stat.(%)	Syst.(%)	(%)
$N_{D^0\bar{D}^0}$	$(1.031 \pm 0.008 \pm 0.013) \times 10^6$	0.8	1.3	+0.1
$\mathcal{B}(D^0 \to K^-\pi^+)$	$(3.891 \pm 0.035 \pm 0.059 \pm 0.035)\%$	0.9	1.8	−3.0
$\mathcal{B}(D^0 \to K^-\pi^+\pi^0)$	$(14.57 \pm 0.12 \pm 0.38 \pm 0.05)\%$	0.8	2.7	−1.1
$\mathcal{B}(D^0 \to K^-\pi^+\pi^+\pi^-)$	$(8.30 \pm 0.07 \pm 0.19 \pm 0.07)\%$	0.9	2.4	−2.4
$N_{D^+D^-}$	$(0.819 \pm 0.008 \pm 0.010) \times 10^6$	1.0	1.2	+0.1
$\mathcal{B}(D^+ \to K^-\pi^+\pi^+)$	$(9.15 \pm 0.10 \pm 0.16 \pm 0.07)\%$	1.1	1.9	−2.3
$\mathcal{B}(D^+ \to K^-\pi^+\pi^+\pi^0)$	$(5.98 \pm 0.08 \pm 0.16 \pm 0.02)\%$	1.3	2.8	−1.0
$\mathcal{B}(D^+ \to K^0_S\pi^+)$	$(1.526 \pm 0.022 \pm 0.037 \pm 0.009)\%$	1.4	2.5	−1.8
$\mathcal{B}(D^+ \to K^0_S\pi^+\pi^0)$	$(6.99 \pm 0.09 \pm 0.25 \pm 0.01)\%$	1.3	3.5	−0.4
$\mathcal{B}(D^+ \to K^0_S\pi^+\pi^+\pi^-)$	$(3.122 \pm 0.046 \pm 0.094 \pm 0.019)\%$	1.5	3.0	−1.9
$\mathcal{B}(D^+ \to K^+K^-\pi^+)$	$(0.935 \pm 0.017 \pm 0.024 \pm 0.003)\%$	1.8	2.6	−1.2
$\mathcal{B}(D^0 \to K^-\pi^+\pi^0)/\mathcal{B}(K^-\pi^+)$	$3.744 \pm 0.022 \pm 0.093 \pm 0.021$	0.6	2.6	+1.9
$\mathcal{B}(D^0 \to K^-\pi^+\pi^+\pi^-)/\mathcal{B}(K^-\pi^+)$	$2.133 \pm 0.013 \pm 0.037 \pm 0.002$	0.6	1.7	+0.5
$\mathcal{B}(D^+ \to K^-\pi^+\pi^+\pi^0)/\mathcal{B}(K^-\pi^+\pi^+)$	$0.654 \pm 0.006 \pm 0.018 \pm 0.003$	0.9	2.7	+1.4
$\mathcal{B}(D^+ \to K^0_S\pi^+)/\mathcal{B}(K^-\pi^+\pi^+)$	$0.1668 \pm 0.0018 \pm 0.0038 \pm 0.0003$	1.1	2.3	+0.5
$\mathcal{B}(D^+ \to K^0_S\pi^+\pi^0)/\mathcal{B}(K^-\pi^+\pi^+)$	$0.764 \pm 0.007 \pm 0.027 \pm 0.005$	0.9	3.5	+2.0
$\mathcal{B}(D^+ \to K^0_S\pi^+\pi^+\pi^-)/\mathcal{B}(K^-\pi^+\pi^+)$	$0.3414 \pm 0.0039 \pm 0.0093 \pm 0.0004$	1.1	2.7	+0.4
$\mathcal{B}(D^+ \to K^+K^-\pi^+)/\mathcal{B}(K^-\pi^+\pi^+)$	$0.1022 \pm 0.0015 \pm 0.0022 \pm 0.0004$	1.5	2.2	+1.1

TABLE VIII Summary of measurements of the $D^0 \to K^-\pi^+$ branching fraction measurements. Only the top six measurements are used in the average by the PDG.

Experiment	Ref.	$\mathcal{B}(D^0 \to K^-\pi^+)$ (%)
CLEO-c	Dobbs *et al.* (2007)	$3.891 \pm 0.035 \pm 0.059 \pm 0.035$
BABAR	Aubert *et al.* (2008b)	$4.007 \pm 0.037 \pm 0.072$
CLEO II[a]	Artuso *et al.* (1998)	$3.82 \pm 0.07 \pm 0.12$
ALEPH	Barate *et al.* (1997)	$3.90 \pm 0.09 \pm 0.12$
ARGUS	Albrecht *et al.* (1994a)	$3.41 \pm 0.12 \pm 0.28$
ALEPH	Decamp *et al.* (1991)	$3.62 \pm 0.34 \pm 0.44$
CLEO-c	He *et al.* (2005)	$3.91 \pm 0.08 \pm 0.09$
CLEO II	Artuso *et al.* (1998)	$3.81 \pm 0.15 \pm 0.16$
CLEO II	Coan *et al.* (1998)	$3.69 \pm 0.11 \pm 0.16$
ARGUS	Albrecht *et al.* (1994b)	$4.5 \pm 0.6 \pm 0.4$
CLEO II	Akerib *et al.* (1993)	$3.95 \pm 0.08 \pm 0.17$
HRS	Abachi *et al.* (1988)	$4.5 \pm 0.8 \pm 0.5$
MARK III	Adler *et al.* (1988)	$4.2 \pm 0.4 \pm 0.4$
MARK II	Schindler *et al.* (1981)	4.1 ± 0.6
LGW	Peruzzi *et al.* (1977)	4.3 ± 1.0
Average		3.89 ± 0.05

[a]This is an average of the results in Akerib *et al.* (1993); Aubert *et al.* (2008b); Coan *et al.* (1998).

interfere constructively to form the K^0_S final state, and destructively to form a K^0_L, we see a rate asymmetry between the K^0_L and K^0_S final states. Using $SU(3)_F$, and in particular the U-spin subgroup, one can predict the asymmetry in $D^0 \to K^0_{S,L}\pi^0$

$$R(D^0) = \frac{\Gamma(D^0 \to K^0_S\pi^0) - \Gamma(D^0 \to K^0_L\pi^0)}{\Gamma(D^0 \to K^0_S\pi^0) + \Gamma(D^0 \to K^0_L\pi^0)} \tag{74}$$

$$\approx 2\tan^2\theta_C = 0.109 \pm 0.001. \tag{75}$$

For the corresponding charged D mode, $D^+ \to K^0_{S,L}\pi^+$ a similar prediction based on $SU(3)$ is not possible. Rather one has to rely on calculations based on factorization or other means of determination of decay amplitudes. For example, flavor-flow diagram approach gives (Bhat-

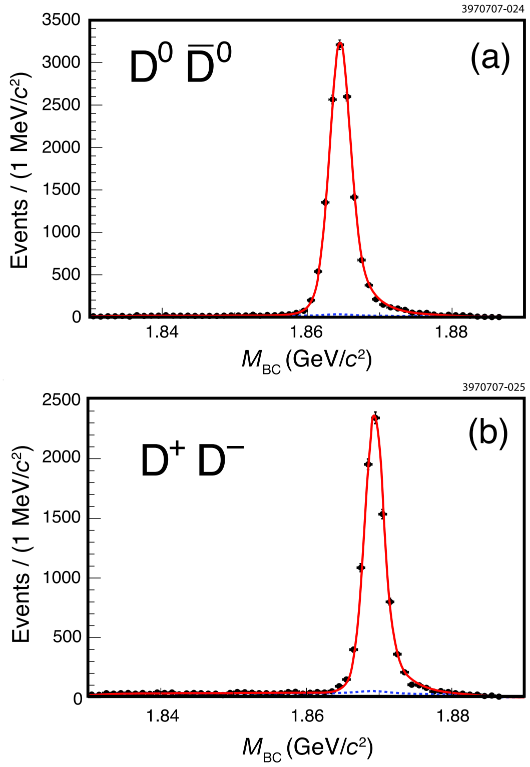

FIG. 17 Projections of the sum of the double tag candidate mass on the $M_{\rm BC}(D)$ axis for (a) the nine $D^0\bar{D}^0$ double tag modes and (b) the 36 D^+D^- double tag modes. The points show the data and the curves the projection of the fit results. The dashed lines shows the background contributions and the solid line the signal shape plus the background. From Dobbs *et al.* (2007).

tacharya and Rosner, 2008)

$$R(D^+) = 2\tan^2\theta_C \ \mathrm{Re}\,\frac{C+A}{T+C} = -0.006^{+0.033}_{-0.028}. \quad (76)$$

We shall discuss the prediction of this ratio in factorization below.

Experimentally these channels are challenging as they involve final states with a K^0_L. CLEO-c has studied these modes (He *et al.*, 2008). They infer the presence of a K^0_L using a missing mass technique after vetoing events with a K^0_S decaying to either a $\pi^+\pi^-$ or $\pi^0\pi^0$ pair if there are tracks or π^0 candidates reconstructed in the event.

In addition to the challenge with the K^0_L final state, these decays are CP eigenstates and at the $\psi(3770)$ where CLEO-c recorded the data for their analysis we need to disentangle the effects from quantum coherence with the rate asymmetry we are interested in here. The effect of the coherently produced $D^0\bar{D}^0$ pairs at the $\psi(3770)$ was discussed in Section III.A.1.

CLEO-c has studied both $D^+\to K^0_{S,L}\pi^+$ and $D^0\to K^0_{S,L}\pi^0$. First the D^+ analysis is discussed as it does not involve the complication of quantum coherence. The branching fraction for $D^+\to K^0_S\pi^+$ is taken from Dobbs *et al.* (2007). In this analysis only the branching fraction for $D^+\to K^0_L\pi^+$ is directly measured. CLEO-c uses a tag technique, in which one charged D is fully reconstructed. Six different charged D tags are used, these modes are the same as in Dobbs *et al.* (2007) described in Sect. V.C. The tag D^- is combined with a π^+ and events consistent with a K^0_S are vetoed. An event is vetoed if an additional charged track or neutral pion, reconstructed in the $\pi^0\to\gamma\gamma$ channel, was found. This veto removes about 90% of the K^0_S background as well as many other backgrounds while retaining 98% efficiency for signal events.

Figure 18 shows the invariant mass distribution recoiling against the tag D and charged pion. The signal peaks at a missing mass square of about 0.25 GeV^2 corresponding to the K^0_L. From the fit to the data CLEO-c extracts a signal of $2,023\pm 54$ events. With 165×10^3 charged D tags and an efficiency of 81.6% for finding the pion the branching fraction is calculated to be

$$\mathcal{B}(D^+\to K^0_L\pi^+) = (1.460\pm 0.040\pm 0.035\pm 0.0005)\%, \quad (77)$$

where the errors are statistical, systematic, and from the branching fraction for $D^+\to K^0_S\pi^+$. The largest contributions to the systematic uncertainty come from the extra track and π^0 veto ($\pm 1.1\%$) and the signal peak width ($\pm 1.6\%$). The sensitivity to the peak width comes from the $D^+\to\eta\pi^+$ events just on the high side of the signal peak as seen in Fig. 18.

Combining the $D^+\to K^0_L\pi^+$ branching fraction with the $D^+\to K^0_S\pi^+$ measured in Dobbs *et al.* (2007), CLEO-c obtains the asymmetry

$$R(D^+) = 0.022\pm 0.016\pm 0.018. \quad (78)$$

There is no evidence for a significant asymmetry in the $D^+\to K^0_{S,L}\pi^+$ mode. Predictions for the asymmetry in charged D decays is more involved than for neutral D decays. D.-N. Gao, based on factorization, predicts (Gao, 2007) this asymmetry to be in the range 0.035 to 0.044, which is consistent with the observed asymmetry.

For the $D^0\to K^0_{S,L}\pi^0$ analysis the effects of the quantum coherence has to be accounted for. In addition, experimentally this mode is more challenging as the resolution for a π^0 is worse than for a charged pion. CLEO-c first measures the branching fraction for $D^0\to K^0_S\pi^0$ without using a $\bar{D}^0$ tag. Next the "branching fraction" for $D^0\to K^0_S\pi^0$ is measured in a tagged analysis where the $\bar{D}^0$ is reconstructed in three modes. Due to the coherence the "branching fraction" measured in the tagged analysis is $\mathcal{B}(D^0\to K^0_S\pi^0)(1-C_f)$, where $C_f = (R_f z_f + y)/(1+R_{WS,f})$, as described in Sect. III.A.1. For the three tag modes C_f can now be calculated. Finally, the "branching fraction" for $D^0\to K^0_L\pi^0$ is measured using the same three tag modes, each of the tag modes give us $\mathcal{B}(D^0\to K^0_L\pi^0)(1+C_f)$, and using the measured values of C_f from above the branching fraction $\mathcal{B}(D^0\to K^0_L\pi^0)$ can be determined.

The K^0_S is reconstructed in the $K^0_S\to\pi^+\pi^-$ final state. There is a background from $D^0\to\pi^+\pi^-\pi^0$. This background is subtracted using the K^0_S mass sideband. The

TABLE IX The efficiency is for the reconstruction of the $K^0_S\pi^0$ after the D tag has been found, the tag yield is the number of D tags reconstructed, the signal yield is the number of $D^0 \to K^0_S\pi^0$ candidates are reconstructed against the tag D, and the tag bias is a correction due to the fact that it is easier to reconstruct the tag in events with the signal than in generic D decays. From He *et al.* (2008).

Tag mode	$K^+\pi^-$	$K^+\pi^-\pi^0$	$K^+\pi^-\pi^+\pi^-$
Efficiency (%)	31.74	31.29	29.97
Tag yield	47,440	63,913	71,040
Signal yield	155	203	256
Tag bias correction (%)	1.000	1.014	1.033
$\mathcal{B}(D^0 \to K^0_S\pi^0)(1-C_f)$	1.03 ± 0.09	1.00 ± 0.09	1.16 ± 0.08

TABLE X The efficiency is for the reconstruction of the $K^0_L\pi^0$, including the K^0_S veto, after the D tag has been found, the tag yield is the number of D tags reconstructed, the signal yield is the number of $D^0 \to K^0_S\pi^0$ candidates are reconstructed against the tag D, and the tag bias is a correction due to the fact that it is easier to reconstruct the tag in events with the signal than in generic D decays. From He *et al.* (2008).

Tag mode	$K^+\pi^-$	$K^+\pi^-\pi^0$	$K^+\pi^-\pi^+\pi^-$
Efficiency (%)	55.21	52.72	49.88
Tag yield	47,440	64,280	71,040
Signal yield	334.8	414.5	466.5
Tag bias correction (%)	1.000	1.037	1.057
$\mathcal{B}(D^0 \to K^0_L\pi^0)(1+C_f)$	1.28 ± 0.08	1.03 ± 0.06	1.12 ± 0.06

signal yield in this analysis is extracted using a cut-and-count technique. CLEO-c looks in a 3 standard deviation window around the nominal values for the beam-constrained mass and ΔE. A sideband in ΔE is used to subtract the combinatorial backgrounds. The number of $D^0\bar{D}^0$ pairs in the data sample is taken from Dobbs *et al.* (2007). CLEO-c obtains the branching fraction

$$\mathcal{B}(D^0 \to K^0_S\pi^0) = (1.240 \pm 0.017 \pm 0.031 \pm 0.047)\% \quad (79)$$

where the last error is due to the π^0 reconstruction efficiency. In the asymmetry $R(D^0)$ this uncertainty will cancel.

Next the "branching fraction" for $\mathcal{B}(D^0 \to K^0_S\pi^0)$ is measured with a $\bar{D}^0$ tag. The three tags modes used are $\bar{D}^0 \to K^+\pi^-$, $\bar{D}^0 \to K^+\pi^-\pi^0$, and $\bar{D}^0 \to K^+\pi^-\pi^+\pi^-$. The results for the tagged analysis is summarized in Table IX. Similarly the tagged "branching fraction" for $D^0 \to K^0_L\pi^0$ was studied using a missing mass technique where the event was fully reconstructed except for the K^0_L. The results are summarized in Table X.

Combining these measurements CLEO-c finds an average asymmetry for the neutral D decays

$$R(D^0) = 0.108 \pm 0.025 \pm 0.024, \quad (80)$$

which is in good agreement with the prediction.

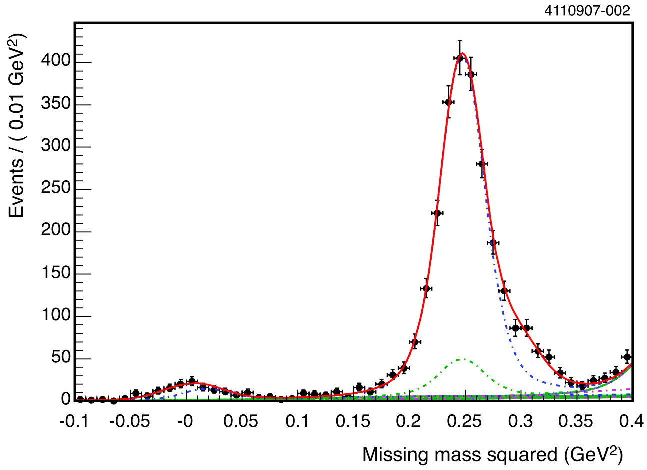

FIG. 18 Missing mass squared distribution for all six tag modes for $D^+ \to X\pi^+$. Events with extra tracks or π^0 candidates have been removed. From He *et al.* (2008).

F. Final states with three kaons

Final states with three kaons are not generally Cabibbo suppressed, but the smaller branching fractions for these decays are due to the small phase space available in these decays. These decays are summarized in Table XI. The decay $D^+ \to K^+K^-K^+$ is Cabibbo suppressed and is included in Sect. VII.D. The limited phase space available has been taken advantage of to measure the D^0 mass (Cawlfield *et al.*, 2007).

G. Summary of Cabibbo favored D^0 and D^+ decays

In Table XII a summary of the Cabibbo favored D^0 and D^+ decays are given. Assuming that $\Gamma(D \to K^0_S X) = \Gamma(D \to K^0_L X)$ for modes where the final states with a K^0_L has not been explicitly measured the Cabibbo favored branching fractions add up to $(50.8 \pm 1.4)\%$ for D^0 meson decays and $(38.3 \pm 1.1)\%$ for D^+ decays. The mode $D^0 \to K^-\pi^+\pi^0\pi^0$ is not included here. An early measurement by MARK III (Adler *et al.*, 1988) reported a large branching fraction of 15±5%. The PDG is not using this result anymore in their summary and there have not been any newer measurements. However, CLEO-c has used this mode for tagging D^0 decays in their studies of semileptonic decays (Ge *et al.*, 2009b). They provide enough information that the branching fraction $\mathcal{B}(D^0 \to K^-\pi^+\pi^0\pi^0) = (7.90 \pm 0.14)\%$ can be calculated. The error quoted only includes the statistical error

TABLE XI Summary of final states with three kaons. If there is more than one measurement we quote here the PDG average.

Mode	Ref.	$\mathcal{B}$ (10^{-3})
$D^0 \to K_S^0 K^+ K^-$	BABAR (Aubert *et al.*, 2005a)	$4.72 \pm 0.03 \pm 0.15 \pm 0.27$
$D^0 \to K_S^0 K_S^0 K_S^0$	PDG Avg. (Amsler *et al.*, 2008)	$0.96 \pm 0.12 \pm 0.05$
$D^0 \to K^+ K^- K^- \pi^+$	PDG Avg. (Amsler *et al.*, 2008)	$0.221 \pm 0.033 \pm 0.009$
$D^0 \to K_S^0 K_S^0 K^\mp \pi^\pm$	FOCUS (Link *et al.*, 2005b)	$0.63 \pm 0.11 \pm 0.06 \pm 0.04$

TABLE XII Summary of branching fractions for Cabibbo favored D^0 and D^+ decays. Averages taken from Amsler *et al.* (2008)

Mode	Branching Fraction
$D^0 \to K^-\pi^+$	$(3.89 \pm 0.05)\%$
$D^0 \to K_S^0\pi^0$	$(1.22 \pm 0.06)\%$
$D^0 \to K_L^0\pi^0$	$(1.00 \pm 0.07)\%$
$D^0 \to K_S^0\pi^+\pi^-$	$(2.99 \pm 0.17)\%$
$D^0 \to K^-\pi^+\pi^0$	$(13.9 \pm 0.5)\%$
$D^0 \to K^-\pi^+\pi^+\pi^-$	$(8.10 \pm 0.20)\%$
$D^0 \to K_S^0\pi^+\pi^-\pi^0$	$(5.4 \pm 0.6)\%$
$D^0 \to K^-\pi^+\pi^+\pi^-\pi^0$	$(4.2 \pm 0.4)\%$
$D^0 \to K_S^0\eta\pi^0$	$(5.6 \pm 1.2) \times 10^{-3}$
$D^0 \to K_S^0\pi^+\pi^+\pi^-\pi^-$	$(2.84 \pm 0.31) \times 10^{-3}$
$D^0 \to K^-\pi^+\pi^+\pi^+\pi^-\pi^-$	$(2.2 \pm 0.6) \times 10^{-4}$
$D^+ \to K_S^0\pi^+$	$(1.45 \pm 0.04)\%$
$D^+ \to K_L^0\pi^+$	$(1.46 \pm 0.05)\%$
$D^+ \to K^-\pi^+\pi^+$	$(9.22 \pm 0.21)\%$
$D^+ \to K_S^0\pi^+\pi^0$	$(6.8 \pm 0.5)\%$
$D^+ \to K^-\pi^+\pi^+\pi^0$	$(6.00 \pm 0.20)\%$
$D^+ \to K_S^0\pi^+\pi^+\pi^-$	$(3.02 \pm 0.12)\%$
$D^+ \to K^-\pi^+\pi^+\pi^+\pi^-$	$(5.6 \pm 0.5) \times 10^{-3}$

and the uncertainty from the $D^0 \to K^-\pi^+$ normalization mode. In particular experimental systematic uncertainties are not included and hence this is not included in the summary. But it does show that there is a substantial branching fraction to the $D^0 \to K^-\pi^+\pi^0\pi^0$ final state.

VI. CABIBBO FAVORED D_s DECAYS

The determination of the absolute branching fraction scale for D_s decays has been a challenge since the discovery of the D_s (Chen *et al.*, 1983). Until recently the focus has been on the final state $D_s^+ \to \phi\pi^+$, followed by $\phi \to K^-K^+$. This final state is easy to reconstruct with small backgrounds; the ϕ is a narrow resonance and the final state consists of all charged particles. However, this final state is not as "clean" as one would wish. There are non-ϕ contributions, such as the $f_0(980)$, to the K^+K^- mass near the ϕ mass that pollute the $D_s^+ \to \phi\pi^+$ signal. Of course, these decays are still real $D_s^+ \to K^+K^-\pi^-$ decays. This is discussed further in Sect. IX.A.12 on Dalitz plot analysis of $D_s^+ \to K^+K^-\pi^+$.

As measurements have gotten more precise the definition of what is measured has had to be made more precise. One of the most recent measurements by CLEO-c (Alexander *et al.*, 2008) does not quote a $D_s^+ \to \phi\pi^+$ branching fraction, but rather partial branching fractions in K^+K^- invariant mass regions near the ϕ. The first attempts at establishing the branching fraction scale for D_s^+ decays were based on model-dependent assumption about equal partial widths for semileptonic decays of the D_s^+ and D^+.

This Section will discuss the different approaches used to measure the D_s absolute branching fractions. The early measurements are described very briefly and the more recent, and precise, measurements are described in more detail.

A. Model-dependent approaches

The NA14 experiment (Alvarez *et al.*, 1990) used the Lund model to estimate the ratio of D_s^+ to D^+ production cross-sections, which allowed them to determine the $D_s^+ \to \phi\pi^+$ branching fractions. The CLEO collaboration (Chen *et al.*, 1989) used estimates of the D_s^+ production rate to determine the branching fraction for $D_s^+ \to \phi\pi^+$.

Several experiments, CLEO (Alexander *et al.*, 1990a; Butler *et al.*, 1994), E687 (Frabetti *et al.*, 1993), ARGUS (Albrecht *et al.*, 1991), and E691 (Anjos *et al.*, 1990) measured the ratio

$$\frac{\mathcal{B}(D_s^+ \to \phi\ell^+\nu_\ell)}{\mathcal{B}(D_s^+ \to \phi\pi^+)}. \tag{81}$$

Using theoretical predictions for the ratio

$$\frac{\Gamma(D_s^+ \to \phi\ell^+\nu_\ell)}{\Gamma(D^+ \to \bar{K}^{*0}\ell^+\nu_\ell)} \tag{82}$$

and the measured D_s^+ and D^+ lifetimes these experiments determined the branching fraction for $D_s^+ \to \phi\pi^+$. Comparing these results require some care as slightly different assumptions were made about the ratio of the semileptonic rates. Also, combining these measurements require care as there are strong systematic correlations between the measurements due to the common, or at least similar, assumptions about partial rates for the semileptonic decays.

All of these measurements use model-dependent assumptions and have associated systematic uncertainties that are hard to quantify. These model dependent measurements are typically no longer used in averages, e.g. by the particle data group (Amsler *et al.*, 2008). With larger data samples model independent measurements became possible.

B. The branching ratio for $D_s \to \phi\pi$ from $B \to D_s^* D^*$

The first statistically significant, see Sect. VI.D, model-independent measurement of the absolute D_s^+ branching fraction was performed by CLEO (Artuso *et al.*, 1996). They used 2.5 fb^{-1} of e^+e^- data collected at the $\Upsilon(4S)$ resonance, corresponding to 2.7×10^6 $B\bar{B}$ pairs, to study $B \to D_s^* D^*$ decays. The same technique has been used by BABAR (Aubert *et al.*, 2005c). They have analyzed a sample with $(123\pm1)\times10^6$ $B\bar{B}$ pairs.

In these analyses the decay $B \to D_s^* D^*$ is reconstructed in two different ways. First, the D_s^* is fully reconstructed using $D_s^{*+} \to D_s^+\gamma$ followed by $D_s^+ \to \phi\pi^+$ and the D^* is partially reconstructed using the slow pion from the D^* decay. In the second method the D^* is fully reconstructed and the $D_s^{*+} \to D_s^+\gamma$ is only identified through the presence of the γ. From this study BABAR quotes $\mathcal{B}(D_s^+ \to \phi\pi^+) = (4.81\pm0.52\pm0.38)\%$ and CLEO $\mathcal{B}(D_s^+ \to \phi\pi^+) = (3.59\pm0.77\pm0.48)\%$.

More recently, BABAR (Aubert *et al.*, 2006c) has presented results based on 210 fb^{-1} of data where they use a tag technique in which one B meson is fully reconstructed. In events with one fully reconstructed B meson candidate BABAR reconstructs one additional $D^{(*)}$ or $D_{s(J)}^{(*)}$ meson. Then they look at the recoil mass against this reconstructed candidate. The recoil masses are shown in Figs. 19 and 20.

From these data BABAR extracts $\mathcal{B}(D_{sJ}(2460)^- \to D_s^{*-}\pi^0) = (56\pm13\pm9)\%$ and $\mathcal{B}(D_{sJ}(2460)^- \to D_s^{*-}\gamma) = (16\pm4\pm3)\%$ in addition to $\mathcal{B}(D_s^- \to \phi\pi^+) = (4.52\pm0.48\pm0.68)\%$. BABAR combines this measurement with their previous measurement discussed above to obtain $\mathcal{B}(D_s^- \to \phi\pi^+) = (4.62\pm0.36\pm0.50)\%$.

C. Study of $D_s^+ \to K^+K^-\pi^+$ in continuum production

Belle (Abe *et al.*, 2007) has used 552.3 pb^{-1} of e^+e^- data to study the process $e^+e^- \to D_s^{*+}D_{s1}^-$ followed by $D_{s1}^- \to D^{*0}K^-$ and $D_s^{*+} \to D_s^+\gamma$. The very large data sample allows Belle to study this exclusive final state in continuum production of D_s mesons. The final state is reconstructed in two ways; either by partially reconstructing the D_{s1} or the D_s^*. Belle obtains the preliminary branching fraction $\mathcal{B}(D_s^+ \to K^+K^-\pi^+) = (4.0\pm0.4\pm0.4)\%$ which is of comparable statistical precision to the other methods discussed above.

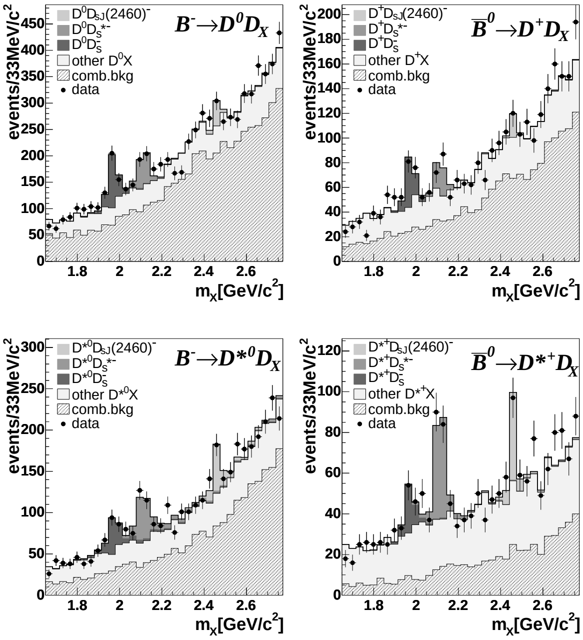

FIG. 19 The recoil mass against a D or D^* in B decays. Top left for $B^- \to D^0 D_X$, top right for $\bar{B}^0 \to D^+ D_X$, lower left for $B^- \to D^{*0} D_X$, and lower right for $\bar{B}^0 \to D^{*+} D_X$. From Aubert *et al.* (2006c).

D. Absolute branching fractions for hadronic D_s decays using double tags

CLEO-c (Alexander *et al.*, 2008) has determined the absolute hadronic branching fractions for D_s meson decays using a double tag technique similar to what was done for the D hadronic branching fractions. The same technique was used by MARK III (Adler *et al.*, 1990b) and BES (Bai *et al.*, 1995). These initial studies were limited by statistics; MARK III observed no events and placed an upper limit while BES observed two events and reported a branching fraction of

$$\mathcal{B}(D_s^+ \to \phi\pi^+) = (3.9^{+5.1+1.8}_{-1.9-1.1})\%. \qquad (83)$$

The BES analysis used 22.3 pb^{-1} recorded at $E_{\rm cm} = 4.03$ GeV.

The CLEO-c analysis used a sample of 298 pb^{-1} of e^+e^- collision data recorded at a center-of-mass energy of 4170 MeV. At this energy D_s mesons are produced, predominantly, as $D_s^+D_s^{*-}$ or $D_s^-D_s^{*+}$ pairs. The eight hadronic final states considered in this analysis by CLEO-c are $K_S^0K^+$, $K_S^0K^-\pi^+\pi^+$, $K^+K^-\pi^+$, $K^+\pi^-\pi^+$, $K^+K^-\pi^+\pi^0$, $\pi^+\pi^-\pi^+$, $\eta\pi^+$, and $\eta'\pi^+$. The analysis proceeds similar to the D hadronic branching fraction analysis described in Sect V.C. Yields and efficiencies for single tags (separately for D_s^+ and D_s^-) and double tags are extracted. The π^0 or γ from the D_s^* decay is not reconstructed in this analysis. The yields, in terms of the efficiencies, branching fractions, and data sample

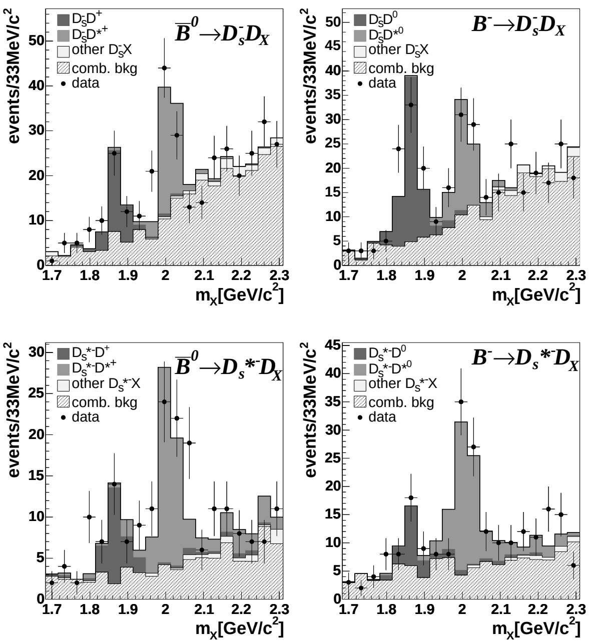

FIG. 20 The recoil mass against a D_s or D_s^* Top left for $\bar{B}^0 \to D_S^- D_X$, top right for $B^- \to D_S^- D_X$, lower left for $\bar{B}^0 \to D_s^{*-} D_X$, and lower right for $B^- \to D_s^{*-} D_X$. From Aubert *et al.* (2006c).

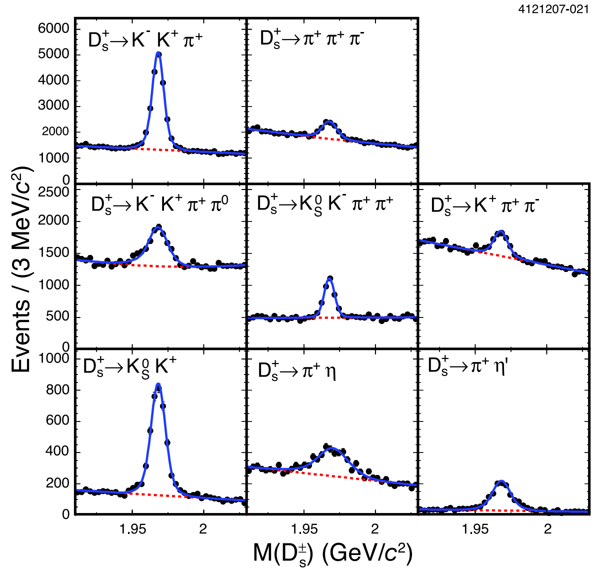

FIG. 21 Single tag yields for D_s modes used in the CLEO-c analysis. Charge conjugate modes are combined. From Alexander *et al.* (2008).

size are given by

$$y_i = N_{D_s^* D_s} \mathcal{B}_i \epsilon_i, \tag{84}$$
$$y_{\bar{j}} = N_{D_s^* D_s} \mathcal{B}_j \epsilon_{\bar{j}}, \tag{85}$$
$$y_{i\bar{j}} = N_{D_s^* D_s} \mathcal{B}_i \mathcal{B}_j \epsilon_{i\bar{j}}, \tag{86}$$

where i indicates a D_s^+ and $\bar{j}$ indicate a D_s^-. In this analysis a total of 16 single tags and 64 double tags are used. The event selection is detailed in Alexander *et al.* (2008). A D_s candidate is referred to as "indirect" if it comes from the decay of the D_s^* in the $e^+e^- \to D_s D_s^*$ interaction. Otherwise the D_s is said to be "direct". The D_s candidates are identified based on their momenta and invariant mass. The direct D_s has a fixed momentum in the e^+e^- restframe, whereas the indirect D_s has momenta in a range due to the extra boost from the $D_s^* \to D_s(\gamma, \pi^0)$ decay. The recoil mass $M_{\rm rec}$ is defined by

$$M_{\rm rec}^2 = \left(E_0 - \sqrt{\mathbf{p}_{D_s}^2 + M_{D_s}^2}\right)^2 - (\mathbf{p}_0 - \mathbf{p}_{D_s})^2, \tag{87}$$

where $(E_0, \mathbf{p}_0)$ is the e^+e^- center-of-mass four-vector, $\mathbf{p}_{D_s}$ is the measured D_s momentum and M_{D_s} is the nominal D_s mass. For direct D_s candidates $M_{\rm rec}$ peaks at the D_s^* mass of 2.112 GeV, while for indirect D_s candidates $M_{\rm rec}$ is spread about evenly over ± 60 MeV around this peak. CLEO-c requires that D_s candidates in a double tag, and for most single tags, satisfies $M_{\rm rec} > 2.051$ GeV. For the three single tag modes, $K^-K^+\pi^+\pi^0$, $\pi^+\pi^+\pi^-$, and $K^+\pi^+\pi^-$, with more substantial backgrounds, it is required that $M_{\rm rec}$ is greater than (2.099, 2.101, 2.099) GeV, respectively. Note that this cut eliminates events from $e^+e^- \to D_s^+ D_s^-$ as these events peak at $M_{\rm rec} = M_{D_s}$. A number of vetoes are applied to reject fake candidates, primarily from $D^* D^*$ events.

The single tag signal yields are extracted from the D_s invariant mass distributions. The single tag event yields in data are shown in Fig. 21. At most one single tag candidate per mode and charge are accepted per event. If more than one candidate pass the selection criteria the candidate with the value of $M_{\rm rec}$ closest to $M_{D_s^*}$ is selected. The data are fit to a signal shape and a background shape. The signal shape is determined from Monte Carlo simulations, but the D_s mass is allowed to float in the fit.

The double tag yields are extracted by a cut-and-count procedure in the plot of the invariant mass of the D_s^+ *vs.* D_s^-. All double tag candidates are shown in Fig. 22. At most one double tag candidate is allowed per event. If there are more than one candidate the combination with the average mass $\hat{M} \equiv (M(D_s^+) + M(D_s^-))/2$ closest to the M_{D_s} is kept. The combinatorial background has structure in $\hat{M}$, but is more uniform in $\Delta M \equiv M(D_s^+) - M(D_s^-)$. The signal region is defined by $|\hat{M} - M_{D_s}| < 12$ MeV and $|\Delta M| < 30$ MeV and the sideband region is defined by $|\hat{M} - M_{D_s}| < 12$ MeV and $50 < |\Delta M| < 140$ MeV. In this analysis the individual double tag yields and efficiencies are determined. The signal and sideband regions are shown in Fig. 22

All yields and efficiencies are combined in a likelihood fit to extract the D_s branching fractions. The branching fraction results from this fit is presented in Table XIII. In addition to the branching fractions, CLEO-c determines

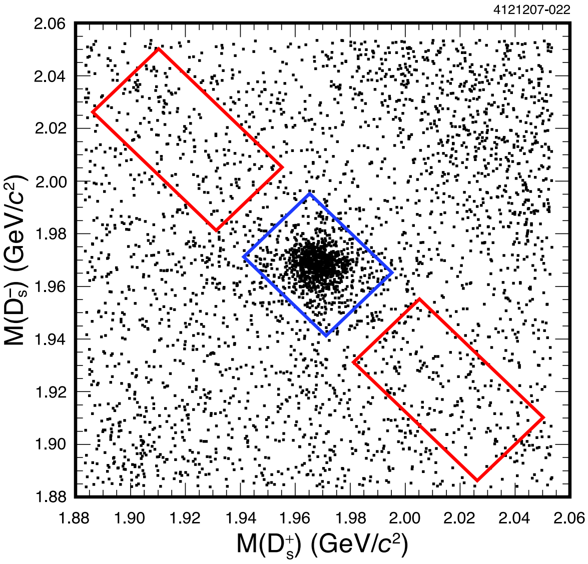

FIG. 22 Double tag yields for D_s modes used in the CLEO-c analysis. The signal region is indicated by the rectangle in the center and the two sideband regions are the diagonally offset rectangles. There are 1089 double tag candidates in the signal region and 339 candidates in the background region. With the signal to background region size of 1:3 this gives a signal to background ratio close to 9:1. From Alexander *et al.* (2008).

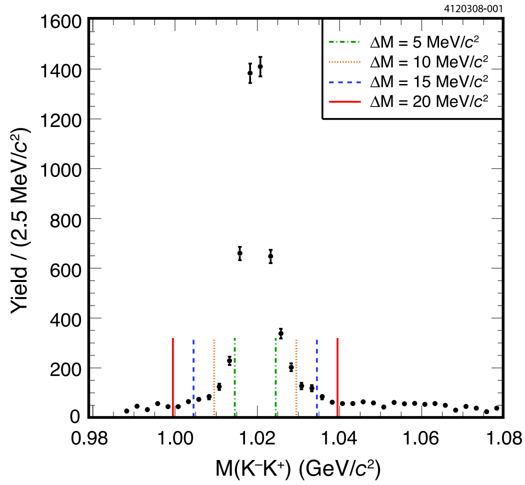

FIG. 23 The K^-K^+ invariant mass near the ϕ resonance in $D_s^+ \to K^-K^+\pi^+$ events from the CLEO-c double tag analysis. The single tag fit procedure used in the CLEO-c analysis is applied to extract the yield in each $M(K^-K^+)$ bin, hence backgrounds are subtracted and the yields shown are for the $D_s^+ \to K^-K^+\pi^+$ signal. The ϕ resonance is clear above an additional broad component. Indicated in the plot are the different mass windows considered by CLEO-c for their partial branching fractions. From Alexander *et al.* (2008)

the number of $D_sD_s^*$ pairs produced in their data sample to be $N_{D_sD_s^*} = (2.93 \pm 0.14 \pm 0.06) \times 10^5$. Combined with the luminosity, $\mathcal{L}_{\rm int} = (298 \pm 3)$ pb^{-1}, they obtain the cross-section $\sigma_{D_sD_s^*}(E_{\rm cm} = 4.17 \text{ GeV}) = (0.983 \pm 0.046 \pm 0.021 \pm 0.010)$ nb, where the last systematic is due to the uncertainty in the luminosity.

CLEO-c does not quote a $D_s^+ \to \phi\pi^+$ branching fraction. The reason for this is that at the precision of this measurement the branching fraction for $D_s^+ \to \phi\pi^+$ is not a well defined quantity. Figure 23 shows the K^+K^- invariant mass near the ϕ resonance. The combination of the relatively broad ϕ resonance and interference with other resonances, such as the $f_0(980)$, requires a complete amplitude analysis to determine the different contributions. Instead, CLEO-c provides partial branching fractions in different mass windows around the ϕ resonance. These partial branching fractions, given in four K^+K^- mass windows centered at the ϕ mass are presented in Table XIV.

Systematic uncertainties from tracking efficiencies, π^0 and K_S^0 reconstruction, and particle identification are common in this analysis to those from the analysis of the D^0 and D^+ absolute branching fractions discussed in Sect. V.C. In additions, for modes containing an η in the final state an uncertainty of $\pm 4.0\%$ is applied per η. Other large systematic uncertainties in this analysis includes the uncertainties from the signal lineshape and the background parameterization in the fits for the yields. These uncertainties are explored by using alternative fits.

The CLEO-c analysis provides the to-date best determination of the hadronic branching fractions for D_s mesons. This analysis is statistics limited; the statistical uncertainty in the $D_s^+ \to K^+K^-\pi^+$ mode is 4.2% and the systematic uncertainty about 3%. The largest systematic uncertainties come from the yield extraction. Both the statistical and systematic uncertainties would improve with additional data. This analysis was based on 298 pb^{-1}; CLEO-c has recorded a total of 589 pb^{-1} of data at this energy.

E. Summary of Cabibbo favored D_s^+ decays

The previous Sections discussed the key measurements that established the absolute branching fraction scale for D_s^+ meson decays. These measurements have evolved from model-dependent determinations, e.g., making use of equal semileptonic widths as for the D^+ decay, to model-independent measurements using tagging techniques. Also as the measurements have become more precise we need to be more precise about what is measured. For example, the often-used normalization mode $D_s^+ \to \phi\pi^+$ suffers from a contamination from the $D_s^+ \to f_0(980)\pi^+$ under the $\phi\pi^+$ signal. The results for the Cabibbo favored modes are summarized in Table XV.

TABLE XIII Branching fractions for D_s decays determined by the CLEO-c analysis described in Alexander *et al.* (2008).

Mode	Branching Fraction $\mathcal{B}$ (%)	$\mathcal{B}/\mathcal{B}(D_s^+ \to K^+K^-\pi^+)$	$\mathcal{A}_{CP}$ (%)
$\mathcal{B}(D_s^+ \to K_S^0 K^+)$	$1.49 \pm 0.07 \pm 0.05$	$0.270 \pm 0.009 \pm 0.008$	$+4.9 \pm 2.1 \pm 0.9$
$\mathcal{B}(D_s^+ \to K^+K^-\pi^+)$	$5.50 \pm 0.23 \pm 0.16$	1	$+0.3 \pm 1.1 \pm 0.8$
$\mathcal{B}(D_s^+ \to K^+K^-\pi^+\pi^0)$	$5.65 \pm 0.29 \pm 0.40$	$1.03 \pm 0.05 \pm 0.08$	$-5.9 \pm 4.2 \pm 1.2$
$\mathcal{B}(D_s^+ \to K_S^0 K^-\pi^+\pi^+)$	$1.64 \pm 0.10 \pm 0.07$	$0.298 \pm 0.014 \pm 0.011$	$-0.7 \pm 3.6 \pm 1.1$
$\mathcal{B}(D_s^+ \to \pi^+\pi^-\pi^+)$	$1.11 \pm 0.07 \pm 0.04$	$0.202 \pm 0.011 \pm 0.009$	$+2.0 \pm 4.6 \pm 0.7$
$\mathcal{B}(D_s^+ \to \pi^+\eta)$	$1.58 \pm 0.11 \pm 0.18$	$0.288 \pm 0.018 \pm 0.033$	$-8.2 \pm 5.2 \pm 0.8$
$\mathcal{B}(D_s^+ \to \pi^+\eta')$	$3.77 \pm 0.25 \pm 0.30$	$0.69 \pm 0.04 \pm 0.06$	$-5.5 \pm 3.7 \pm 1.2$
$\mathcal{B}(D_s^+ \to K^+\pi^+\pi^-)$	$0.69 \pm 0.05 \pm 0.03$	$0.125 \pm 0.009 \pm 0.005$	$+11.2 \pm 7.0 \pm 0.9$

TABLE XIV Partial branching fractions in the mode $D_s^+ \to K^+K^-\pi^+$ for events with a K^+K^- invariant mass within ΔM MeV of the ϕ, $|m_{K^+K^-} - m_\phi| < \Delta M$. From the CLEO-c study described in Alexander *et al.* (2008).

ΔM	Partial Branching Fraction (%)
5	$1.69 \pm 0.08 \pm 0.06$
10	$1.99 \pm 0.10 \pm 0.05$
15	$2.14 \pm 0.10 \pm 0.05$
20	$2.24 \pm 0.11 \pm 0.06$

TABLE XV Summary of branching fractions for Cabibbo favored D_s^+ decays. Averages taken from Amsler *et al.* (2008) unless otherwise noted.

Mode	Branching Fraction
$D_s^+ \to K^+K_S^0$	$(1.49 \pm 0.09)\%$
$D_s^+ \to K^+K^-\pi^+$	$(5.50 \pm 0.28)\%$
$D_s^+ \to K^+K^-\pi^+\pi^0$	$(5.6 \pm 0.5)\%$
$D_s^+ \to K_S^0 K^+\pi^+\pi^-$	$(9.6 \pm 1.3) \times 10^{-3}$
$D_s^+ \to K_S^0 K^-\pi^+\pi^+$	$(1.64 \pm 0.12)\%$
$D_s^+ \to K^+K^-\pi^+\pi^+\pi^-$	$(8.8 \pm 1.6) \times 10^{-3}$
$D_s^+ \to K_S^0 K_S^0 \pi^+\pi^+\pi^-$	$(8.4 \pm 3.5) \times 10^{-4}$
$D_s^+ \to \pi^+\pi^+\pi^-$	$(1.11 \pm 0.08)\%$
$D_s^+ \to \pi^+\pi^+\pi^-\pi^0$	$< 14\%$
$D_s^+ \to \pi^+\pi^+\pi^+\pi^-\pi^-$	$(8.0 \pm 0.9) \times 10^{-3}$
$D_s^+ \to \pi^+\pi^+\pi^+\pi^-\pi^-\pi^0$	$(4.9 \pm 3.2)\%$
$D_s^+ \to \eta\pi^+$	$(1.58 \pm 0.21)\%$
$D_s^+ \to \omega\pi^+$ [a]	$(2.3 \pm 0.5) \times 10^{-3}$
$D_s^+ \to \omega\pi^0\pi^+$ [a]	$(2.78 \pm 0.70)\%$
$D_s^+ \to \omega\pi^+\pi^-\pi^+$ [a]	$(1.58 \pm 0.46)\%$
$D_s^+ \to \omega\pi^+\eta$ [a]	$< 2.13\%$
$D_s^+ \to \eta\rho^+$	$(13.0 \pm 2.2)\%$
$D_s^+ \to \eta'\pi^+$	$(3.8 \pm 0.4)\%$
$D_s^+ \to \eta'\rho^+$	$(12.2 \pm 2.0)\%$

[a] Includes results from Ge *et al.* (2009a).

VII. CABIBBO SUPPRESSED DECAYS OF D^0, D^+, AND D_s^+ MESONS

A. Theoretical issues

Studies of hadronic singly Cabibbo-suppressed decays of charmed mesons are important for several reasons. First, these decays hold the potential for future observation of direct (*i.e.*, not associated with $D^0\overline{D}^0$ mixing (Bianco *et al.*, 2003; Gedalia and Perez, 2010; Petrov, 2004)) CP violation in the D-system. In the Standard Model, this is due to the fact that the final state particles contain at least one pair of a quark and antiquark of the same flavor, making possible a contribution from penguin-type amplitudes. Those amplitudes provide an access to the third generation of quarks (b-quarks in the loops), needed for observation of CP violation in the Standard Model (Bianco *et al.*, 2003; Buccella *et al.*, 1993). New physics can also make an entrance through those transitions, affecting both the amplitudes and CP-violating asymmetries (Grossman *et al.*, 2007). Second, it offers new ground for studying strong dynamics in hadronic decays, in particular, the issue of flavor $SU(3)_F$ breaking in D decays. For example, one of the famous failures of the applications of $SU(3)_F$ symmetry involves the prediction that the decay rates for $D^0 \to K^+K^-$ and $D^0 \to \pi^+\pi^-$ are equal. In reality, the first rate is about three times larger than the second one. Other puzzles include the fact that the rates for decays like $D^+ \to K^{*+}\overline{K}^{*0}$ are so much enhanced by strong dynamics that their values appear to be as large as the ones of Cabibbo-favored decays. One popular explanation for such phenomena include resonant final-state interactions (Chau and Cheng, 1989; Kamal and Verma, 1987) that affect not only D decays, but also $D^0\overline{D}^0$ mixing (Falk *et al.*, 1999; Golowich and Petrov, 1998). There are also other explanations (Chau and Cheng, 1992; Savage, 1991). In order to study those phenomena it is convenient to select a base formalism for studies of hadronic transitions.

It is convenient to use the topological diagram approach to predict unknown branching ratios for singly-Cabibbo-suppressed decays. The analysis, done in Chiang *et al.* (2003) and repeated in Bhattacharya and Rosner (2008) and Bhattacharya and Rosner (2009) with updated experimental data, is displayed in Tables XVI through XIX.

1. $D \to PP$ transitions

Topological diagram approach to singly Cabibbo-suppressed transitions can make use of the information obtained from the fits of CF decays discussed above. In particular, the ratio of primed (SCS) to unprimed (CF) amplitudes is fixed, it is just $\lambda' = \tan\theta_C = 0.23$. Table XVI, taken from Bhattacharya and Rosner (2008), presents the most recent compilation of the branching ratios, amplitudes, and representations in terms of reduced amplitudes for singly Cabibbo-suppressed charm decays involving pions and kaons. The extracted topological amplitudes, in units of 10^{-7} GeV, are

$$T' = 6.44 \; ; \quad (88)$$
$$C' = -4.15 - 2.25i \; ; \quad (89)$$
$$E' = -1.76 + 3.48i \; ; \quad (90)$$
$$A' = 0.55 - 1.14i \; . \quad (91)$$

The deviations from flavor $SU(3)$ in Table XVI are discussed below.

Note that the decay $D^0 \to K^0\overline{K}^0$ is forbidden by $SU(3)_F$. Estimates of $SU(3)_F$-breaking effects lead to predictions for $\mathcal{B}(D^0 \to K^0\overline{K}^0)$ that are consistent with experimental observations, but are by no means reliable (Dai *et al.*, 1999; Eeg *et al.*, 2001; Lipkin, 1980; Pham, 1987). We shall discuss those below.

Final states with η and η' require additional considerations. In particular, new topological amplitudes, flavor-singlet singlet-exchange SE' and singlet-annihilation SA'. The amplitudes C and E extracted from Cabibbo-favored charm decays imply values of $C' = \lambda' C$ and $E' = \lambda' E$ which may be used in constructing amplitudes for singly-Cabibbo-suppressed D^0 decays involving η and η'.

2. $D \to PV$ transitions

A similar technique can be applied to describe $D \to PV$ transitions. In this case, similar topological amplitudes are denoted by a subscript "V". We present the most recent results in Tables XVIII (Bhattacharya and Rosner, 2009).

B. Cabibbo suppressed D^0 and D^+ decays

Experimentally, Cabibbo suppressed or doubly Cabibbo suppressed decays of D^0 or D^+ mesons are almost always measured relative to a Cabibbo favored normalization mode. This includes most CLEO-c analyses as the branching fractions for Cabibbo suppressed modes are typically suppressed by $|V_{cd}/V_{cs}|^2 \approx 0.05$ and the statistics in these modes using a tagged analysis would be limited. In some cases, e.g. the CLEO-c analysis of $D^0 \to K\bar{K}$ final states (Bonvicini *et al.*, 2008a), CLEO has normalized against the number of produced $D\bar{D}$ events and measured directly the branching fraction.

1. Two-body decays of D^0 and D^+

There is a substantial amount of data on the two-body decays of D^0 and D^+. The first measurements of Cabibbo suppressed D^0 decays were for $D^0 \to K^-K^+$ and $D^0 \to \pi^-\pi^+$ done by the Mark II experiment (Abrams *et al.*, 1979b). Since the first observation of these modes they have been measured by many experiments with increased precision. In these measurements the $D^0 \to K^-K^+$ and $D^0 \to \pi^-\pi^+$ branching fractions are measured relative to the $D^0 \to K^-\pi^+$ yield. Experiments operating above the $c\bar{c}$ threshold tag the D^0 by looking at the D^0–D^{*+} mass difference in the decay $D^{*+} \to D^0\pi^+$.

The results for the $D^0 \to K^-K^+$ and $D^0 \to \pi^-\pi^+$ decays are summarized in Table XIX. The most precise measurement is that of CDF (Acosta *et al.*, 2005), in the $D^0 \to K^-K^+$ they reconstruct about 16,000 signal candidates.

As can be seen from Table XIX, the rate for $D^0 \to K^+K^-$ is larger than the rate for $D^0 \to \pi^+\pi^-$ by a factor of three. In the $SU(3)_F$ (or in the U-spin) symmetry limit, those rates should be the same. $SU(3)_F$ is, in general, expected to work to 30%, so this is a rather severe violation of this symmetry.

This problem has been around since the 80s (Chau and Cheng, 1986; Lipkin, 1980), yet it still received no completely satisfactory solution. While the one popular explanation for this puzzle involves final-state interactions (*e.g.* a presence of a resonance that couples stronger to K^+K^- compared to $\pi^+\pi^-$ state or other type (Chau and Cheng, 1986; Donoghue and Holstein, 1980)), it might be tempting to try to understand the issue in factorization (Chau and Cheng, 1992; Sanda, 1980). Neglecting for a moment the annihilation diagram contribution,

$$\frac{\mathcal{A}_{K\overline{K}}}{\mathcal{A}_{\pi\overline{\pi}}} = \frac{f_K}{f_\pi} \frac{m_D^2 - m_K^2}{m_D^2 - m_\pi^2} \frac{F^{DK}(m_K^2)}{F^{D\pi}(m_\pi^2)}. \quad (92)$$

With the recent lattice evaluations $f_K/f_\pi = 1.218 \pm 0.002^{+0.011}_{-0.024}$ from a recent lattice QCD calculation with domain-wall fermions (Beane *et al.*, 2007) (which is consistent with experimental determinations of the decay constants that can also be used, see Artuso *et al.* (2008); Bianco *et al.* (2003)), assuming a modified pole dominance for the form-factors $F^{DK}(m_K^2)$ and $F^{D\pi}(m_\pi^2)$, and extracting them from semileptonic D decays (see Artuso *et al.* (2008) for a recent review and Besson *et al.* (2009) for recent determination of parameters), we get

$$\mathcal{A}_{K\overline{K}} \simeq 1.32 \mathcal{A}_{\pi\overline{\pi}}. \quad (93)$$

TABLE XVI Branching ratios, amplitudes, decomposition in terms of reduced amplitudes, and predicted branching ratios for singly-Cabibbo-suppressed charm decays involving pions and kaons. Predictions for the branching ratios are from Bhattacharya and Rosner (2008).

Meson	Decay mode	$\mathcal{B}$ (10^{-3})	p^* (MeV)	$\lvert\mathcal{A}\rvert$ $(10^{-7}$ GeV)	Rep.	Predicted $\mathcal{B}$ (10^{-3})
D^0	$\pi^+\pi^-$	1.40±0.02	921.9	4.61±0.03	$-(T'+E')$	2.23
	$\pi^0\pi^0$	0.80±0.08	922.6	3.49±0.17	$-(C'-E')/\sqrt{2}$	1.27
	K^+K^-	3.93±0.07	791.0	8.35±0.08	$(T'+E')$	1.92
	$K^0\overline{K}^0$	0.37±0.06	788.5	2.57±0.35	0	0
D^+	$\pi^+\pi^0$	1.24±0.07	924.7	2.73±0.08	$-(T'+C')/\sqrt{2}$	0.87
	$K^+\overline{K}^0$	6.17±0.20	792.6	6.58±0.11	$T'-A'$	5.12
D_s^+	π^+K^0	2.44±0.30	915.7	5.84±0.36	$-(T'-A')$	2.56
	π^0K^+	0.75±0.28	917.1	3.24±0.60	$-(C'+A')/\sqrt{2}$	0.87

TABLE XVII Real and imaginary parts of amplitudes for SCS charm decays involving η and η', in units of 10^{-7} GeV, from Chiang *et al.* (2003).

Amplitude	Expression	Re	Im	$\lvert\mathcal{A}_{\rm exp}\rvert$
$-\sqrt{6}\mathcal{A}(D^0\to\pi^0\eta)$	$2E'-C'+SE'$	0.63	9.21	7.79 ± 0.54
$\frac{\sqrt{3}}{2}\mathcal{A}(D^0\to\pi^0\eta')$	$\frac{1}{2}(C'+E')+SE'$	−2.95	0.62	3.54 ± 0.35
$\frac{3}{2\sqrt{2}}\mathcal{A}(D^0\to\eta\eta)$	$C'+SE'$	−4.14	−2.25	5.91 ± 0.34
$-\frac{3\sqrt{2}}{7}\mathcal{A}(D^0\to\eta\eta')$	$\frac{1}{7}(C'+6E')+SE'$	−2.10	2.66	3.48 ± 0.38
$\sqrt{3}\mathcal{A}(D^+\to\pi^+\eta)$	$T'+2C'+2A'+SA'$	−0.75	−6.77	8.21±0.26
$-\frac{\sqrt{6}}{4}\mathcal{A}(D^+\to\pi^+\eta')$	$\frac{1}{4}(T'-C'+2A')+SA'$	2.92	−0.01	3.72±0.15
$-\sqrt{3}\mathcal{A}(D_s^+\to\eta K^+)$	$-(T'+2C')+SA'$	1.85	4.50	8.05±0.88
$\frac{\sqrt{6}}{4}\mathcal{A}(D_s^+\to\eta' K^+)$	$\frac{1}{4}(2T'+C'+3A')+SA'$	2.59	−1.41	3.43±0.57

It is interesting to note that the effect of $SU(3)_F$ breaking in the decay constants works in the *opposite* direction to the effect due to different phase space of K^+K^- and $\pi^+\pi^-$ final states (Chau and Cheng, 1992). In other words, factorization predicts about 30% breaking of $SU(3)_F$ in spectator amplitudes (c.f. Chau and Cheng (1992)). Clearly, this is not sufficient for the resolution of the puzzle.

There is a recent suggestion (Bianco *et al.*, 2003) attributing this effect to the difference between $SU(3)_F$ breaking in exclusive vs. inclusive modes. This fact can also be interpreted in terms of final state interactions, as final-state interactions do not simply enhance a given decay channel, but rather redistribute the strength of different channels composing the inclusive decay rate. The fact that the ratio of $\Gamma(D\to KK\pi\pi)$ and $\Gamma(D\to 4\pi)$ exhibits behavior opposite to the ratio of $\Gamma(D\to KK)$ and $\Gamma(D\to\pi\pi)$ (see Tables XXII and XXIII) buttresses this conclusion. The presence of final-state interaction-enhanced exchange amplitude is also crucial for the explanation of this phenomenon.

A number of other two-body final states to pseudoscalars and have been studied. These decays are summarized in Table XX.

The most complete study of D mesons decays to final states containing η and η' mesons is done by CLEO-c (Artuso *et al.*, 2008). This analysis uses 281 pb^{-1} of data collected at the $\psi(3770)$ resonance. In this study CLEO-c makes use of single tags; the modes studied here have sufficiently small branching fractions that using D tagging is not useful. The π^0 and η mesons are reconstructed in the $\gamma\gamma$ final state. In addition, for modes with two η mesons in the final state ($\eta\eta$ and $\eta\eta'$) the $\eta\to\pi^+\pi^-\pi^0$ channel is used to reconstruct η mesons. The η' is reconstructed in the channel $\eta'\to\eta\pi^+\pi^-$. It is required that $402 < M_{\eta\pi^+\pi^-} - M_\eta < 418$ MeV.

The yields are extracted by fitting the $M_{\rm BC}$ distributions after selecting events consistent with $\Delta E = 0$. In Figs. 24 and 25 the observed signals are shown. The significance for all modes are over 4σ except for the $D^0\to\eta'\pi^+\pi^-$ mode where the significance is estimated to be 3.2σ. The observed yields and branching fractions are summarized in Table XXI. These data make it possible to constrain new singlet exchange SE' amplitudes introduced in Sect. VII.A.1. In order to do that, one can rewrite four equations for D^0 decay amplitudes to the final states with $\eta^{(\prime)}$:

$$-\sqrt{6}\mathcal{A}(D^0\to\eta\pi^0) \ = \ 2E'-C'+SE', \qquad (94)$$

$$\frac{\sqrt{3}}{2}\mathcal{A}(D^0\to\eta'\pi^0) \ = \ \frac{1}{2}\left(E'+C'\right)+SE', \qquad (95)$$

TABLE XVIII Branching ratios and invariant amplitudes for singly-Cabibbo-suppressed decays of charmed mesons to one pseudoscalar and one vector meson (from Bhattacharya and Rosner (2009)).

Meson	Decay mode	Representation	$\mathcal{B}$ (Amsler *et al.*, 2008) (%)	p^* (MeV)	$\lvert\mathcal{A}\rvert$ (10^{-6})
D^0	$\pi^+\rho^-$	$-(T_V{}' + E_P{}')$	0.497±0.023	763.8	1.25±0.03
	$\pi^-\rho^+$	$-(T_P{}' + E_V{}')$	0.980±0.040	763.8	1.76±0.04
	$\pi^0\rho^0$	$\frac{1}{2}(E_P{}' + E_V{}' - C_P{}' - C_V{}')$	0.373±0.022	764.2	1.08±0.03
	K^+K^{*-}	$T_V{}' + E_P{}'$	0.153±0.015	609.8	0.97±0.05
	K^-K^{*+}	$T_P{}' + E_V{}'$	0.441±0.021	609.8	1.65±0.04
	$K^0\overline{K}^{*0}$	$E_V{}' - E_P{}'$	<0.18	605.3	
	$\overline{K}^0K^{*0}$	$E_P{}' - E_V{}'$	<0.09	605.3	
	$\pi^0\phi$	$\frac{1}{\sqrt{2}}C_P{}'$	0.124±0.012	644.7	0.81±0.04
	$\pi^0\omega$	$\frac{1}{2}(E_P{}' + E_V{}' - C_P{}' + C_V{}')$		761.2	
	$\eta\rho^0$	$\frac{1}{\sqrt{6}}(2C_V{}' - C_P{}' - E_P{}' - E_V{}')$		652.0	
	$\eta\omega$	$-\frac{1}{\sqrt{6}}(2C_V{}' + C_P{}' + E_P{}' + E_V{}')$	0.221±0.023	648.1	1.07±0.11
	$\eta\phi$	$\frac{1}{\sqrt{3}}(C_P{}' - E_P{}' - E_V{}')$	0.014±0.005	488.8	0.41±0.15
	$\eta'\rho^0$	$\frac{1}{2\sqrt{3}}(E_P{}' + E_V{}' + C_P{}' + C_V{}')$		342.5	
	$\eta'\omega$	$\frac{1}{2\sqrt{3}}(E_P{}' + E_V{}' + C_P{}' - C_V{}')$		333.5	
D^+	$\rho^0\pi^+$	$\frac{1}{\sqrt{2}}(A_P{}' - A_V{}' - C_P{}' - T_V{}')$	0.082±0.015	767	0.32±0.03
	$\omega\pi^+$	$-\frac{1}{\sqrt{2}}(A_P{}' + A_V{}' + C_P{}' + T_V{}')$	<0.034	764	
	$\phi\pi^+$	$C_P{}'$	0.620±0.070	647	1.13±0.06
	$\overline{K}^{*0}K^+$	$(T_V{}' - A_V{}')$	0.435±0.048	611	1.03±0.06
	$\pi^0\rho^+$	$\frac{1}{\sqrt{2}}(A_V{}' - A_P{}' - C_V{}' - T_P{}')$		767	
	$\eta\rho^+$	$\frac{1}{\sqrt{3}}(A_V{}' + A_P{}' + 2C_V{}' + T_P{}')$	<0.7	656	
	$\eta'\rho^+$	$\frac{1}{\sqrt{6}}(C_V{}' - A_V{}' - A_P{}' - T_P{}')$	<0.5	349	
	$\overline{K}^0K^{*+}$	$(T_P{}' - A_P{}')$	3.18±1.38	612	2.78±0.60
D_s^+	π^+K^{*0}	$(A_V{}' - T_V{}')$	0.225±0.039	773	0.79±0.07
	π^0K^{*+}	$-\frac{1}{\sqrt{2}}(C_V{}' + A_V{}')$		775	
	ηK^{*+}	$\frac{1}{\sqrt{3}}(T_P{}' + 2C_V{}' + A_P{}' - A_V{}')$		661	
	$\eta'K^{*+}$	$\frac{1}{\sqrt{6}}(2T_P{}' + C_V{}' + 2A_P{}' + A_V{}')$		337	
	$K^0\rho^+$	$(A_P{}' - T_P{}')$		743	
	$K^+\rho^0$	$-\frac{1}{\sqrt{2}}(C_P{}' + A_P{}')$	0.27±0.05	745	0.92±0.09
	$K^+\omega$	$-\frac{1}{\sqrt{2}}(C_P{}' - A_P{}')$		741	
	$K^+\phi$	$T_V{}' + C_P{}' + A_V{}'$	<0.057	607	

TABLE XIX Measurements of $D^0 \to K^-K^+$ and $D^0 \to \pi^-\pi^+$. The branching fractions have been recalculated using $\mathcal{B}(D^0 \to K^-\pi^+) = (3.89 \pm 0.05)\%$.

Experiment	$\mathcal{B}(D^0 \to K^-K^+)$ (10^{-3})	$\mathcal{B}(D^0 \to \pi^-\pi^+)$ (10^{-3})
CLEO-c (Bonvicini *et al.*, 2008a; Rubin *et al.*, 2006)	$4.08 \pm 0.08 \pm 0.09$	$1.41 \pm 0.04 \pm 0.03$
BES II (Ablikim *et al.*, 2005)	$4.75 \pm 0.43 \pm 0.17$	
CDF (Acosta *et al.*, 2005)	$3.859 \pm 0.043 \pm 0.069$	$1.40 \pm 0.02 \pm 0.03$
FOCUS (Link *et al.*, 2003)	$3.863 \pm 0.054 \pm 0.074$	$1.37 \pm 0.05 \pm 0.03$
CLEO II (Csorna *et al.*, 2002)	$4.05 \pm 0.13 \pm 0.13$	$1.36 \pm 0.06 \pm 0.07$
E791 (Aitala *et al.*, 1998a)	$4.24 \pm 0.12 \pm 0.13$	$1.56 \pm 0.08 \pm 0.12$
CLEO II (Asner *et al.*, 1996)	$4.51 \pm 0.27 \pm 0.28$	
E687 (Frabetti *et al.*, 1994a)	$4.24 \pm 0.27 \pm 0.35$	
E691 (Anjos *et al.*, 1991)	$4.16 \pm 0.39 \pm 0.39$	
CLEO (Alexander *et al.*, 1990b)	$4.55 \pm 0.39 \pm 0.28$	
Average	3.98 ± 0.07	1.40 ± 0.03

TABLE XX Measurements of D^0 and D^+ decays to Cabibbo suppressed, non-strange, two-body final states. The averages are from Amsler *et al.* (2008).

Mode	$\mathcal{B}$ (10^{-3})
$D^0 \to \pi^+\pi^-$	1.40 ± 0.02
$D^0 \to \pi^0\pi^0$	0.80 ± 0.08
$D^0 \to \eta\pi^0$	0.57 ± 0.14
$D^0 \to \omega\pi^0$	< 0.26
$D^+ \to \pi^0\pi^+$	1.24 ± 0.07
$D^+ \to \pi^+\eta$	3.39 ± 0.29
$D^+ \to \pi^+\omega$	< 0.34

$$\frac{3}{2\sqrt{2}}\mathcal{A}(D^0 \to \eta\eta) = C' + SE', \quad (96)$$

$$-\frac{3\sqrt{2}}{7}\mathcal{A}(D^0 \to \eta'\eta') = \frac{1}{7}(C' + 6E') + SE'. \quad (97)$$

It is interesting to note that the right-hand side of each of Eqs.(94) determines a vector in a complex plane. Since both amplitudes and phases of C' and E' are known from Eq. (88), these four equations contain a common complex off-set, SE'. Since only the magnitudes of the right-hand sides of these equations are known, they each define a circle in the complex plane with the radius given by that magnitude. Plotting them on the same graph then determines SE'.

This is done in Fig. 26. Notice that all circles intersect in two points, which determine two possible solutions for SE'. The smaller values for $SE' = (-0.7 \pm 0.4) \times 10^{-7}$ GeV $+ i(-1.0 \pm 0.6) \times 10^{-7}$ GeV are theoretically preferable, as SE' is an Okubo-Zweig-Iizuka (OZI)-suppressed amplitude (Iizuka, 1966; Okubo, 1977; Zweig, 1964).

TABLE XXI Yields and branching fractions for D meson decays to final states with η and η' mesons. From Artuso *et al.* (2008).

Mode	Yield	Branching Fraction (10^{-4})
$\mathcal{B}(D^+ \to \eta\pi^+)$	1033 ± 42	$34.3 \pm 1.4 \pm 1.7$
$\mathcal{B}(D^+ \to \eta'\pi^+)$	352 ± 20	$44.2 \pm 2.5 \pm 2.9$
$\mathcal{B}(D^0 \to \eta\pi^0)$	156 ± 24	$6.4 \pm 1.0 \pm 0.4$
$\mathcal{B}(D^0 \to \eta'\pi^0)$	50 ± 9	$8.1 \pm 1.5 \pm 0.6$
$\mathcal{B}(D^0 \to \eta\eta)$	255 ± 22	$16.7 \pm 1.4 \pm 1.3$
$\mathcal{B}(D^0 \to \eta\eta')$	46 ± 9	$12.6 \pm 2.5 \pm 1.1$
$\mathcal{B}(D^0 \to \eta\pi^+\pi^-)$	257 ± 32	$10.9 \pm 1.3 \pm 0.9$
$\mathcal{B}(D^+ \to \eta\pi^+\pi^0)$	149 ± 34	$13.8 \pm 3.1 \pm 1.6$
$\mathcal{B}(D^0 \to \eta'\pi^+\pi^-)$	21 ± 8	$4.5 \pm 1.6 \pm 0.5$
$\mathcal{B}(D^+ \to \eta'\pi^+\pi^0)$	33 ± 9	$15.7 \pm 4.4 \pm 2.5$

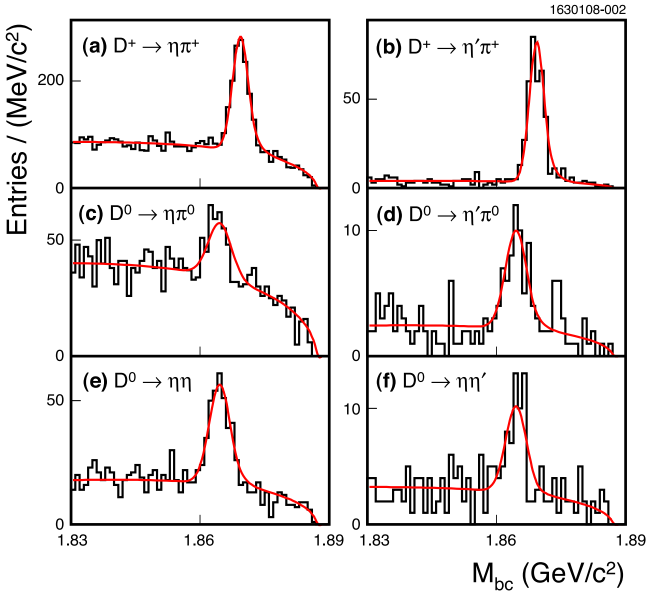

FIG. 24 Yields for a) $D^+ \to \eta\pi^+$, b) $D^+ \to \eta'\pi^+$, c) $D^0 \to \eta\pi^0$, d) $D^0 \to \eta'\pi^0$, e) $D^0 \to \eta\eta$, and $D^0 \to \eta\eta'$. From Artuso *et al.* (2008).

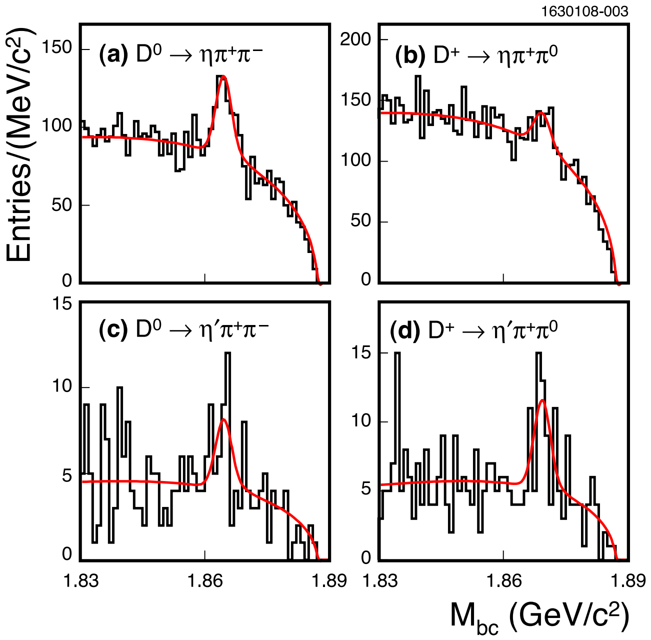

FIG. 25 Yields for a) $D^0 \to \eta\pi^+\pi^-$, b) $D^+ \to \eta\pi^+\pi^0$, c) $D^0 \to \eta'\pi^+\pi^-$, and d) $D^+ \to \eta'\pi^+\pi^0$. From Artuso *et al.* (2008).

2. Multibody decays with kaons and pions

Multibody decays of D^0 and D^+ mesons has also been extensively studied. While theoretical studies of those transitions are limited, some of those decays can be

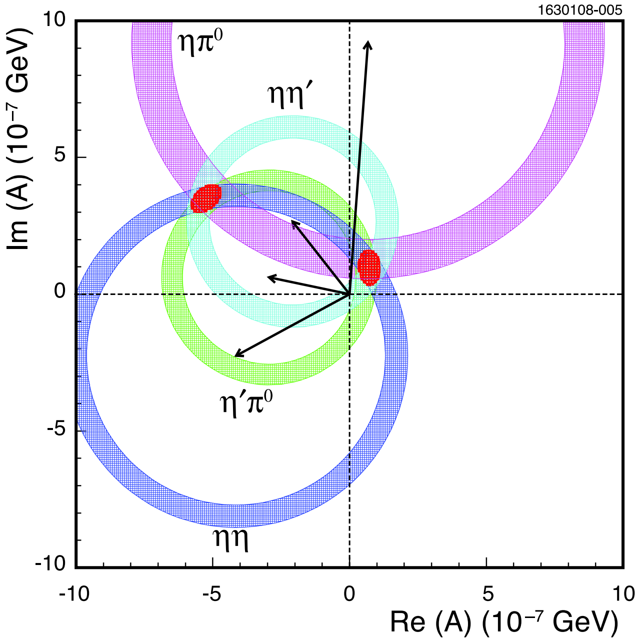

FIG. 26 Graphical representation of Eqs. (94) used to determine SE' from the amplitude analysis for $D \to \eta^{(\prime)}\eta(\pi^0)$ Artuso *et al.* (2008). Circles represent absolute values of the decay amplitudes. The intersection points provide two possible solutions for SE' (see text).

used in the Dalitz-plot analyses of $D^0\overline{D}^0$ mixing (Artuso *et al.*, 2008). Measurements of branching fractions to final states with three or more pions, including final states with η and ω mesons, can be found in Table XXII. In Section IX Dalitz plot analysis of three-body final states are discussed.

TABLE XXII Measurements of D^0 and D^+ decays to Cabibbo suppressed final states with three or more pions in the final states. Final states with η and ω mesons are also included. Limits are given at 90% C.L. Averages from Amsler *et al.* (2008).

Mode	$\mathcal{B}$ (10^{-3})
$D^0 \to \pi^+\pi^-\pi^0$	14.1 ± 0.6
$D^0 \to \pi^+\pi^-\pi^+\pi^-$	7.44 ± 0.21
$D^0 \to \pi^+\pi^-\pi^+\pi^-\pi^0$	4.2 ± 0.5
$D^0 \to \pi^0\pi^0\pi^0$	< 0.35
$D^0 \to \pi^+\pi^-\pi^0\pi^0$	10.0 ± 0.9
$D^0 \to \pi^+\pi^-\pi^+\pi^-\pi^+\pi^-$	0.42 ± 0.12
$D^+ \to \pi^+\pi^+\pi^-$	3.21 ± 0.19
$D^+ \to \pi^+\pi^0\pi^0$	4.6 ± 0.4
$D^+ \to \pi^+\pi^+\pi^-\pi^0$	11.4 ± 0.8
$D^+ \to \pi^+\pi^+\pi^-\pi^+\pi^-$	1.63 ± 0.16

In addition to the $D^0 \to KK$ decays discussed above, many other Cabibbo suppressed decays with two kaon in the final states have been studied. Dalitz plot analyses have been performed on some three-body final states as discussed in Sect. IX. The final states with two kaons in the final state are summarized in Table XXIII.

TABLE XXIII Measurements of branching fractions for D^0 and D^+ decays to Cabibbo suppressed final states with two kaons. Averages from Amsler *et al.* (2008).

Mode	$\mathcal{B}$ (10^{-3})
$D^0 \to K^0_S K^-\pi^+$	3.5 ± 0.5
$D^0 \to K^0_S K^+\pi^-$	2.7 ± 0.5
$D^0 \to K^+K^-\pi^0$	3.29 ± 0.14
$D^0 \to K^0_S K^0_S \pi^0$	< 0.59
$D^0 \to K^+K^-\pi^+\pi^-$	2.43 ± 0.012
$D^0 \to K^0_S K^0_S \pi^+\pi^-$	1.30 ± 0.24
$D^0 \to K^0_S K^-\pi^+\pi^+\pi^-$	< 0.15
$D^0 \to K^+K^-\pi^+\pi^-\pi^0$	3.1 ± 2.0
$D^+ \to K^+K^-\pi^+$	9.63 ± 0.31
$D^+ \to K^+K^0_S\pi^+\pi^-$	1.69 ± 0.18
$D^+ \to K^0_S K^-\pi^+\pi^+$	2.32 ± 0.18
$D^+ \to K^+K^-\pi^+\pi^+\pi^-$	2.3 ± 1.2

C. Cabibbo suppressed D_s decays

The Cabibbo suppressed D_s decays are final states with one or three kaons. The measured decays are listed in Table XXIV. This table also includes the doubly Cabibbo suppressed decay $D^+ \to K^+K^+\pi^-$. CLEO-c (Adams *et al.*, 2007) has performed a systematic study of two-body D_s decays.

D. Doubly Cabibbo suppressed decays

The doubly Cabibbo suppressed decays have two Cabibbo suppressed weak couplings. Naively, the rates for the doubly Cabibbo suppressed decays are smaller than the Cabibbo favored decay rates by a factor of $\tan^4\theta_C \approx 2.8 \times 10^{-3}$. Since those rates are quite small, one may wonder if they can be affected by some kind of new physics contributions. It has been proven (Bergmann and Nir, 1999), however, that phenomenological constraints imply that the new physics contributions are quite small compared to the standard model amplitudes. Since all quarks in the decay vertex of the DCS diagram are of different flavors, the set of new physics models that could possibly affect those decays are indeed not that big.

The first observation of a doubly Cabibbo suppressed decay was in the decay channel $D^0 \to K^+\pi^-$ (Cinabro *et al.*, 1994). Experimentally, the flavor, D^0 or $\bar{D}^0$, of the initial state is tagged by the charged of the slow pion in the decay $D^{*+} \to D^0\pi^+$. The simplest measurements observe the time integrated rate of D^0 decays and do not separated direct decay contributions from mixing,

TABLE XXIV Cabibbo suppressed D_s^+ decays.

Mode	Ref.	$\mathcal{B}(10^{-3})$
$D_s^+ \to K^+\pi^0$	(Adams *et al.*, 2007)	0.82 ± 0.22
$D_s^+ \to K_S^0\pi^+$	(Adams *et al.*, 2007; Link *et al.*, 2008)	1.25 ± 0.15
$D_s^+ \to K^+\eta$	(Adams *et al.*, 2007)	1.41 ± 0.31
$D_s^+ \to K^+\eta'$	(Adams *et al.*, 2007)	1.6 ± 0.5
$D_s^+ \to K^+\pi^+\pi^-$	(Alexander *et al.*, 2008)	6.9 ± 0.5
$D_s^+ \to K_S^0\pi^+\pi^+\pi^-$	(Link *et al.*, 2008)	3.1 ± 1.1
$D_s^+ \to K^+K^+K^-$	(Link *et al.*, 2002b)	0.49 ± 0.17
$D_s^+ \to K^+K^+\pi^-$	(Link *et al.*, 2005c)	0.29 ± 0.11

where a D^0 oscillated to a $\bar{D}^0$ and decayed via a Cabibbo favored decays.

The D^0 doubly Cabibbo suppressed decays that have been studied are summarized in Table XXV. The three most precise measurements of the $D^0 \to K^+\pi^-$ decay by CDF (Aaltonen *et al.*, 2008), BABAR (Aubert *et al.*, 2007b), and Belle (Zhang *et al.*, 2006) obtained branching ratios with respect to $D^0 \to K^-\pi^+$ of $(4.15 \pm 0.10) \times 10^{-3}$, $(3.53 \pm 0.08 \pm 0.04) \times 10^{-3}$, and $(3.77 \pm 0.08 \pm 0.05) \times 10^{-3}$ respectively. The agreement between these measurements is not very good, the PDG applies a scale factor of 3.3 for the error on their average to obtain the average ratio of branching fractions to be $(3.80 \pm 0.18) \times 10^{-3}$.

TABLE XXV Doubly Cabibbo suppressed D^0 decays. The first column ($\mathcal{B}$) shows the branching fraction for the decay and the second column (R) shows the ratio of the branching fraction with respect to the corresponding Cabibbo favored decay. Averages from Amsler *et al.* (2008).

Mode	$\mathcal{B}$ (10^{-4})	R (10^{-3})
$D^0 \to K^+\pi^-$	1.48 ± 0.07	3.80 ± 0.18
$D^0 \to K^+\pi^-\pi^0$	3.05 ± 0.17	2.20 ± 0.10
$D^0 \to K^+\pi^-\pi^+\pi^-$	$2.62^{+0.21}_{-0.19}$	$3.23^{+0.25}_{-0.22}$

The decay $D^0 \to K^+\pi^-\pi^0$ was first observed by CLEO (Brandenburg *et al.*, 2001). The PDG average is dominated by the more recent measurements from BABAR (Aubert *et al.*, 2006b) and Belle (Tian *et al.*, 2005).

The first significant $D^0 \to K^+\pi^-\pi^+\pi^-$ observation was made by CLEO (Dytman *et al.*, 2001). The most recent and precise measurement of this decay was done by Belle (Tian *et al.*, 2005).

Both CLEO-c (Dytman *et al.*, 2006) and BABAR (Aubert *et al.*, 2006a) have studied the doubly Cabibbo suppressed decay $D^+ \to K^+\pi^0$. CLEO-c has reconstructed candidates in a 281 pb^{-1} sample of e^+e^- data recorded at the $\psi(3770)$. BABAR has used a sample of 124 fb^{-1} recorded at the $\Upsilon(4S)$. CLEO-c and BABAR finds branching fractions in good agreement with each other, $\mathcal{B}(D^+ \to K^+\pi^0) = (2.24 \pm 0.36 \pm 0.15 \pm 0.08) \times 10^{-4}$ and $\mathcal{B}(D^+ \to K^+\pi^0) = (2.52 \pm 0.46 \pm 0.24 \pm 0.08) \times 10^{-4}$, respectively. The average branching fraction obtained is $(2.37 \pm 0.32) \times 10^{-4}$.

The final state $D^+ \to K^+\pi^+\pi^-$ has been studied by E687 (Frabetti *et al.*, 1995b), E791 (Aitala *et al.*, 1997), and FOCUS (Link *et al.*, 2004b). The average branching fraction from these measurements is $\mathcal{B}(D^+ \to K^+\pi^+\pi^-) = (6.2 \pm 0.7) \times 10^{-4}$.

The decay $D^+ \to K^+K^+K^-$ has been observed by FOCUS (Link *et al.*, 2002b). They measure the ratio of branching fractions $\mathcal{B}(D^+ \to K^+K^+K^-)/\mathcal{B}(D^+ \to K^-\pi^+\pi^+) = (9.49 \pm 2.17 \pm 0.22) \times 10^{-4}$. This gives the branching fraction $\mathcal{B}(D^+ \to K^+K^+K^-) = (8.7 \pm 2.0) \times 10^{-5}$.

VIII. FINAL STATE INTERACTIONS AND AMPLITUDE ANALYSIS

One of the simplest ways to analyze decays of D-mesons is to employ the flavor flow diagram technique described earlier. One potential problem with the application of this technique[1] to charm decays involves assignment of quark amplitudes ($\mathcal{T}$, $\mathcal{A}$, etc.) to a particular decay. The root of the problem involves inelastic final state interactions.

A. Hadronic decays into meson states

Historically, the issue came up with decays of the type $D^0 \to \phi K^0$, which have been claimed to originate entirely from quark exchange amplitudes. Thus, in the topological $SU(3)$ or flavor-flow analysis of this transition only an exchange amplitude $\mathcal{E}$ should be assigned to this decay. However, final-state interaction contributions of the type

$$D^0 \to \eta^{(\prime)} \bar{K}^{0*} \to \phi \bar{K}^0 \tag{98}$$

[1] Similar problems could affect charm decay analysis using the factorization approximation.

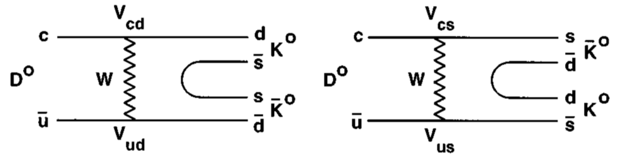

FIG. 27 The two quark diagrams that contribute to the decay $D^0 \to K_S^0 K_S^0$. Since $V_{cd} = -V_{us}$ the two amplitudes represented by these diagrams largely cancel. In the limit that the d and s quark masses where the same the cancellation would have been exact.

could proceed through the color-suppressed internal W-emission diagram $\mathcal{C}$ followed by strong-interaction rescattering $\eta^{(\prime)}\bar{K}^{0*} \to \phi\bar{K}^0$. This contribution is not optional, but is, in fact, required by unitarity (Donoghue, 1986). While in the example above partial cancellation occurs between the intermediate $\eta\bar{K}^{0*}$ and $\eta'\bar{K}^{0*}$ states (Lipkin, 1987), this cancellation is not generic. Similar processes are also possible in D_s-meson decays (Fajfer *et al.*, 2003; Gronau and Rosner, 2009). If large, the contributions of this type could be important in the topological flavor-flow amplitude analysis of charm decays (Cheng, 2003).

One way to study the importance of inelastic final-state interaction contributions in charm decays is to seek guidance from experimental studies of "annihilation" decays, i.e. decays whose contribution is dominated by weak annihilation or exchange amplitudes in the topological flavor-flow analysis.

Another related decay mode that is interesting from this perspective is $D^0 \to K_S K_S$. Naively, there are two W exchange diagrams that contribute to this final state as illustrated in Fig. 27. Since $V_{cd} = -V_{us}$, these amplitudes interfere destructively, so in the flavor $SU(3)_F$ limit the branching ratio for this process is zero. Thus, in addition to being the "pure annihilation" decay, the rate of the $D^0 \to K_S K_S$ transition explicitly probes $SU(3)_F$-breaking corrections. It should be rather small.

Interestingly enough, a naive calculation of this decay rate in factorization gives exactly zero,

$$\begin{aligned} \mathcal{A}(D^0 \to K_S K_S) &= \frac{1}{2}\mathcal{A}(D^0 \to K^0\overline{K}^0) \\ &= f_D p_D \cdot (p_{K^0} - p_{\bar{K}^0}) = 0, \end{aligned} \quad (99)$$

so $\mathcal{B}_{\rm fact}(D^0 \to K_S K_S) = 0$. As we discuss later in this Section, experimental analyses of this transition, however, clearly yield a non-zero result.

The ratio of branching fractions $\mathcal{B}(K_S^0 K_S^0)/\mathcal{B}(K_S^0\pi^+\pi^-)$ has been measured by CLEO (Alexander *et al.*, 1990b), E687 (Frabetti *et al.*, 1994c), CLEO II (Asner *et al.*, 1996), and FOCUS (Link *et al.*, 2005b). CLEO-c (Bonvicini *et al.*, 2008a) has studied this decay using a single tag technique and normalized to the number of $D^0\bar{D}^0$ events produced. These measurements are summarized in Table XXVI. Measurements of the branching ratios $\mathcal{B}(K_S^0 K_S^0)/\mathcal{B}(K_S^0\pi^+\pi^-)$ has been rescaled using $\mathcal{B}(K_S^0\pi^+\pi^-) = (2.99 \pm 0.17)\%$ (Amsler *et al.*, 2008).

The most recent, and most precise, measurement from CLEO-c gives the smallest central value. Given the large uncertainties in the earlier measurements there is no strong inconsistency between the different measurements. This clearly points to shortcomings of factorization calculation outlined above.

One way to understand this branching ratio would be to assume that non-factorizable pieces, dropped in Eq. (99), dominate the branching ratio for $D^0 \to K_S K_S$. There is, however, no reliable way to estimate those (see, however, Eeg *et al.* (2001)). Another way would be to accept that this, and similar branching ratios are dominated by final-state interactions (Lipkin, 1980; Pham, 1987). A simple two-channel model estimates give

$$\Gamma(D^0 \to K^0\overline{K}^0) = \Gamma(D^0 \to K^+K^-)\tan^2\left(\frac{1}{2}(\delta_0 - \delta_1)\right), \quad (100)$$

where δ_0 and δ_1 are the phase shifts for $I = 0$ and $I = 1$ amplitudes. Estimates with other models of final-state interactions give comparable results (Dai *et al.*, 1999). While these estimates are by no means reliable, they serve as an indication of the importance of final-state interactions in charm hadronic decays.

B. Baryonic decay $D_s^+ \to p^+\bar{n}$

Final states with baryons are not possible for the D^0 and D^+. The lightest neutral final state $p\bar{p}$ has a mass of 1876.54 MeV and is just above the D^0 and D^+ mass. However, the D_s^+ is kinematically allowed to decay to $p^+\bar{n}$. This decay is also quite interesting because the flavors of all valence quarks that constitute the initial state ($c\bar{s}$) differ from the flavors of the final-state quarks composing the $p^+\bar{n}$ pair. Thus, it is quite tempting to declare that the transition $D_s^+ \to p^+\bar{n}$ proceeds only via the weak annihilation graph (Chen *et al.*, 2008; Pham, 1980a,b).

A factorization ansatz can be employed in order to estimate the branching ratio for this process (Chen *et al.*, 2008). It must be emphasized again that contrary to hadronic B decays, simple factorization has not been proven in charm transitions, especially as applied to annihilation amplitudes. Nevertheless, a factorized decay amplitude is

$$A(D_s^+ \to p^+\bar{n}) = \frac{G_F}{\sqrt{2}} V_{cs}V_{ud}^* a_1 f_{D_s} p_{D_s}^\mu \langle p\bar{n}|\overline{u}\gamma_\mu (1-\gamma_5)\, d|0\rangle, \quad (101)$$

where $p_{D_s} = p_p + p_{\bar{n}}$ is the four-momentum of a D_s-meson. The matrix element between the vacuum and the final state can be parametrized. First, let us note that vector current conservation implies that

$$p_{D_s}^\mu \langle p\bar{n}|\overline{u}\gamma_\mu (1-\gamma_5)\, d|0\rangle = (m_p + m_{\bar{n}})\langle p\bar{n}|\overline{u}\gamma_5 d|0\rangle, \quad (102)$$

TABLE XXVI The observed branching fractions for $D^0 \to K_S^0 K_S^0$. The errors are statistical, systematic, and from normalization branching fraction $K_S^0\pi^+\pi^-$ when used.

Experiment	Events	$\mathcal{B}(D^0 \to K_S^0 K_S^0)$ (10^{-4})
CLEO-c (Bonvicini *et al.*, 2008a)	68 ± 15	$1.46 \pm 0.32 \pm 0.09$
FOCUS (Link *et al.*, 2005b)	79 ± 17	$4.31 \pm 0.96 \pm 0.48 \pm 0.24$
CLEO II (Asner *et al.*, 1996)	26	$3.02 \pm 0.66 \pm 0.48 \pm 0.17$
E687 (Frabetti *et al.*, 1994c)	20 ± 7	$11.7 \pm 3.9 \pm 3.9 \pm 0.7$
CLEO (Alexander *et al.*, 1990b)	5	$6.3^{+3.3}_{-2.4} \pm 0.6 \pm 0.4$
Average		1.93 ± 0.30

so the decay amplitude can be parameterized as

$$A(D_s^+ \to p^+\bar{n}) = \frac{G_F}{\sqrt{2}} V_{cs} V_{ud}^* a_1 f_{D_s} \times \left(2m_N g_1^{p\bar{n}} + \frac{m_{D_s}^2}{2m_N} g_3^{p\bar{n}}\right) \overline{u}_p \gamma_5 v_{\bar{n}} \tag{103}$$

where $g_i^{p\bar{n}}$ are the formfactors parameterizing the baryon current, and m_N is the nucleon's mass. The two formfactors $g_1^{p\bar{n}}$ and $g_3^{p\bar{n}}$ can be related to each other (Chen *et al.*, 2008; Pham, 1980a,b),

$$g_3^{p\bar{n}}(p_{D_s}^2) = -\frac{4m_N^2}{p_{D_s}^2 - m_\pi^2} g_1^{p\bar{n}}(p_{D_s}^2), \tag{104}$$

so that the decay amplitude takes the form,

$$A(D_s^+ \to p^+\bar{n}) = \frac{2G_F}{\sqrt{2}} V_{cs} V_{ud}^* a_1 f_{D_s} \times m_N \left(\frac{m_\pi}{m_{D_s}}\right)^2 g_1^{p\bar{n}} \; \overline{u}_p \gamma_5 v_{\bar{n}}. \tag{105}$$

This amplitude leads to the estimate of the decay branching ratio $\mathcal{B}(D_s^+ \to p^+\bar{n})$ in the factorization approximation (Chen *et al.*, 2008),

$$\mathcal{B}(D_s^+ \to p^+\bar{n})_{\rm th} = (0.4^{+1.1}_{-0.3}) \times 10^{-6}. \tag{106}$$

The theoretical error quoted in Eq. (106) is entirely due to the uncertainty in the form-factor value of $g_1^{p\bar{n}}(m_{D_s}^2)$ (Chen *et al.*, 2008), which was obtained by extrapolation of the nucleon data with a particularly assumed shape of q^2-dependence. This estimate gives a rather small branching ratio, which nevertheless can be tested experimentally. CLEO-c has studied this final state (Athar *et al.*, 2008).

As (anti-)neutrons are hard to reconstruct, CLEO-c uses a missing mass technique to identify this signal. All particles in the event, except for the (anti-)neutron, is reconstructed and the signal is extracted by looking in the missing mass distribution of the events, which for signal will peak at the neutron mass.

CLEO-c use 325 pb^{-1} of e^+e^- annihilation data collected at a center-of-mass energy of 4170 MeV. CLEO-c uses 8 tag modes ($K^+K^-\pi^-$, $K_S^0K^-$, $\eta\pi^-$, $\eta'\pi^-$, $\phi\rho^-$, $\pi^-\pi^+\pi^-$, $K^{*-}K^{*0}$, and $\eta\rho^-$) to first reconstruct a D_s^- candidate. It is required that this D_s candidate has a reconstructed invariant mass which is within 2.5σ of the known D_s mass. Next, this candidate is combined with a photon. The recoil mass squared against the $D_s^-\gamma$ is calculated and required to be consistent with the mass of the D_s. Note here that it does not matter if the photon came from the D_s^* that is the parent of the D_s^- or from the parent of the other D_s in the event. This missing mass squared distribution is fit to determine the number of tags, CLEO-c reports finding 16,995 D_s tags. This yield will be used as the denominator in the branching fraction calculation.

CLEO-c then searches for the proton candidate in the momentum range from 150 to 550 MeV. In this momentum range CLEO-c uses dE/dx to identify the proton, 550 MeV is below Cherenkov threshold. Kinematic fits are performed to the D_s^-, photon, and proton candidate. Applying these kinematic constraints improve the resolution on the missing mass by a factor of two.

In Fig. 28 the distribution of the recoil mass against the proton shown. There are 13 candidate events consistent with the $D_s^+ \to p^+\bar{n}$ signal. From this yield, the number of tags, and the efficiency for reconstructing the proton, CLEO-c determines the branching fraction

$$\mathcal{B}(D_s^+ \to p^+\bar{n})_{\rm exp} = (1.30 \pm 0.36^{+0.12}_{-0.16}) \times 10^{-3}. \tag{107}$$

This result shows quite unambiguously that the factorization-ansatz estimate of Eq. (106) fails by more than three orders of magnitude. This could be because of the following two reasons. First, the use of a factorization ansatz could be completely misleading for the description of $D_s^+ \to p^+\bar{n}$. This could be due to the fact that the charm quark is too light for the factorization approach to be reliable. In fact, since the mass of the D_s lies right in the middle of the region populated by highly excited light quark resonances, it is possible that the presence of nearby states could significantly affect the decay. In addition, the decay happens almost at the threshold for $p\bar{n}$ production, with no large energy release – something that factorization-based approaches usually require. Second, there could be other decay mechanisms that contribute to this transition besides annihilation. For example, inelastic rescattering discussed above could be responsible

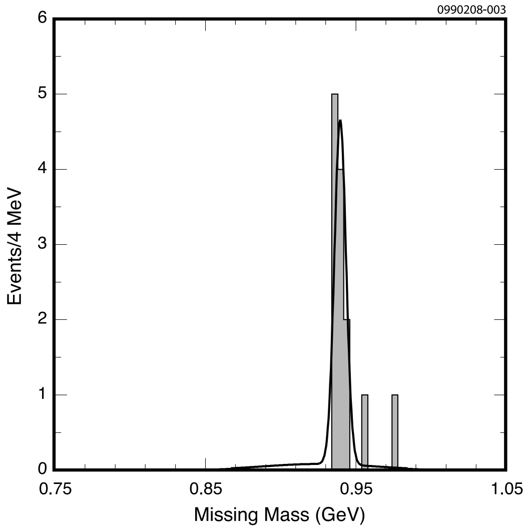

FIG. 28 The missing mass distribution for all $D_s^+ \to p^+\bar{n}$ candidates. CLEO-c sees 13 signal candidates. From Athar *et al.* (2008).

for the bulk of the result. An example of this mechanism would be a tree-level transition $D_s^+ \to \eta^{(\prime)}\pi^+$ with subsequent rescattering $\eta^{(\prime)}\pi^+ \to p^+\bar{n}$. It has been argued (Chen *et al.*, 2008) that this mechanism can provide a contribution that is consistent with the experimentally-measured branching ratio. More work is definitely needed for complete theoretical understanding of this and related processes.

IX. DALITZ DECAYS OF D MESONS

In this Section multibody decays of D mesons are discussed. The most extensive studies of multibody decays are the Dalitz plot studies performed in three-body decays. We give an overview of the analysis techniques used, and discuss some of the final states that have been investigated. Last, a few four-body final states have also been investigated and they are discussed here.

A. Three-body Dalitz plot analyses

Many hadronic three-body final states of D^0, D^+, and D_s^+ meson decays have been studied using a Dalitz plot analysis in which the resonant substructure has been probed. From these analyses we learn about the amplitudes and phases of the different components that contribute to these final states. It is seen that most three-body final states are dominated by pseudo two-body decays.

There is an enormous number of applications of three-body decays of D-mesons. One of the most important applications involves proper determination of branching fractions of quasi-two-body decays, such as $D \to \rho\pi$. Also, the possibility of determination of all relative decay amplitudes and phases in the Dalitz analysis of D^0 decays allows for novel studies of $D^0\overline{D}^0$ mixing and searches of CP violation in the charm system. Finally, Dalitz analyses of D decays offer unique ways to study formation of light-quark structures (such as σ and κ) that are not reachable in direct e^+e^--annihilation experiments.

In a Dalitz plot analysis the dynamics of a decay is investigated by analyzing the kinematic distributions by plotting the data such that the event density is proportional to the matrix element squared (Dalitz, 1953). For the three-body decay $D \to abc$ where a, b, and c are pseudoscalars the decay rate can be written (Amsler *et al.*, 2008)

$$d\Gamma = \frac{1}{32(2\pi)^3 M_D^3} |\mathcal{M}|^2 \; dm_{ab}^2 \; dm_{bc}^2, \qquad (108)$$

where $\mathcal{M}$ is the decay matrix element and $m_{ij}^2 = (p_i + p_j)^2$ is the invariant mass squared of particles i and j. Note that for $\mathcal{M}$ = constant, the Dalitz plot in variables (m_{ab}^2, m_{bc}^2) of Eq. (108) represents a homogeneously-filled shape. Any apparent structures would then represent interactions of the final-state particles.

1. Formalism for Dalitz plot fits

In general, the amplitude for the process $D \to Rc$, $R \to ab$ where R is an intermediate resonance and a, b, and c are particles of arbitrary spin, can be written

$$\mathcal{M}_R(L, m_{ab}, m_{bc}) = \sum_\lambda \langle ab|R_\lambda\rangle T_R(m_{ab}) \langle cR_\lambda|D\rangle \quad (109)$$

where L is the spin of resonance R, and the sum is over the helicity states λ of R. It is customary to break the amplitude of Eq. (109) into three parts,

$$\mathcal{M}_R(L, m_{ab}, m_{bc}) = Z(L, \mathbf{p}, \mathbf{q}) \; B_L^D(|\mathbf{p}|) \; B_L^R(|\mathbf{q}|) \; T_R(m_{ab}), \quad (110)$$

where Z depends on the spin of resonance R and describes the angular distribution of the decay products. If all final-state particles are spin-0, which is the case for all of the decays described here (see Eq. (108)), it reduces to Legendre's polynomials. The B_L's are the spin-dependent Blatt-Weisskopf penetration functions that incorporate effects due to finite-size of the final-state hadrons, and T_R is a function that describes dynamics of the final-state mesons that incorporate a prescription on how to treat the final-state resonances R. The momenta $\mathbf{p}$ and $\mathbf{q}$ of c and a, respectively, are defined in the R rest frame (e.g. $|\mathbf{q}| = \sqrt{(m_R^2 - (m_a + m_b)^2)(m_R^2 - (m_a - m_b)^2)}/2m_R$. The main difference between various analyses of Dalitz plots is related to the chosen model for T_R.

The most common description of Dalitz plots in three-body decays is the so called *isobar model*. In this model amplitudes are added coherently for each resonance. A nonresonant contribution, which describes a direct decay of the D into a 3-body final state, is usually added as a coherent contribution uniformly distributed across the Dalitz plot, making the total amplitude

$$\mathcal{M} = \mathcal{M}_{NR} + \sum_R \mathcal{M}_R(L, m_{ab}, m_{bc}). \tag{111}$$

In the isobar model each resonance is described by a Breit-Wigner lineshape,

$$T_R(m_{ab}) = \left[m_R^2 - m_{ab}^2 - i m_R \Gamma_{ab}(q)\right]^{-1}. \tag{112}$$

Here $\Gamma_{ab}(q)$ describes a momentum-dependent width of the resonance R, which generalizes the narrow-width approximation,

$$\Gamma_{ab}(q) = \Gamma_R \left(\frac{q}{q_0}\right)^{2L+1} \left(\frac{m_0}{m_{ab}}\right) B'_L(q, q_0)^2. \tag{113}$$

Resonant fractions, or fit fractions, are defined, for each resonance R, as

$$f_R = \frac{\int |\mathcal{M}_R|^2}{\int |\mathcal{M}_{NR} + \sum_R \mathcal{M}_R|^2}, \tag{114}$$

where the integration above is over the whole Dalitz plot. The sum of fractions, so defined, is not required to be unity. One must remember that the isobar model is breaking unitarity partly due to the result of interference terms, missing from the denominator, and partly due to kinematic limits imposed on the integrals (Edera, 2004).

The *K-matrix model* is used when a proper description of a Dalitz plot dominated by broad scalar resonances is needed. The K-matrix formalism is, by construction, unitary. It follows from a specific parameterization of the scattering matrix,

$$S_{if} = \delta_{if} + 2iT_{if} = \delta_{if} + 2i\{\rho_i\}^{1/2}\ \hat{T}_{if}\ \{\rho_f\}^{1/2}, \tag{115}$$

where $\hat{T}_{if}$ is a Lorentz-invariant scattering amplitude and $\rho_i = 2q_i/m_i$ are the diagonal elements of the (diagonal) phase space matrix. Here $q_i = m_i\sqrt{1 - 4m_i^2/s}$ is the breakup momentum for decay channel i.

The K-matrix represents a particular parameterization of $\hat{T}$,

$$\hat{T} = \left(\hat{I} - i\hat{K}\hat{\rho}\right)^{-1} \hat{K}. \tag{116}$$

The final-state resonances appear in the K-matrix as a sum of poles. A particular parameterization of the K-matrix can be chosen, which incorporates data from scattering experiments. One useful parameterization of the K-matrix can be found in (Anisovich and Sarantsev, 2003). A good description of K-matrix formalism can be found in (Chung *et al.*, 1995). See also D. Asner's review in (Amsler *et al.*, 2008).

In addition to the isobar model and the K-matrix models presented above, several experiments have used the Model-Independent Partial Wave Analysis (MIPWA). This approach was first used by the E791 collaboration (Aitala *et al.*, 2006). Instead of trying to describe the S-wave as a sum of broad Breit-Wigner resonances, which often leads to unitarity violation when they overlap, or using the K-matrix parameterization, this method parameterizes the amplitude and phase by dividing the $\pi^+\pi^-$ mass spectrum into discrete slices. The amplitude and phase are interpolated using a Relaxed Cubic Spline (Kölbig and Lipps, 1990).

2. Experimental considerations

When analyzing data using a Dalitz plot analysis there are several experimental effects to consider. The reconstruction efficiency for the D candidates is not uniform across the Dalitz plot. The momentum spectrum of the observed particles will depend on the position in the Dalitz plot and affect the efficiency for finding and reconstructing the particles. The effect of efficiency variations across the Dalitz plot is typically incorporated using a Monte Carlo simulation and parameterization of the efficiency as a function of the Dalitz plot variables.

The finite detector resolution is usually neglected as the resonances studied are mostly broad compared to the detector resolution. There are a few exceptions such as $\phi \to K^+K^-$ and $\omega \to \pi^+\pi^-$. In these cases the resolution function has to be convolved with the truth level probability distribution. A related effect is resolution effects near the phase-space boundary in the Dalitz plot. To avoid smearing near the phase-space boundary the final state particles momenta can be recalculated using a constraint to the D mass. This forces the phase-space boundary to be strictly respected.

Experimentally we also have to consider backgrounds that pass the event selection criteria. The backgrounds can be classified into different categories. Combinatorial backgrounds where the selected particles do not all come from the decay of a D. This background may contain resonances, such as a K^* or ρ. We also have backgrounds where all candidates come from a D decay but are not signal. These backgrounds include final states with identical particles, e.g. $D^0 \to K_S^0\pi^0$ contributing to $D^0 \to \pi^+\pi^-\pi^0$ or a $\bar{D}^0$ decay incorrectly identified as a D^0, or misidentified particles such as $D^+ \to \pi^-\pi^+\pi^+$ reconstructed as $D^+ \to K^-\pi^+\pi^+$.

In the following Sections different Dalitz plot analyses will be discussed. As in general it is impossible to average the results of different analysis the most recent, or precise, results are discussed in more detail for each mode.

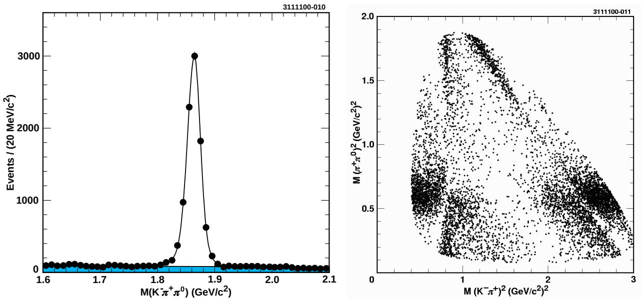

FIG. 29 The left plot shows the $D^0 \to K^-\pi^+\pi^0$ reconstructed mass distribution. The plot to the right shows the $M^2(\pi^+\pi^0)$ versus $M^2(K^-\pi^+)$ Dalitz plot for the 7,070 $D^0 \to K^-\pi^+\pi^0$ candidates. From Kopp *et al.* (2001).

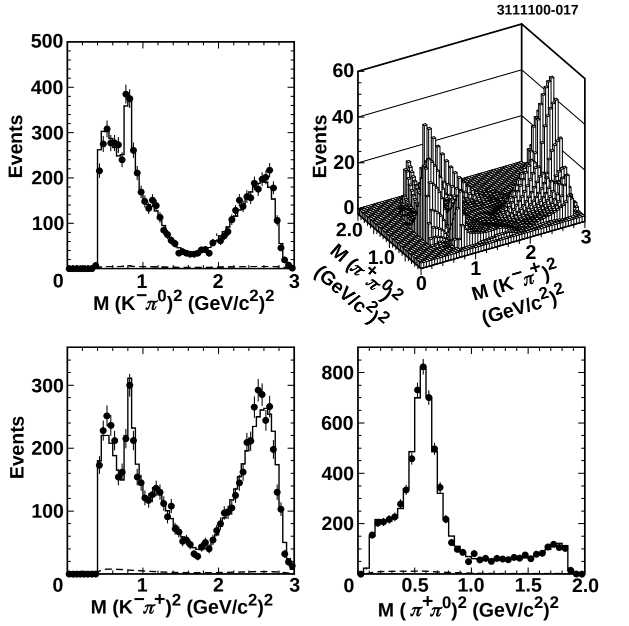

FIG. 30 The $D^0 \to K^-\pi^+\pi^0$ Dalitz fit. From Kopp *et al.* (2001).

3. $D^0 \to K^-\pi^+\pi^0$

The decay $D^0 \to K^-\pi^+\pi^0$ has been studied by the tagged photon spectrometer at Fermilab (Summers *et al.*, 1984), MARK III (Adler *et al.*, 1987), E691 (Anjos *et al.*, 1993) E687 (Frabetti *et al.*, 1994b), and CLEO II (Kopp *et al.*, 2001). The first of these analyses was a simplified Dalitz analysis that did not include the interference. The data was fit to an incoherent sum of $K^-\rho^+$, $\bar{K}^{*0}\pi^0$, $K^{*-}\pi^+$, and nonresonant decays. The latest analysis by CLEO II has about a factor of 10 higher statistics than any of the earlier measurements.

The analysis by CLEO II used 4.7 fb^{-1} of e^+e^- collision data collected at $\sqrt{s} = 10.6$ GeV. The D^0 candidate is required to come from a $D^{*+} \to D^0\pi^+$ decay. The D^0 candidate is required to form a D^{*+} candidate which satisfies $144.9 < M(D^{*+}) - M(D^0) < 145.9$ MeV. The invariant mass distribution of the $K^-\pi^+\pi^0$ candidates and the 7,070 event selected for the Dalitz plot analysis are shown in Fig. 29. This sample has a purity of $96.7 \pm 1.1\%$. The large K^{*0}, ρ^+, and K^{*-} resonances and their interference is easily seen in the Dalitz plot and in the projections of the Dalitz plot fit in Fig. 30. The results of the Dalitz plot fit are summarized in Table XXVII. The $\rho(770)^+$ resonance dominates the Dalitz plot with a fit fraction of 78.8%.

4. $D^0 \to K^0_S\pi^+\pi^-$

The decay $D^0 \to K^0_S\pi^+\pi^-$ is of interest for the extraction of the CKM angle γ in the decays $B^\mp \to D^{(*)}K^\mp$ and $B^\mp \to \bar{D}^{(*)}K^\mp$ (Atwood *et al.*, 2001). When the decay of the D^0 or $\bar{D}^0$ in these decays is to a common final states, such as $K^0_S\pi^+\pi^-$, the two decays above interfere and this allow us to measure the CKM angle γ. To extract γ from this analysis a good understanding of the $D^0 \to K^0_S\pi^+\pi^-$ Dalitz plot is required.

This final state has been investigated by many experiments. The first studies were performed by (Adler *et al.*, 1987; Albrecht *et al.*, 1993; Anjos *et al.*, 1993; Frabetti *et al.*, 1992, 1994b). CLEO was the first experiment to include doubly Cabibbo suppressed decays in the Dalitz plot analysis (Muramatsu *et al.*, 2002) of this decay. They used 10 resonances in their fit: $K^0_S\rho^0$, $K^0_S\omega$, $K^0_S f_0(980)$, $K^0_S f_2(1270)$, $K^0_S f_0(1370)$, $K^*(892)^-\pi^+$, $K^*_0(1430)^-\pi^+$, $K^*_2(1430)^-\pi^+$, $K^*(1680)^-\pi^+$, and the Cabibbo suppressed mode $K^*(892)^+\pi^-$. CLEO found a very small fit fraction for the nonresonant contribution of $(0.9\pm0.4^{+1.0+1.7}_{-0.3-0.2})\%$. They also determined that the phase difference between the Cabibbo allowed $K^*(892)^-\pi^+$ and the doubly Cabibbo suppressed decay $K^*(892)^+\pi^-$ is consistent with 180° as expected from the Cabibbo factors. The significance of the $K^*(892)^+\pi^-$ resonance is 5.5 standard deviations in the study by CLEO.

Both BABAR (Aubert *et al.*, 2005b, 2008a) and Belle (Abe *et al.*, 2008; Poluektov *et al.*, 2006) have studied this decay with samples well over an order of magnitude larger than CLEO in their program to determine the CKM angle γ. BABAR (Aubert *et al.*, 2008a) has used a data sample of 351 fb^{-1} collected at the $\Upsilon(4S)$ to study the $D^0 \to K^0_S\pi^+\pi^-$ Dalitz plot. They reconstruct 487,000 $D^{*+} \to D^0\pi^+$, $D^0 \to K^0_S\pi^+\pi^-$ decays with a purity of 97.7%. The Dalitz plot is fit to a sum of eight different P and D wave resonances. They use three Cabibbo favored resonances $K^*(892)^-$, $K^*(1680)^-$, and $K^*_2(1430)^-$; two doubly Cabibbo suppressed resonances $K^*(892)^+$ and $K^*_2(1430)^+$, and three CP eigenstates $\rho(770)^0$, $\omega(782)$, and $f_2(1270)$. The K-matrix formalism with the P-vector approximation is used to describe the contribution to the amplitude from the $\pi^+\pi^-$ S-wave.

TABLE XXVII Dalitz plot parameters from CLEO II analysis of $D^0 \to K^-\pi^+\pi^0$, from Kopp *et al.* (2001). The errors shown are statistical, experimental systematic, and modeling systematic respectively.

Mode	Fit fraction	Phase (deg)
$\rho(770)^+K^-$	$0.788 \pm 0.019 \pm 0.013 \pm 0.046$	0.0 (fixed)
$K^*(892)^-\pi^+$	$0.161 \pm 0.007 \pm 0.007^{+0.026}_{-0.008}$	$163 \pm 2.3 \pm 3.1 \pm 4.3$
$\bar{K}^*(892)^0\pi^0$	$0.127 \pm 0.009 \pm 0.005 \pm 0.015$	$-0.2 \pm 3.3 \pm 2.2 \pm 7.0$
$\rho(1700)^+K^-$	$0.057 \pm 0.008 \pm 0.007 \pm 0.006$	$171 \pm 6 \pm 5^{+6.1}_{-55}$
$\bar{K}_0^*(1430)^0\pi^0$	$0.041 \pm 0.006 \pm 0.007^{+0.031}_{-0.005}$	$166 \pm 5 \pm 4.6 \pm 12$
$K_0^*(1430)^-\pi^+$	$0.033 \pm 0.006 \pm 0.007 \pm 0.012$	$55.5 \pm 5.8 \pm 3.3^{+4.2}_{-13}$
$K^*(1680)^-\pi^+$	$0.013 \pm 0.003 \pm 0.003 \pm 0.003$	$103 \pm 8 \pm 7 \pm 14$
Nonresonant	$0.075 \pm 0.009 \pm 0.006^{+0.056}_{-0.009}$	$31 \pm 4 \pm 5.5^{+14}_{-3.7}$

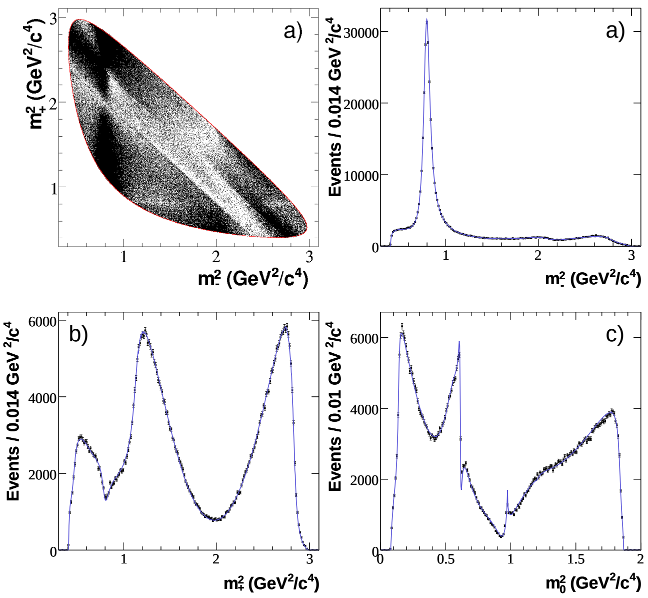

FIG. 31 BABAR $D^0 \to K_S^0\pi^+\pi^-$ Dalitz plot analysis. From Aubert *et al.* (2008a).

TABLE XXVIII Dalitz plot parameters from the BABAR analysis, Aubert *et al.* (2008a), of $D^0 \to K_S^0\pi^+\pi^-$. The errors for the amplitudes and phases include only the statistical errors. The fit fractions quoted include also the systematic uncertainties. Upper limits on fit fractions are quoted at 95% confidence level.

Resonance	Amplitude	Phase (deg)	Fit fraction
$K^*(892)^-$	1.740 ± 0.010	139.0 ± 0.3	55.7 ± 2.8
$K_0^*(1430)^-$	8.2 ± 0.7	153 ± 8	10.2 ± 1.5
$K_2^*(1430)^-$	1.410 ± 0.022	138.4 ± 1.0	2.2 ± 1.6
$K^*(1680)^-$	1.46 ± 0.10	-174 ± 4	0.7 ± 1.9
$K^*(892)^+$	0.158 ± 0.003	-42.7 ± 1.2	0.46 ± 0.23
$K_0^*(1430)^+$	0.32 ± 0.06	143 ± 11	< 0.05
$K_2^*(1430)^+$	0.091 ± 0.016	85 ± 11	< 0.12
$\rho(770)^0$	1 (fixed)	0 (fixed)	21.0 ± 1.6
$\omega(782)$	0.0527 ± 0.0007	126.5 ± 0.9	0.9 ± 1.0
$f_2(1270)$	0.606 ± 0.026	157.4 ± 2.2	0.6 ± 0.7
$\pi\pi$ S-wave			11.9 ± 2.6

The $K\pi$ S-wave includes the $K_0^*(1430)^-$ and $K_0^*(1430)^+$ resonances and a nonresonant component. The data and the fit projections are shown in Fig. 31. The result of the fit is shown in Table XXVIII.

Belle (Poluektov *et al.*, 2006) has used a 357 fb^{-1} sample collected at the $\Upsilon(4S)$ to study the $D^0 \to K_S^0\pi^+\pi^-$ Dalitz plot. They select a sample of 271,621 events for their analysis with an estimated purity of 96.8%. They fit their data to a sum of 15 resonances plus a nonresonant amplitude. The data and projections of their fit are shown in Fig. 32. The result of their fit is summarized in Table XXIX. For the two σ resonances that are included in the fit Belle obtained $M_{\sigma_1} = 519 \pm 6$ MeV, $\Gamma_{\sigma_1} = 454 \pm 12$ MeV, $M_{\sigma_2} = 1050 \pm 6$ MeV, and $\Gamma_{\sigma_2} = 101 \pm 7$ MeV. The wide σ_1 resonance is highly correlated with the nonresonant component. Belle has also reported a preliminary study (Abe *et al.*, 2008) using 605 fb^{-1} of data to study this Dalitz plot.

At this point the uncertainties in γ are limited by statistics. Contributions to the uncertainty on γ from these measurements are not limited by the Dalitz plot uncertainty. But with increased statistics the γ measurement should improve and a better understanding of the Dalitz plot is required. CLEO-c (Briere *et al.*, 2009) has performed a CP- and flavor-tagged Dalitz plot analysis using 818 pb^{-1} of data collected at the $\psi(3770)$ resonance. In this analysis the final states $K_S^0\pi^+\pi^-$ and $K_L^0\pi^+\pi^-$ are studied in decays where they recoil against a flavor-tagged, CP-tagged, or $K_S^0\pi^+\pi^-$ decay of the other D meson in the $\psi(3770)$ decay. The Dalitz plot is binned into eight regions and fit for the average interference between the D^0 and $\bar{D}^0$ in the bin. This allows the extraction of the relative strong phase between $D^0 \to K_s^0\pi^+\pi^-$ and $\bar{D}^0 \to K_s^0\pi^+\pi^-$, which is required for the extraction of the CKM angle γ. The CLEO-c measurement reduces the systematic uncertainty from the strong phase difference on the determination of γ to about 1.7°.

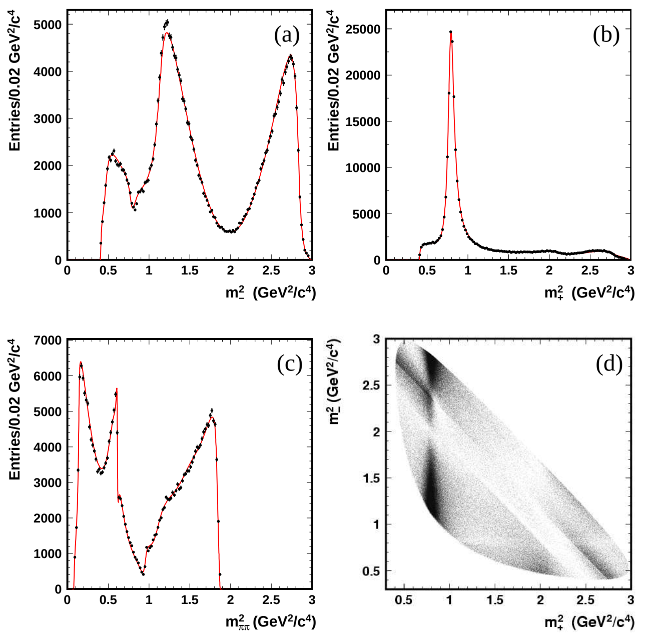

FIG. 32 Belle $D^0 \to K_S^0\pi^+\pi^-$ Dalitz plot analysis. (a) the $m^2(K_S^0\pi^+)$, (b) the $m^2(K_S^0\pi^-)$, and (c) the $m^2(\pi^-\pi^+)$ distributions are shown and in (d) the Dalitz plot distribution. The points with error bars show the data and the smooth curve is the result of the fit. From Poluektov *et al.* (2006).

5. $D^0 \to \pi^-\pi^+\pi^0$

The Dalitz plot of $D^0 \to \pi^-\pi^+\pi^0$ has been studied by BABAR as a means to extract information about the CKM parameter γ (Aubert *et al.*, 2007c) similar to what was done with $D^0 \to K_S^0\pi^+\pi^-$. CLEO has also studied this decay (Muramatsu *et al.*, 2002). BABAR reconstructs $44,780 \pm 250$ signal events over a background of 830 ± 70 events. The Dalitz plot of these events is shown in Fig. 33. The three ρ bands are clearly visible with a strong destructive interference. BABAR used 15 resonances plus a nonresonant contribution to fit the data. The results of the fit are summarized in Table XXX. The $\rho(770)$ resonances are clearly the strongest features on the Dalitz plot, with fit fractions adding to (128.6 ± 1.6)%. The $\rho(1700)$ resonances contribute with fit fractions of 3 to 5% each, much smaller than the dominant contributions. The remaining amplitudes, including nonresonant, are much smaller. The large, destructively interfering, $\rho\pi$ amplitudes are suggestive of an $I = 0$ dominated final state (Zemach, 1965). This is consistent with the observation that $D^0 \to 3\pi^0$ is strongly suppressed.

6. $D^0 \to K^+K^-\pi^0$

CLEO (Besson *et al.*, 2006) and BABAR (Aubert *et al.*, 2007a) have both studied the Dalitz plot of this decay. The BABAR analysis used 358 fb^{-1} of e^+e^- collision data collected near the $\Upsilon(4S)$ resonance. A sample with a high purity of about 98.1% was selected for this study containing $11,278\pm110$ $D^{*+} \to D^0\pi^+$ tagged candidates. The Dalitz plot and the best isobar fit is shown in Fig. 34. The isobar model allows for several different solutions that each give a similarly good description of the data. At low K^+K^- invariant mass an S-wave K^+K^- contribution is needed, but the fit can not dis-

TABLE XXIX Dalitz plot parameters from Belle analysis of $\bar{D}^0 \to K_S^0\pi^+\pi^-$, from Poluektov *et al.* (2006). Errors are statistical only.

Resonance	Amplitude	Phase (deg)	Fit fraction (%)
$K_S^0\sigma_1$	1.43 ± 0.07	212 ± 3	9.8
$K_S^0\rho^0$	1 (fixed)	0 (fixed)	21.6
$K_S^0\omega$	$(31.4 \pm 0.8) \times 10^{-3}$	110.8 ± 1.6	0.4
$K_S^0 f_0(980)$	0.365 ± 0.006	201.9 ± 1.9	4.9
$K_S^0\sigma_2$	0.23 ± 0.02	237 ± 11	0.6
$K_S^0 f_2(1270)$	1.32 ± 0.04	348 ± 2	1.5
$K_S^0 f_0(1370)$	1.44 ± 0.10	82 ± 6	1.1
$K_S^0\rho(1370)^0$	0.66 ± 0.07	9 ± 8	0.4
$K^*(892)^+\pi^-$	1.644 ± 0.010	132.1 ± 0.5	61.2
$K^*(892)^-\pi^+$	0.144 ± 0.004	320.3 ± 1.5	0.55
$K^*(1410)^+\pi^-$	0.61 ± 0.06	113 ± 4	0.05
$K^*(1410)^-\pi^+$	0.45 ± 0.04	254 ± 5	0.14
$K_0^*(1430)^+\pi^-$	2.15 ± 0.04	353.6 ± 1.2	7.4
$K_0^*(1430)^-\pi^+$	0.47 ± 0.04	88 ± 4	0.43
$K_2^*(1430)^+\pi^-$	0.88 ± 0.03	318.7 ± 1.9	2.2
$K_2^*(1430)^-\pi^+$	0.25 ± 0.02	265 ± 6	0.09
$K^*(1680)^+\pi^-$	1.39 ± 0.27	103 ± 12	0.36
$K^*(1680)^-\pi^+$	1.2 ± 0.2	118 ± 11	0.11
Nonresonant	3.0 ± 0.3	164 ± 5	9.7

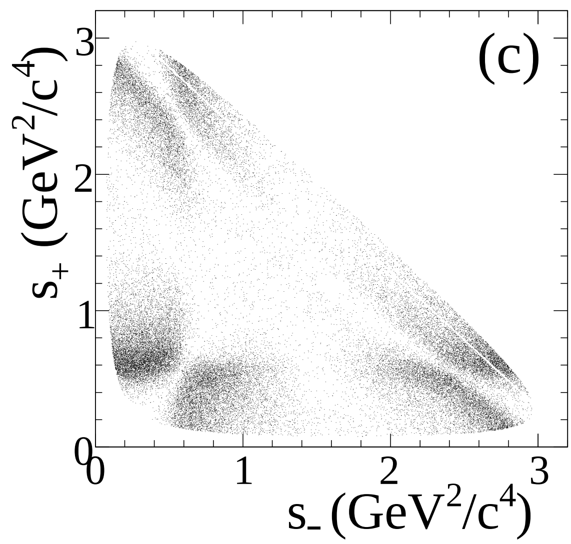

FIG. 33 BABAR Dalitz plot of $s_+ = m^2_{\pi^+\pi^0}$ *vs.* $s_- = m^2_{\pi^-\pi^0}$ for the $D^0 \to \pi^+\pi^-\pi^0$ decay. From Aubert *et al.* (2007c).

TABLE XXX Dalitz plot parameters from BABAR analysis, Aubert *et al.* (2007c), of $D^0 \to \pi^-\pi^+\pi^0$.

Resonance	Amplitude ratio (%)	Phase (deg)	Fit fraction
$\rho(770)^+$	100 (fixed)	0 (fixed)	$67.8 \pm 0.0 \pm 0.6$
$\rho(770)^0$	$58.8 \pm 0.6 \pm 0.2$	$16.2 \pm 0.6 \pm 0.4$	$26.2 \pm 0.5 \pm 1.1$
$\rho(770)^-$	$71.4 \pm 0.8 \pm 0.3$	$-2.0 \pm 0.6 \pm 0.6$	$34.6 \pm 0.8 \pm 0.3$
$\rho(1450)^+$	$21 \pm 6 \pm 13$	$-146 \pm 18 \pm 24$	$0.11 \pm 0.07 \pm 0.12$
$\rho(1450)^0$	$33 \pm 6 \pm 4$	$10 \pm 8 \pm 12$	$0.30 \pm 0.11 \pm 0.07$
$\rho(1450)^-$	$82 \pm 5 \pm 4$	$16 \pm 3 \pm 3$	$1.79 \pm 0.22 \pm 0.12$
$\rho(1700)^+$	$225 \pm 18 \pm 14$	$-17 \pm 2 \pm 3$	$4.1 \pm 0.7 \pm 0.7$
$\rho(1700)^0$	$251 \pm 15 \pm 13$	$-17 \pm 2 \pm 2$	$5.0 \pm 0.6 \pm 1.0$
$\rho(1700)^-$	$100 \pm 11 \pm 7$	$-50 \pm 3 \pm 3$	$3.2 \pm 0.4 \pm 0.6$
$f_0(980)$	$1.50 \pm 0.12 \pm 0.17$	$-59 \pm 5 \pm 4$	$0.25 \pm 0.04 \pm 0.04$
$f_0(1370)$	$6.3 \pm 0.9 \pm 0.9$	$156 \pm 9 \pm 6$	$0.37 \pm 0.11 \pm 0.09$
$f_0(1500)$	$5.8 \pm 0.6 \pm 0.6$	$12 \pm 9 \pm 5$	$0.39 \pm 0.08 \pm 0.07$
$f_0(1710)$	$11.2 \pm 1.4 \pm 1.7$	$51 \pm 8 \pm 7$	$0.31 \pm 0.07 \pm 0.08$
$f_2(1270)$	$104 \pm 3 \pm 21$	$-171 \pm 3 \pm 4$	$1.32 \pm 0.08 \pm 0.10$
$\sigma(400)$	$6.9 \pm 0.6 \pm 1.2$	$8 \pm 4 \pm 8$	$0.82 \pm 0.10 \pm 0.10$
Nonresonant	$57 \pm 7 \pm 8$	$-11 \pm 4 \pm 2$	$0.84 \pm 0.21 \pm 0.12$

tinguish between an $a_0(980)$ and a $f_0(980)$. Similarly, at intermediate K^+K^- invariant mass either a $f_2'(1525)$ or an f_0 with a similar mass works. In the study of this Dalitz plot the relative amplitude and phase of the amplitudes for $D^0 \to K^{*-}K^+$ to $D^0 \to K^{*+}K^-$ can be measured. Defining r_D and δ_D by

$$r_D e^{i\delta_D} \equiv \frac{a_{D^0\to K^{*-}K^+}}{a_{D^0\to K^{*+}K^-}}, \tag{117}$$

BABAR obtains

$$r_D = 0.599 \pm 0.013(\text{stat}) \pm 0.011(\text{syst}) \tag{118}$$

and

$$\delta_D = -35.5^\circ \pm 1.9^\circ(\text{stat}) \pm 2.2^\circ(\text{syst}) \tag{119}$$

consistent with the earlier CLEO results.

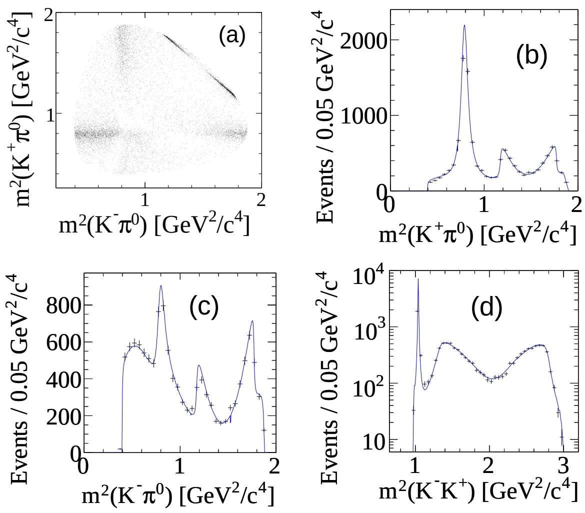

FIG. 34 BABAR $D^0 \to K^+K^-\pi^0$ Dalitz plot analysis. From Aubert *et al.* (2007a).

7. $D^0 \to K^+K^-K^0_S$

The $D^0 \to K^+K^-K^0_S$ mode has been studied by BABAR (Aubert *et al.*, 2005a, 2008a) as part of an analysis for γ determination. BABAR uses a sample of 69,000 reconstructed $D^0 \to K^+K^-K^0_S$ decays with a purity of 99.3%. The data, shown in Fig. 35 was fit to an isobar model which includes eight resonances. The result of this fit is summarized in Table XXXI. In the fit BABAR floats the mass and width of the $\phi(1020)$. The $a_0(980)$ resonance has a mass very close to KK threshold and decays primarily to $\eta\pi$ and is described by a coupled channel Breit-Wigner line shape. The data is well described by the fit, BABAR finds a reduced χ^2 of 1.09 for 6,856 degrees of freedom.

8. $D^0 \to K^0_S\eta\pi^0$

The decay $D^0 \to K^0_S\eta\pi^0$ has been studied using a 9.0 fb^{-1} data sample collected using the CLEO II.V detector in e^+e^- collisions at the $\Upsilon(4S)$ resonance (Rubin *et al.*, 2004). The sample contained 155 $D^0 \to K^0_S\eta\pi^0$ candidate events. The two large contributions to this decay come from $K^*(892)^0\eta$ and $a_0(980)^0K^0_S$. The projections of the Dalitz plot fit is shown in Fig. 36. Fixing the amplitude for $a_0(980)^0K^0_S$ to be 1 with a zero phase CLEO measured

$$a_{K^*(892)^0\eta} = 0.249 \pm 0.032 \pm 0.013 \pm 0.018, \tag{120}$$

$$\phi_{K^*(892)^0\eta} = (259 \pm 12 \pm 9 \pm 6)^\circ, \tag{121}$$

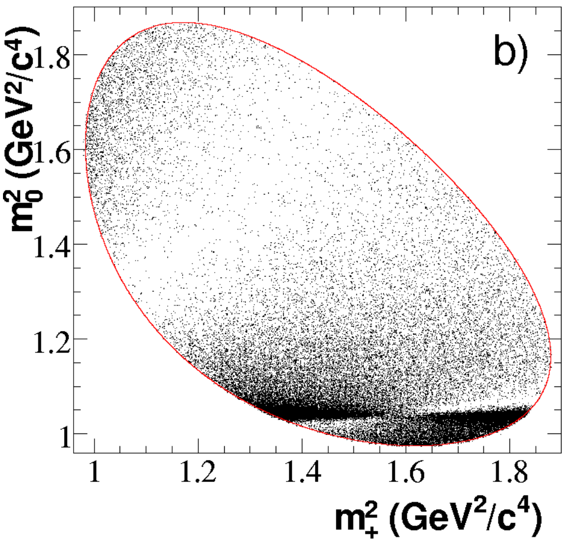

FIG. 35 Dalitz plot distribution from the BABAR analysis of $D^0 \to K^+K^-K^0_S$. The invariant mass squares plotted are $m_0^2 = m^2(K^+K^-)$ and $m_+^2 = m^2(K^+K^0_S)$ for a D^0 decay and the charge conjugate particles are used for the $\bar{D}^0$ decay. From Aubert *et al.* (2008a).

TABLE XXXI Dalitz plot parameters from BABAR analysis of $D^0 \to K^+K^-K^0_S$. Errors are only statistical. From (Aubert *et al.*, 2008a).

Resonance	Amplitude	Phase (deg)	Fit fraction (%)
$K^0_S a_0(980)^0$	1	0	55.8
$K^0_S \phi(1020)^0$	0.227 ± 0.005	56.2 ± 1.0	44.9
$K^0_S f_0(1370)$	0.04 ± 0.06	2 ± 80	0.1
$K^0_S f_2(1370)$	0.261 ± 0.020	9 ± 6	0.3
$K^0_S a_0(1450)^0$	0.65 ± 0.09	95 ± 10	12.6
$K^- a_0(980)^+$	0.562 ± 0.015	179 ± 3	16.0
$K^- a_0(1450)^+$	0.84 ± 0.04	97 ± 4	21.8
$K^+ a_0(1450)^-$	0.118 ± 0.015	138 ± 7	0.7

$$\mathrm{FF}(K^*(892)^0\eta) = 0.293 \pm 0.062 \pm 0.029 \pm 0.019, \quad (122)$$
$$\mathrm{FF}(a_0(980)^0 K^0_S) = 1.19 \pm 0.09 \pm 0.20 \pm 0.16, \quad (123)$$
$$(124)$$

where the errors are statistical, systematic, and model dependence respectively. For the model dependence CLEO considered alternative models where they added additional resonances. They considered four different alternative fits including: a nonresonant component, $K_0^*(1430)\eta$, $K_0^*(1430)\eta + a_2(1320)K^0_S$, and $\kappa\eta$. The fit probability for these different fits were 6.4%, 19.4%, 64.7%, and 49.9% respectively. The fit with only two resonances had a probability of 0.8%. From these alternative fits CLEO-c derives a fit fraction of $0.246 \pm 0.092 \pm 0.024 \pm 0.087$ for any additional components beyond the $K^*(892)^0\eta$ and $a_0(980)^0K^0_S$.

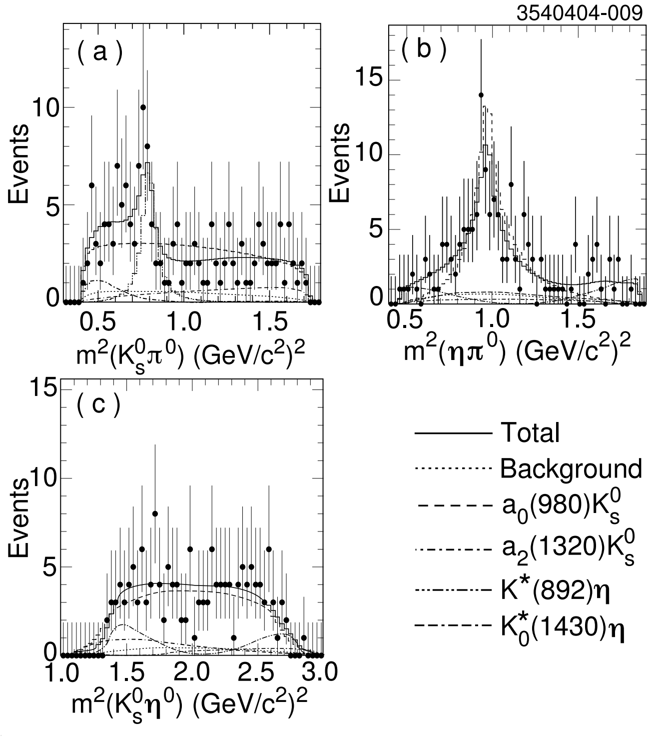

FIG. 36 CLEO $D^0 \to K^0_S\eta\pi^0$ Dalitz plot analysis. From Rubin *et al.* (2004).

9. $D^+ \to K^-\pi^+\pi^+$

The decay $D^+ \to K^-\pi^+\pi^+$ is one of the largest decays of the D^+. CLEO-c has measured the branching fraction to be $\mathcal{B}(D^+ \to K^-\pi^+\pi^+) = (9.15 \pm 0.10 \pm 0.16 \pm 0.07)\%$. The Dalitz plot for this decay has been studied by several experiments MARK III (Adler *et al.*, 1987), NA14 (Alvarez *et al.*, 1991), E691 (Anjos *et al.*, 1993), E687 (Frabetti *et al.*, 1994b), E791 (Aitala *et al.*, 2002, 2006), CLEO-c (Bonvicini *et al.*, 2008b), and most recently by FOCUS (Link *et al.*, 2009). This Dalitz plot is interesting as the only clear resonant contribution from $K^*(892)^0$ only has a 12% fit fraction and a contribution of over 60% from $K\pi$ S-wave. E791 (Aitala *et al.*, 2002) obtained a good fit including a large low-mass $K^-\pi^+$ scalar resonance κ. This fit obtained fit fractions that were significantly different from earlier studies. E791 (Aitala *et al.*, 2006) re-analyzed the data using a model-independent partial wave analysis. The CLEO-c analysis also uses the same model independent partial wave analysis.

The CLEO-c study is based on 572 pb^{-1} of e^+e^- collision data collected at the $\psi(3770)$ resonance. The data sample selected for the Dalitz plot analysis consists of 140,793 events with a background of about 1.1%. The projections of the Dalitz plot is shown in Fig. 37. The CLEO-c analysis finds that in order to get a good description of the data, either in the isobar model or using the model-independent partial wave analysis for the $K\pi$ S-wave, they need to include a $I = 2$ $\pi^+\pi^+$ S-wave.

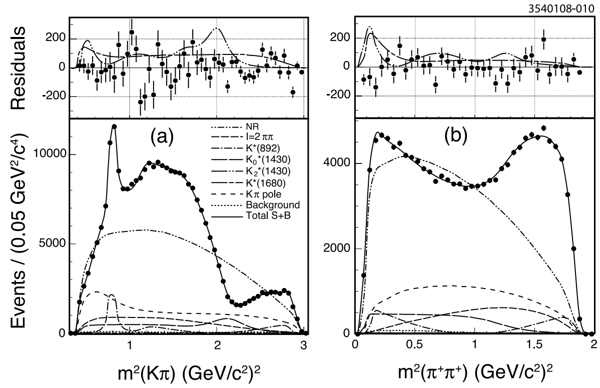

FIG. 37 Projections of the Dalitz plot fit in the CLEO-c Dalitz plot analysis of $D^+ \to K^-\pi^+\pi^+$ in a) for $m^2(K\pi)$ (two entries per candidate, b) for $m^2(\pi^+\pi^+)$. The data are shown as points with error bars. The insets on top shows the residuals between the data and the as points with error bars. The small contributions in the fit from the $K^*(1680)$ and $K_2^*(1430)$ resonances are also shown in the insets enhanced by a factor of 10. From Bonvicini *et al.* (2008b).

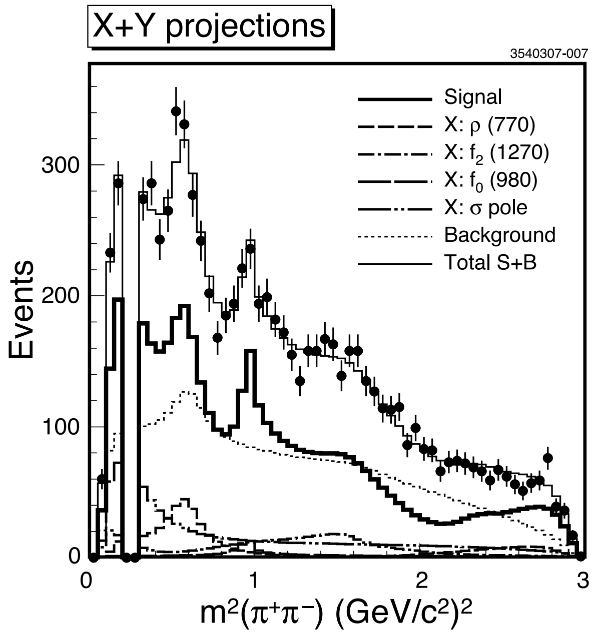

FIG. 38 CLEO-c $D^+ \to \pi^+\pi^-\pi^+$ Dalitz plot analysis. From Bonvicini *et al.* (2007).

CLEO-c implements this $I = 2$ $\pi^+\pi^+$ S-wave either using an analytic form or using a model-independent partial wave analysis. The model-independent partial wave analysis results agree with the analytic form and both give a good fit. CLEO-c finds a fit fraction of about 10 to 15% for the $I = 2$ $\pi^+\pi^+$ S-wave. The almost constant $K\pi$ S-wave amplitude from threshold to about 1.4 GeV with a slow phase variation does not show evidence for a κ resonance.

The FOCUS analysis used a sample of 53,595 events with a purity of 98.8% to perform a model independent partial wave analysis to study the $K\pi$ S-wave. The result for the $K\pi$ S-wave is consistent with CLEO-c, only small amplitude variations below 1.4 GeV and a smoothly changing phase.

TABLE XXXII Dalitz plot parameters obtained by the CLEO-c analysis, from Bonvicini *et al.* (2007), of $D^+ \to \pi^+\pi^-\pi^+$.

Resonance	Amplitude	Phase (deg)	Fit fraction (%)
$\rho(770)^0\pi^+$	1 (fixed)	0 fixed	$20.0 \pm 2.3 \pm 0.9$
$f_0(980)\pi^+$	$1.4 \pm 0.2 \pm 0.2$	$12 \pm 10 \pm 5$	$4.1 \pm 0.9 \pm 0.3$
$f_2(1270)\pi^+$	$2.1 \pm 0.2 \pm 0.1$	$-123 \pm 6 \pm 3$	$18.2 \pm 2.6 \pm 0.7$
$f_0(1370)\pi^+$	$1.3 \pm 0.4 \pm 0.2$	$-21 \pm 15 \pm 14$	$2.6 \pm 1.8 \pm 0.6$
$f_0(1500)\pi^+$	$1.1 \pm 0.3 \pm 0.2$	$-44 \pm 13 \pm 16$	$3.4 \pm 1.0 \pm 0.8$
σ pole	$3.7 \pm 0.3 \pm 0.2$	$-3 \pm 4 \pm 2$	$41.8 \pm 1.4 \pm 2.5$

10. $D^+ \to \pi^+\pi^+\pi^-$

The $D^+ \to \pi^+\pi^+\pi^-$ decay has been studied by E687 (Frabetti *et al.*, 1997), E691 (Anjos *et al.*, 1989), E791(Aitala *et al.*, 2001a), FOCUS (Link *et al.*, 2004a), and CLEO-c (Bonvicini *et al.*, 2007). The most recent analysis, with the largest data sample, is the CLEO-c analysis. The earlier analysis by E791 had reported the need to add a $\sigma(500)$ Breit-Wigner to the $\pi^+\pi^-$ S-wave in order to get an acceptable fit. FOCUS analyzed this mode using a K-matrix description of the $\pi^+\pi^-$ S-wave. They obtained an acceptable fit, but did not rule out the need for a $\sigma(500)$. CLEO-c has studied these decays with a sample of about 2,600 signal events, excluding the K_S^0 events. The nominal fit using the isobar model supports the need for a $\sigma\pi^+$ component. The fit to the isobar model is shown in Figure 38 and the result from the fit is summarized in Table XXXII.

11. $D^+ \to K^+K^-\pi^+$

The Dalitz plot of the Cabibbo suppressed decay $D^+ \to K^+K^-\pi^+$ has been studied by E687 (Frabetti *et al.*, 1995a) and CLEO-c (Rubin *et al.*, 2008). The CLEO-c analysis uses a sample about 20 times larger than E687. For the Dalitz analysis a sample with about 23,000 events were used with a purity of (84.3 ± 0.1)% was used.

The best fit (labeled 'Fit B' in the CLEO-c paper) is shown in Fig. 39 and the result of the fit is summarized in Table XXXIII. The total fit fraction is (86.1 ± 1.1)% and the fit had a χ^2/d.o.f.=895/708. CLEO-c also report results from two additional fits with different $K\pi$ S-wave parameterizations. Instead of the $\kappa(800)$ they tried a non-resonant contribution and a parameterization from the LASS experiment (Aston *et al.*, 1988). Both of these fits were of similar quality.

TABLE XXXIII Dalitz plot parameters from CLEO-c analysis, from Rubin *et al.* (2008), of $D^+ \to K^+K^-\pi^+$, results are from their 'Fit B'.

Resonance	Amplitude	Phase (deg)	Fit fraction (%)
$\bar{K}^*(892)^0K^+$	1 (fixed)	0 (fixed)	$25.7 \pm 0.5^{+0.4+0.1}_{-0.3-1.2}$
$\bar{K}_0^*(1430)^0K^+$	$4.56 \pm 0.13^{+0.10+0.42}_{-0.01-0.39}$	$70 \pm 6^{+1+16}_{-6-23}$	$18.8 \pm 1.2^{+0.6+3.2}_{-0.1-3.4}$
$\phi\pi^+$	$1.166 \pm 0.015^{+0.001+0.025}_{-0.009-0.009}$	$-163 \pm 3^{+1+14}_{-1-5}$	$27.8 \pm 0.4^{+0.1+0.2}_{-0.3-0.4}$
$a_0(1450)^0\pi^+$	$1.50 \pm 0.10^{+0.09+0.92}_{-0.06-0.33}$	$116 \pm 2^{+1+7}_{-1-14}$	$4.6 \pm 0.6^{+0.5+7.2}_{-0.3-1.8}$
$\phi(1680)\pi^+$	$1.86 \pm 0.20^{+0.02+0.62}_{-0.08-0.77}$	$-112 \pm 6^{+3+19}_{-4-12}$	$0.51 \pm 0.11^{+0.01+0.37}_{-0.04-0.15}$
$\bar{K}_2^*(1430)^0K^+$	$7.6 \pm 0.8^{+0.5+2.4}_{-0.6-4.8}$	$171 \pm 4^{+0+24}_{-2-11}$	$1.7 \pm 0.4^{+0.3+1.2}_{-0.2-0.7}$
$\kappa(800)\pi^+$	$2.30 \pm 0.13^{+0.01+0.52}_{-0.11-0.29}$	$-87 \pm 6^{+2+15}_{-3-10}$	$7.0 \pm 0.8^{+0.0+3.5}_{-0.6-1.9}$

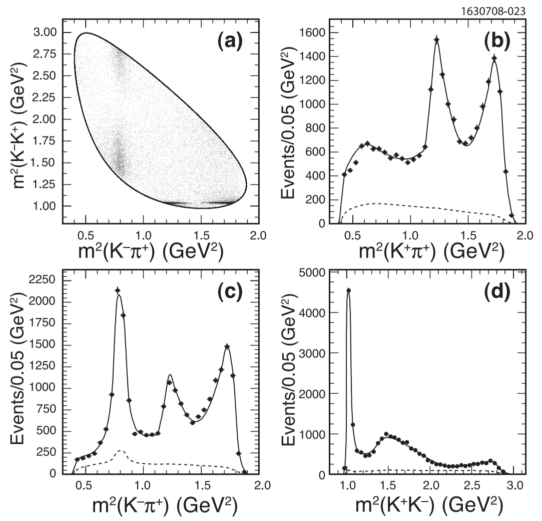

FIG. 39 CLEO-c $D^+ \to K^+K^-\pi^+$ Dalitz plot analysis, from Rubin *et al.* (2008). (a) The Dalitz plot distribution. (b)-(d) the projections of the fit (solid) line and the data (points). The dashed line shows the background contribution.

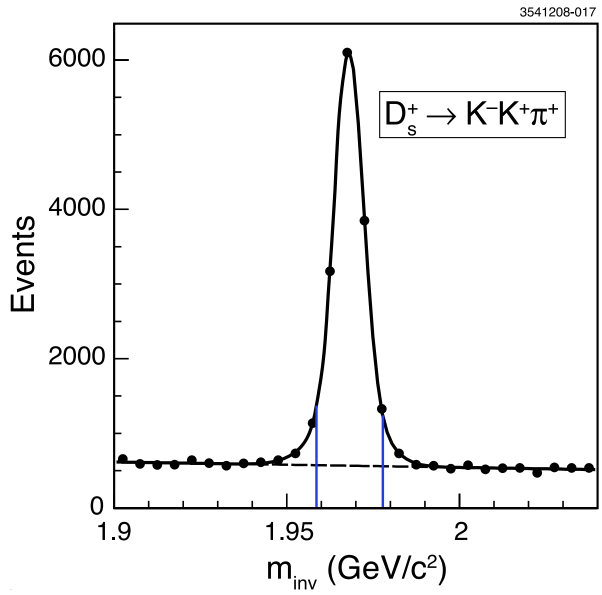

FIG. 40 The $K^+K^-\pi^+$ invariant mass for the signal candidates in the CLEO-c Dalitz plot analysis of $D_s^+ \to K^+K^-\pi^+$. From Mitchell *et al.* (2009).

12. $D_s^+ \to K^+K^-\pi^+$

The Dalitz plot for $D_s^+ \to K^+K^-\pi^+$ is of interest as it contains the large $D_s^+ \to \phi\pi^+$ contribution that traditionally has been the reference branching fraction for D_s^+ decays. The decay $D_s^+ \to K^+K^-\pi^+$ has been studied by E687 (Frabetti *et al.*, 1995a) using a sample of 701 events. This analysis showed evidence for a large $D_s^+ \to f_0(980)\pi^+$ contribution. FOCUS has also reported a preliminary study of this Dalitz plot (Malvezzi, 2002). Most recently CLEO-c (Mitchell *et al.*, 2009) has reported results from their study of the Dalitz plot in this decay.

The CLEO-c analysis uses 586 pb^{-1} of e^+e^- collision data collected at $\sqrt{s} = 4.17$ GeV. In this analysis about 14,400 $D_s^+ \to K^+K^-\pi^+$ candidates are reconstructed with a background of about 15%. The invariant mass distribution for the $K^+K^-\pi^+$ candidates are shown in Fig. 40. The Dalitz plot is shown in Fig. 41. Clearly visible in this plot are the ϕ and K^{*0} resonances.

The data are fit to an isobar model including the $f_0(980)$, ϕ, $f_0(1370)$, $f_0(1710)$, $K^*(892)$, and $K_0^*(1430)$ resonances. CLEO-c finds that all resonances studied by E687 are significant, but that in order to obtain a good fit they need to add an additional K^+K^- resonance. Several resonant, or nonresonant, contributions give a similar improvement of the fit quality, though the $f_0(1370)$ gives the best fit and is used in the main result. The result of this fit is shown in Fig. 42. A summary of the amplitudes and phases extracted from this fit is shown in Table XXXIV. CLEO-c obtains a reasonably good fit, $\chi^2/\text{d.o.f} = 178/117$, using these resonances. It is interesting to note the large $f_0(980)$ contribution in the same mass regions as the $\phi(1020)$. As the $f_0(980)$ is spin zero and the $\phi(1020)$ is spin one the angular distributions are very different for the produced K^+K^- pair for the two resonances.

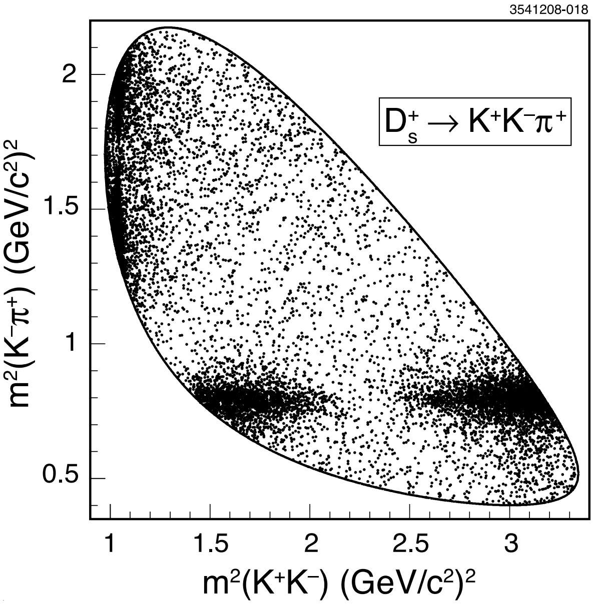

FIG. 41 The Dalitz plot for $D_s^+ \to K^+K^-\pi^+$ candidates in the CLEO-c analysis of $D_s^+ \to K^+K^-\pi^+$. From Mitchell *et al.* (2009).

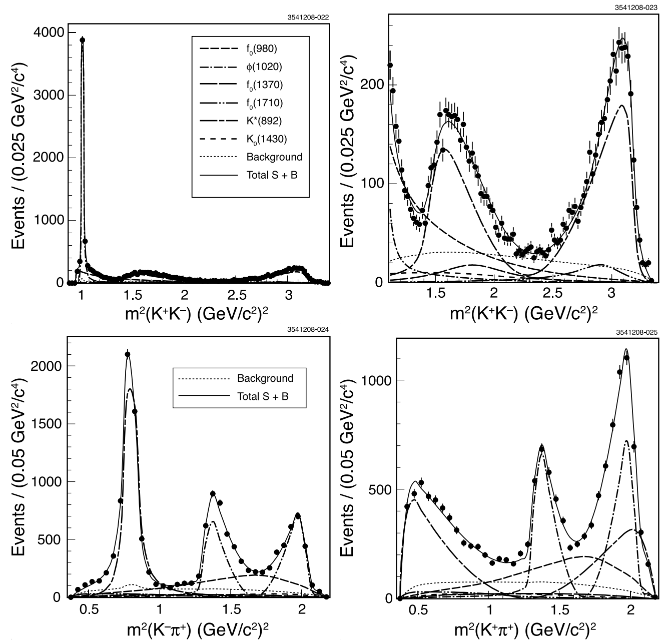

FIG. 42 The CLEO-c Dalitz plot fit for $D_s^+ \to K^+K^-\pi^+$ candidates. From Mitchell *et al.* (2009).

13. $D_s^+ \to \pi^+\pi^-\pi^+$

The decay $D_s^+ \to \pi^+\pi^-\pi^+$ has been studied by E791 (Aitala *et al.*, 2001b), FOCUS (Link *et al.*, 2004a), and BABAR (Aubert *et al.*, 2009). The BABAR analysis selects 13,179 events with a purity of 80%. The invariant mass distribution of the $D_s^+ \to \pi^+\pi^-\pi^+$ candidates is shown in Fig. 43 and the symmetrized Dalitz plot distribution is shown in Fig. 44. The symmetrized plot shows two entries in the Dalitz plot for each candidate. The analysis by BABAR includes three resonances, $f_2(1270)\pi^+$, $\rho(770)\pi^+$, and $\rho(1450)\pi^+$. In addition to these P- and D-wave resonances the MIPWA is used for the $\pi^+\pi^-$ S-wave. This method parameterizes the amplitude and phase by dividing the $\pi^+\pi^-$ mass spectrum into 29 slices. The results for the amplitudes and phases from the fit for the parameterization of the S-wave clearly show the $f_0(980)$ resonance. There is also some evidence for the $f_0(1370)$ and $f_0(1500)$. In Table XXXV the summary of the fit is given. The S-wave parameterization accounts for a fit fraction of $(83.0 \pm 0.9 \pm 1.9)$%. This decay also has an important contribution from a spin-2 resonance, $D_s^+ \to f_2(1270)\pi^+$.

TABLE XXXIV Dalitz plot parameters from CLEO-c analysis, Mitchell *et al.* (2009), of $D_s^+ \to K^-K^+\pi^+$.

Resonance	Amplitude	Phase (deg)	Fit fraction (%)
$\bar{K}^*(892)^0K^+$	1 (fixed)	0 (fixed)	48.2 ± 1.2
$\bar{K}_0^*(1430)^0K^+$	1.76 ± 0.12	145 ± 8	5.3 ± 0.7
$f_0(980)\pi^+$	3.67 ± 0.13	156 ± 3	16.8 ± 1.1
$\phi(1020)\pi^+$	1.15 ± 0.02	-15 ± 4	42.7 ± 1.3
$f_0(1710)\pi^+$	1.27 ± 0.07	102 ± 4	4.4 ± 0.4

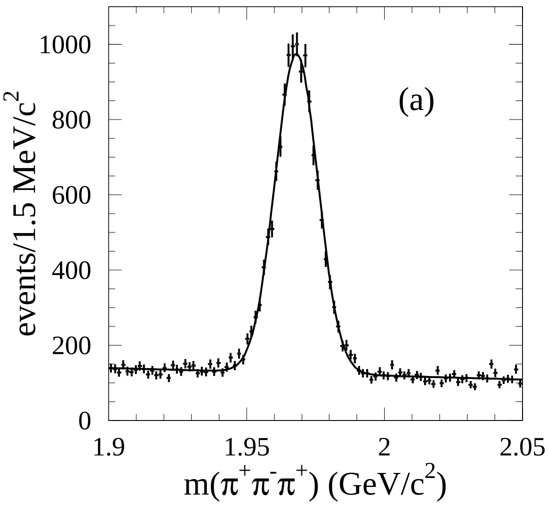

FIG. 43 The $\pi^+\pi^-\pi^+$ invariant mass for the signal candidates in the BABAR Dalitz plot analysis of $D_s^+ \to \pi^+\pi^-\pi^+$. From Aubert *et al.* (2009).

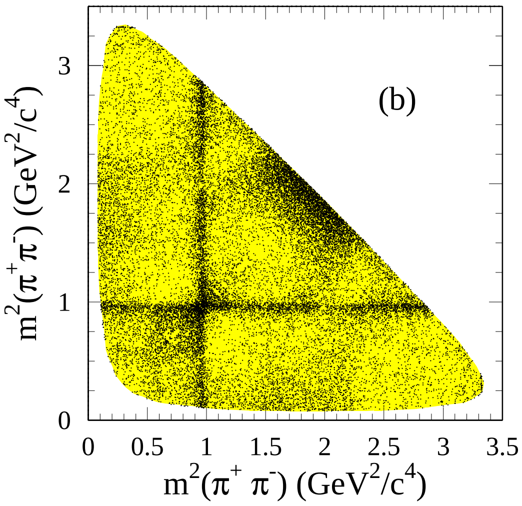

FIG. 44 The Dalitz plot for signal candidates in the BABAR Dalitz plot analysis of $D_s^+ \to \pi^+\pi^-\pi^+$. From Aubert *et al.* (2009).

TABLE XXXV Dalitz plot parameters from BABAR analysis, Aubert *et al.* (2009), of $D_s^+ \to \pi^+\pi^-\pi^+$.

Resonance	Amplitude	Phase (rad)	Fit fraction (%)
$f_2(1270)\pi^+$	1 (fixed)	0 (fixed)	$10.1 \pm 1.5 \pm 1.1$
$\rho(770)^0\pi^+$	$0.19 \pm 0.02 \pm 0.12$	$1.1 \pm 0.1 \pm 0.2$	$1.8 \pm 0.5 \pm 1.0$
$\rho(1450)^0\pi^+$	$1.2 \pm 0.3 \pm 1.0$	$4.1 \pm 0.2 \pm 0.5$	$2.3 \pm 0.8 \pm 1.7$
S-wave	See Ref. Aubert *et al.* (2009)		$83.0 \pm 0.9 \pm 1.9$

B. Four-body decays

Similar to the three-body decays discussed in the previous Section the resonant substructure can be studied in higher multiplicity final states. A four-body final state has a five-dimensional phase space which is hard to visualize.

MARK III (Adler *et al.*, 1990a) studied the decay $D^0 \to K^-\pi^+\pi^-\pi^+$. They performed an unbinned maximum likelihood fit in the five-dimensional phase space to extract amplitudes for two-body decays. MARK III selected a sample of $1,281 \pm 45$ $D^0 \to K^-\pi^+\pi^-\pi^+$ candidates. The result of the fit to this samples is summarized in Table XXXVI. The largest two-body decay contributing to this final state is $D^0 \to K^-a_1(1260)^+$ with a fit fraction of $0.492 \pm 0.024 \pm 0.08$. The fit gives a fit fraction of $0.242 \pm 0.025 \pm 0.06$ for nonresonant four-body final states, but it is likely that this includes contributions from other wide resonances.

The decay $D^0 \to K^+K^-\pi^+\pi^-$ has been studied by E687 (Frabetti *et al.*, 1995c), E791 (Aitala *et al.*, 1998b), and FOCUS (Link *et al.*, 2005e). The FOCUS study used $1,279 \pm 48$ events. They performed an unbinned maximum likelihood fit including 10 resonances. The amplitudes are summarized in Table XXXVII. The dominant contribution to the decay rate, about 55%, comes from decays to intermediate states with an axial vector and a pseudoscalar. The second largest contribution, about 30%, comes from intermediate states with two vectors mesons. The remaining contributions are from three body intermediate states $D \to VPP$ and $D \to SPP$.

TABLE XXXVI Fit fractions and phases from the MARK III analysis (Adler *et al.*, 1990a) of the decay $D^0 \to K^-\pi^+\pi^-\pi^+$.

Resonance	Fit fraction (%)	Phase (rad)
$\bar{K}^{*0}\rho^0$ Transverse (S-wave)	$0.142 \pm 0.016 \pm 0.05$	-1.39 ± 0.09
$K^-a_1(1260)^+$	$0.492 \pm 0.024 \pm 0.08$	0
$K_1(1270)^-\pi^+$	$0.066 \pm 0.019 \pm 0.03$	0.71 ± 0.25
$\bar{K}^{*0}\pi^+\pi^-$	$0.140 \pm 0.018 \pm 0.04$	3.07 ± 0.09
$K^-\rho^0\pi^+$	$0.084 \pm 0.022 \pm 0.04$	-0.30 ± 0.13
Four-body nonresonant	$0.242 \pm 0.025 \pm 0.06$	-1.07 ± 0.08

The decay $D^0 \to \pi^+\pi^-\pi^+\pi^-$ has been studied by FOCUS (Link *et al.*, 2007). They performed a likelihood fit to a sample of 6,153 events using an isobar model. The result of the fit is summarized in Table XXXVIII. The dominant contribution to the decay rate, about 60%, comes from decays to intermediate states with an a_1 resonance. The second largest contribution, about 25%, comes from $\rho^0\rho^0$ intermediate final states. The goodness of fit is estimated with a χ^2 technique. A very low probability of about 10^{-17} is obtained. FOCUS tried adding additional resonances, but did not find any significant improvements in the fit probability.

Another use of four-body decays of D mesons is the search by FOCUS (Link *et al.*, 2005d) for CP violation using triple-product correlations. FOCUS studied the time reversal odd product $\mathbf{p_1} \cdot (\mathbf{p_2} \times \mathbf{p_3})$ by forming the asymmetry

$$A_T \equiv \frac{\Gamma(\mathbf{p_1} \cdot (\mathbf{p_2} \times \mathbf{p_3}) > 0) - \Gamma(\mathbf{p_1} \cdot (\mathbf{p_2} \times \mathbf{p_3}) < 0)}{\Gamma(\mathbf{p_1} \cdot (\mathbf{p_2} \times \mathbf{p_3}) > 0) + \Gamma(\mathbf{p_1} \cdot (\mathbf{p_2} \times \mathbf{p_3}) < 0)}. \tag{125}$$

However, strong phases can cause a non-zero value of A_T without the presence of CP violation. A true T-violating signal can be established by measuring a non-zero value of

$$A_{T_{\rm viol}} \equiv \frac{1}{2}(A_T - \bar{A}_T), \tag{126}$$

where $\bar{A}_T$ is the T-odd asymmetry measured for the CP-conjugate process. FOCUS considered three different four-body decays in this analysis and measure the following asymmetries

$$A_{T_{\rm viol}}(D^0 \to K^-K^+\pi^-\pi^+) = 0.010 \pm 0.057 \pm 0.037, \tag{127}$$
$$A_{T_{\rm viol}}(D^+ \to K_S^- K^+\pi^-\pi^+) = 0.023 \pm 0.062 \pm 0.022, \tag{128}$$
$$A_{T_{\rm viol}}(D_s^+ \to K_S^- K^+\pi^-\pi^+) = -0.036 \pm 0.067 \pm 0.023 \tag{129}$$

all consistent with no T violation.

TABLE XXXVII Fit fractions and phases from the FOCUS (Link *et al.*, 2005e) analysis of the decay $D^0 \to K^- K^+ \pi^- \pi^+$.

Mode	Magnitude	Phase (°)	Fraction (%)
$K_1(1270)^+K^-,\ K_1 \to \rho(770)^0K^+$	1 (fixed)	0 (fixed)	$18 \pm 6 \pm 3$
$K_1(1270)^+K^-,\ K_1 \to K_0^*(1430)^0\pi^+$	$0.27 \pm 0.08 \pm 0.06$	$354 \pm 19 \pm 19$	$2 \pm 1 \pm 0$
$K_1(1270)^+K^-,\ K_1 \to K^*(892)^0\pi^+$	$0.94 \pm 0.16 \pm 0.13$	$12 \pm 12 \pm 15$	$16 \pm 4 \pm 5$
$K_1(1270)^+K^-$	–	–	$33 \pm 6 \pm 4$
$K_1(1400)^+K^-$	$1.18 \pm 0.19 \pm 0.09$	$259 \pm 11 \pm 13$	$22 \pm 3 \pm 4$
$K^*(892)^0\bar{K}^*(892)^0$	$0.39 \pm 0.09 \pm 0.11$	$28 \pm 13 \pm 10$	$3 \pm 2 \pm 1$
$\phi(1020)\rho(770)^0$	$1.30 \pm 0.11 \pm 0.07$	$49 \pm 11 \pm 12$	$29 \pm 2 \pm 1$
$\rho(770)^0K^+K^-$	$0.33 \pm 0.12 \pm 0.16$	$278 \pm 26 \pm 20$	$2 \pm 2 \pm 2$
$\phi(1020)\pi^+\pi^-$	$0.30 \pm 0.06 \pm 0.06$	$163 \pm 16 \pm 15$	$1 \pm 1 \pm 0$
$K^*(892)^0K^+\pi^-$	$0.83 \pm 0.09 \pm 0.10$	$234 \pm 10 \pm 11$	$11 \pm 2 \pm 1$
$f_0(980)\pi^+\pi^-$	$0.91 \pm 0.13 \pm 0.05$	$240 \pm 11 \pm 17$	$15 \pm 3 \pm 2$

TABLE XXXVIII Amplitudes, phases, and fit fractions from the FOCUS (Link *et al.*, 2007) analysis of the decay $D^0 \to \pi^-\pi^+\pi^-\pi^+$.

Mode	Magnitude	Phase (°)	Fraction (%)
$a_1^+\pi^-,\ a_1^+ \to \rho^0\pi^+$ (S-wave)	1 (fixed)	0 (fixed)	$43.3 \pm 2.5 \pm 1.9$
$a_1^+\pi^-,\ a_1^+ \to \rho^0\pi^+$ (D-wave)	$0.241 \pm 0.033 \pm 0.024$	$82 \pm 5 \pm 4$	$2.5 \pm 0.5 \pm 0.4$
$a_1^+\pi^-,\ a_1^+ \to \sigma\pi^+$	$0.439 \pm 0.026 \pm 0.021$	$193 \pm 4 \pm 4$	$8.3 \pm 0.7 \pm 0.6$
$a_1^+\pi^-$ (all)	...	...	$60.0 \pm 3.0 \pm 2.4$
$\rho^0\rho^0$ (parallel)	$0.157 \pm 0.027 \pm 0.020$	$120 \pm 7 \pm 8$	$1.1 \pm 0.3 \pm 0.3$
$\rho^0\rho^0$ (perpendicular)	$0.384 \pm 0.020 \pm 0.015$	$163 \pm 3 \pm 3$	$6.4 \pm 0.6 \pm 0.5$
$\rho^0\rho^0$ (longitudinal)	$0.624 \pm 0.023 \pm 0.015$	$357 \pm 3 \pm 3$	$16.8 \pm 1.0 \pm 0.8$
$\rho^0\rho^0$ (all)	...	...	$24.5 \pm 1.3 \pm 1.0$
$f_0(980)\pi^+\pi^-$	$0.233 \pm 0.019 \pm 0.015$	$261 \pm 7 \pm 4$	$2.4 \pm 0.5 \pm 0.4$
$f_2(1270)\pi^+\pi^-$	$0.338 \pm 0.021 \pm 0.016$	$317 \pm 4 \pm 4$	$4.9 \pm 0.6 \pm 0.5$
$\sigma\pi^+\pi^-$	$0.432 \pm 0.027 \pm 0.022$	$254 \pm 4 \pm 5$	$8.2 \pm 0.9 \pm 0.7$
$R\pi^+\pi^-$ (all)	...	...	$20.0 \pm 1.2 \pm 1.0$

X. CONCLUSIONS

Charm decays remain an exciting field for both theoretical and experimental investigations. In fact, most discoveries in heavy flavor physics in the last five years involved charm quarks one way or another. These include $D^0\overline{D}^0$ mixing, new open-charm D_{sJ} states, charmonium states X, Y, Z states with ordinary and exotic quantum numbers, etc.

In this review, we touched only a part of a vast field of charm physics, the hadronic transitions of charmed mesons. We did not review many other exciting developments in charm physics. For example, a set of hadronic resonant states with new and exciting properties has been discovered in both open- and hidden-charm quark systems (see, *e.g.*, Swanson (2006); Voloshin (2008) for recent reviews), many exciting results were obtained in theoretical (lattice) computations and experimental measurements of leptonic and semi-leptonic decays of charmed mesons (Artuso *et al.*, 2008; Bianco *et al.*, 2003), $D^0\overline{D}^0$-mixing was discovered and used to constrain new physics at the scales of several TeV (Golowich *et al.*, 2007), etc. Also, experimental searches for CP violation in charm transitions remains one of the primary ways of probing new physics in low-energy interactions (Grossman *et al.*, 2007). Finally, we did not discuss inclusive charm decays, lifetimes of charmed states (Bianco *et al.*, 2003; Gabbiani *et al.*, 2004) (for older references, see Bigi (1995); Bigi *et al.* (1992)), as well as charmed spectroscopy and decays of charmed baryons (Voloshin, 1999).

Our knowledge of hadronic charm decays has improved significantly over the last few years. The B-factory experiments, BABAR and Belle, have very large charm data samples that have allowed them to do very precise studies, including the absolute hadronic branching fractions for but D^0 and D_s^+ mesons. In addition, the unique CLEO-c data samples allow detailed studies of D^0, D^+, and D_s^+ decays. In this review we have covered the status of the determination of the absolute branching fractions first for D^0 and D^+ mesons. These measurements are dominated by results from CLEO-c and BABAR and have statistical uncertainties now below $\pm 1\%$ and systematic uncertainties of about $\pm 1.8\%$. The determination of D_s^+ branching fractions is dominated by CLEO-

c. The previously commonly used normalization mode $D_s^+ \to \phi\pi^+$ is not used by CLEO-c any more as it is ambiguous at the level of precision now obtained by CLEO-c. CLEO-c instead quotes partial branching fractions for different K^+K^- mass ranges around the ϕ resonance. These partial branching fractions do not try to disentangle the contributions from the ϕ or other resonance contributing to the rate. The CLEO-c measurement obtains a statistical precision of about 4.2% and systematic uncertainties of about 3% in the $D_s^+ \to K^+K^-\pi^+$ mode. This result should improve when CLEO-c includes their full data sample. The large charm samples now available have allowed more detailed studies of Cabibbo suppressed D and D_s decays. Decays with smaller branching fractions have been explored as well as final states with π^0 and η mesons that traditionally have been harder to reconstruct, but thanks the excellent electromagnetic calorimeters of the BABAR, Belle, and CLEO-c are now accessible. Finally, a summary of Dalitz decay studies of D mesons is given. Many of the three-body final states have now been analyzed for their resonant substructure, and also a few final states with more than three particles in the final state have been studied. These studies show that most of the D decays proceed via pseudo two-body decays.

The study of charm will continue with new experiments. The upgraded BES III experiment has started to take data at the $\psi(3770)$ in 2010. In their first run they have recorded about 900 pb^{-1}, of comparable size to the CLEO-c data sample at this energy. BES III will carry on a similar physics program as CLEO-c with increased statistics. Running at design luminosity for one year, e.g. at the $\psi(3770)$ resonance, would provide a data sample a factor of six times larger than the CLEO-c data sample. Analysis that are statistics limited will be improved with the larger data samples. However, analyses that are limited by systematic uncertainties will see smaller gains. LHCb has just started taking data in 2010 at the LHC. LHCb has a sophisticated trigger designed for B-physics, but will also select a very large charm sample. Future e^+e^- Super B factories will produce very large charm samples, the goal of the Super B factories is to produce data sample at least an order of magnitude larger than the current B factories. In particular this will provide very tight constraints on CP-violating observables. All these experiments will continue to provide new data on charm physics. New measurements will play a big role in the development of the theoretical understanding of hadronic D mesons decays. For example, they will allow tuning of the models of hadronic decays. Experiments with quantum-coherent initial states will produce measurements of the phases of decay amplitudes, i.e. the quantities that QCD-based calculations can predict. Finally, measurements of the new hadronic modes will allow complete fits of the flavor-flow amplitudes, and thus better predictions of new decay rates, especially for the PV, VV, AV, and other final states. While lattice QCD had enormous influence on the studies of leptonic and semileptonic transitions, the internal limitations of the lattice approach, i.e. the fact that the calculations are done in the Euclidean space-time, means that lattice QCD will only have limited impact on the studies of hadronic D-decays. These experimental and theoretical developments will allow us to understand in more detail the charm decays reviewed in this article and hopefully allow us to explore new physics beyond the Standard Model.

Acknowledgments

We would like to thank David Cinabro and Rob Harr for careful reading the manuscript and insightful comments. A.R. was supported in part by the U.S. National Science Foundation under Grant PHY-0757894 and CAREER Award PHY-0846388. A.R. also thanks the Alfred P. Sloan foundation for their support. A.A.P. was supported in part by the U.S. National Science Foundation under CAREER Award PHY-0547794, and by the U.S. Department of Energy under Contract DE-FG02-96ER41005.

References

Aaltonen, T., *et al.* (CDF), 2008, Phys. Rev. Lett. **100**, 121802.

Abachi, S., *et al.* (HRS), 1988, Phys. Lett. **B205**, 411.

Abe, K., *et al.* (Belle), 2007, eprint hep-ex/0701053.

Abe, K., *et al.* (Belle), 2008, eprint 0803.3375v1.

Ablikim, M., *et al.* (BES), 2005, Phys. Lett. **B622**, 6.

Ablikim, M., *et al.* (BES), 2006a, Phys. Rev. Lett. **97**, 121801.

Ablikim, M., *et al.* (BES), 2006b, Phys. Lett. **B641**, 145.

Ablikim, M., *et al.* (BES), 2007, Phys. Rev. **D76**, 122002.

Ablikim, M., *et al.* (BES), 2008, Phys. Lett. **B659**, 74.

Abrams, G. S., *et al.*, 1979a, Phys. Rev. Lett. **43**, 477.

Abrams, G. S., *et al.*, 1979b, Phys. Rev. Lett. **43**, 481.

Acosta, D. E., *et al.* (CDF), 2005, Phys. Rev. Lett. **94**, 122001.

Adam, N. E., *et al.* (CLEO), 2005, Phys. Rev. Lett. **94**, 232002.

Adams, G. S., *et al.* (CLEO), 2007, Phys. Rev. Lett. **99**, 191805.

Adler, J., *et al.* (MARK-III), 1987, Phys. Lett. **B196**, 107.

Adler, J., *et al.* (MARK-III), 1988, Phys. Rev. Lett. **60**, 89.

Adler, J., *et al.* (MARK-III), 1990a, Phys. Rev. Lett. **64**, 2615.

Adler, J., *et al.* (MARK-III), 1990b, Phys. Rev. Lett. **64**, 169.

Aitala, E. M., *et al.* (E791), 1997, Phys. Lett. **B404**, 187.

Aitala, E. M., *et al.* (E791), 1998a, Phys. Lett. **B421**, 405.

Aitala, E. M., *et al.* (E791), 1998b, Phys. Lett. **B423**, 185.

Aitala, E. M., *et al.* (E791), 2001a, Phys. Rev. Lett. **86**, 770.

Aitala, E. M., *et al.* (E791), 2001b, Phys. Rev. Lett. **86**, 765.

Aitala, E. M., *et al.* (E791), 2002, Phys. Rev. Lett. **89**, 121801.

Aitala, E. M., *et al.* (E791), 2006, Phys. Rev. **D73**, 032004.

Akerib, D. S., *et al.* (CLEO), 1993, Phys. Rev. Lett. **71**, 3070.

Albrecht, H., *et al.* (ARGUS), 1990, Phys. Lett. **B241**, 278.

Albrecht, H., *et al.* (ARGUS), 1991, Phys. Lett. **B255**, 634.

Albrecht, H., *et al.* (ARGUS), 1993, Phys. Lett. **B308**, 435.
Albrecht, H., *et al.* (ARGUS), 1994a, Phys. Lett. **B324**, 249.
Albrecht, H., *et al.* (ARGUS), 1994b, Phys. Lett. **B340**, 125.
Alexander, J. P., *et al.* (CLEO), 1990a, Phys. Rev. Lett. **65**, 1531.
Alexander, J. P., *et al.* (CLEO), 1990b, Phys. Rev. Lett. **65**, 1184.
Alexander, J. P., *et al.* (CLEO), 2008, Phys. Rev. Lett. **100**, 161804.
Alvarez, M. P., *et al.* (NA14/2), 1990, Phys. Lett. **B246**, 261.
Alvarez, M. P., *et al.* (NA14/2), 1991, Z. Phys. **C50**, 11.
Amsler, C., *et al.* (Particle Data Group), 2008, Phys. Lett. **B667**, 1.
Anisovich, V. V., and A. V. Sarantsev, 2003, Eur. Phys. J. **A16**, 229.
Anjos, J. C., *et al.*, 1989, Phys. Rev. Lett. **62**, 125.
Anjos, J. C., *et al.*, 1990, Phys. Rev. **D41**, 2705.
Anjos, J. C., *et al.*, 1991, Phys. Rev. **D44**, 3371.
Anjos, J. C., *et al.* (E691), 1993, Phys. Rev. **D48**, 56.
Artuso, M., B. Meadows, and A. A. Petrov, 2008, Ann. Rev. Nucl. Part. Sci. **58**, 249.
Artuso, M., *et al.* (CLEO), 1996, Phys. Lett. **B378**, 364.
Artuso, M., *et al.* (CLEO), 1998, Phys. Rev. Lett. **80**, 3193.
Artuso, M., *et al.*, 2003, Nucl. Instrum. Meth. **A502**, 91.
Artuso, M., *et al.* (CLEO), 2008, Phys. Rev. **D77**, 092003.
Ashmanskas, B., *et al.* (CDF-II), 2004, Nucl. Instrum. Meth. **A518**, 532.
Asner, D. M., and W. M. Sun, 2006, Phys. Rev. **D73**, 034024, erratum ibid. **D**77, 019901 (2008).
Asner, D. M., *et al.* (CLEO), 1996, Phys. Rev. **D54**, 4211.
Asner, D. M., *et al.*, 2008, eprint 0809.1869.
Aston, D., *et al.*, 1988, Nucl. Phys. **B296**, 493.
Athar, S. B., *et al.* (CLEO), 2008, Phys. Rev. Lett. **100**, 181802.
Atwood, D., I. Dunietz, and A. Soni, 2001, Phys. Rev. **D63**, 036005.
Atwood, D., and A. A. Petrov, 2005, Phys. Rev. **D71**, 054032.
Atwood, D., and A. Soni, 2002, Phys. Lett. **B533**, 37.
Aubert, B., *et al.* (BABAR), 2005a, Phys. Rev. **D72**, 052008.
Aubert, B., *et al.* (BABAR), 2005b, Phys. Rev. Lett. **95**, 121802.
Aubert, B., *et al.* (BABAR), 2005c, Phys. Rev. **D71**, 091104.
Aubert, B., *et al.* (BABAR), 2005d, Phys. Rev. **D72**, 091101.
Aubert, B., *et al.* (BABAR), 2006a, Phys. Rev. **D74**, 011107.
Aubert, B., *et al.* (BABAR), 2006b, Phys. Rev. Lett. **97**, 221803.
Aubert, B., *et al.* (BABAR), 2006c, Phys. Rev. **D74**, 031103.
Aubert, B., *et al.* (BABAR), 2007a, Phys. Rev. **D76**, 011102.
Aubert, B., *et al.* (BABAR), 2007b, Phys. Rev. Lett. **98**, 211802.
Aubert, B., *et al.* (BABAR), 2007c, Phys. Rev. Lett. **99**, 251801.
Aubert, B., *et al.* (BABAR), 2008a, Phys. Rev. **D78**, 034023.
Aubert, B., *et al.* (BABAR), 2008b, Phys. Rev. Lett. **100**, 051802.
Aubert, B., *et al.* (BABAR), 2009, Phys. Rev. **D79**, 032003.
Aubert, J. J., *et al.* (E598), 1974, Phys. Rev. Lett. **33**, 1404.
Augustin, J. E., *et al.*, 1974, Phys. Rev. Lett. **33**, 1406.
Augustin, J. E., *et al.*, 1975, Phys. Rev. Lett. **34**, 233.
Bai, J. Z., *et al.* (BES), 1994, Nucl. Instrum. Meth. **A344**, 319.
Bai, J. Z., *et al.* (BES), 1995, Phys. Rev. **D52**, 3781.
Bai, J. Z., *et al.* (BES), 2001, Nucl. Instrum. Meth. **A458**, 627.
Bai, J. Z., *et al.* (BES), 2005, Phys. Lett. **B605**, 63.
Balest, R., *et al.* (CLEO), 1994, Phys. Rev. Lett. **72**, 2328.
Baltrusaitis, R. M., *et al.* (MARK-III), 1986, Phys. Rev. Lett. **56**, 2140.
Barate, R., *et al.* (ALEPH), 1997, Phys. Lett. **B403**, 367.
Barberio, E., and Z. Was, 1994, Comput. Phys. Commun. **79**, 291.
Bartelt, J. E., *et al.* (CLEO), 1998, Phys. Rev. Lett. **80**, 3919.
Bauer, M., B. Stech, and M. Wirbel, 1987, Z. Phys. **C34**, 103.
Beane, S. R., P. F. Bedaque, K. Orginos, and M. J. Savage, 2007, Phys. Rev. **D75**, 094501.
Beneke, M., G. Buchalla, M. Neubert, and C. T. Sachrajda, 1999, Phys. Rev. Lett. **83**, 1914.
Benvenuti, A. C., *et al.*, 1975a, Phys. Rev. Lett. **35**, 1199.
Benvenuti, A. C., *et al.*, 1975b, Phys. Rev. Lett. **34**, 419.
Bergmann, S., Y. Grossman, Z. Ligeti, Y. Nir, and A. A. Petrov, 2000, Phys. Lett. **B486**, 418.
Bergmann, S., and Y. Nir, 1999, JHEP **09**, 031.
Bernabeu, J., F. J. Botella, and J. Roldan, 1988, Phys. Lett. **B211**, 226.
Bernstein, D., *et al.*, 1984, Nucl. Instr. Meth. **A226**, 301.
Besson, D., *et al.* (CLEO), 2006, Phys. Rev. Lett. **96**, 092002.
Besson, D., *et al.* (CLEO), 2009, Phys. Rev. **D80**, 032005.
Bhattacharya, B., and J. L. Rosner, 2008, Phys. Rev. **D77**, 114020.
Bhattacharya, B., and J. L. Rosner, 2009, Phys. Rev. **D79**, 034016, erratum ibid. **D**79, 034016 (2009).
Bianco, S., F. L. Fabbri, D. Benson, and I. Bigi, 2003, Riv. Nuovo Cim. **26N7**, 1.
Bigi, I. I. Y., 1995, eprint hep-ph/9508408.
Bigi, I. I. Y., N. G. Uraltsev, and A. I. Vainshtein, 1992, Phys. Lett. **B293**, 430.
Bigi, I. I. Y., and H. Yamamoto, 1995, Phys. Lett. **B349**, 363.
Björken, B. J., and S. L. Glashow, 1964, Phys. Lett. **11**, 255.
Bloch, F., and A. Nordsieck, 1937, Phys. Rev. **52**, 54.
Blok, B., and M. A. Shifman, 1993, Nucl. Phys. **B399**, 441.
Bonvicini, G., *et al.* (CLEO), 2007, Phys. Rev. **D76**, 012001.
Bonvicini, G., *et al.* (CLEO), 2008a, Phys. Rev. **D77**, 091106.
Bonvicini, G., *et al.* (CLEO), 2008b, Phys. Rev. **D78**, 052001.
Brandenburg, G., *et al.* (CLEO), 2001, Phys. Rev. Lett. **87**, 071802.
Briere, R. A., *et al.* (CLEO Collaboration), 2001, Cornell report, No. CLNS 01/1742.
Briere, R. A., *et al.* (CLEO), 2009, Phys. Rev. **D80**, 032002.
Buccella, F., M. Lusignoli, G. Miele, A. Pugliese, and P. Santorelli, 1995, Phys. Rev. **D51**, 3478.
Buccella, F., M. Lusignoli, and A. Pugliese, 1996, Phys. Lett. **B379**, 249.
Buccella, F., *et al.*, 1993, Phys. Lett. **B302**, 319.
Buras, A. J., J. M. Gerard, and R. Ruckl, 1986, Nucl. Phys. **B268**, 16.
Butler, F., *et al.* (CLEO), 1992, Phys. Rev. Lett. **69**, 2041.
Butler, F., *et al.* (CLEO), 1994, Phys. Lett. **B324**, 255.
Cawlfield, C., *et al.* (CLEO), 2007, Phys. Rev. Lett. **98**, 092002.
Chau, L. L., and H. Y. Cheng, 1986, Phys. Rev. Lett. **56**, 1655.
Chau, L.-L., and H.-Y. Cheng, 1989, Phys. Lett. **B222**, 285.
Chau, L.-L., and H.-Y. Cheng, 1992, Phys. Lett. **B280**, 281.
Chen, A., *et al.* (CLEO), 1983, Phys. Rev. Lett. **51**, 634.
Chen, C.-H., H.-Y. Cheng, and Y.-K. Hsiao, 2008, Phys. Lett. **B663**, 326.
Chen, W. Y., *et al.* (CLEO), 1989, Phys. Lett. **B226**, 192.
Cheng, H.-Y., 2003, Eur. Phys. J. **C26**, 551.

Chiang, C.-W., Z. Luo, and J. L. Rosner, 2003, Phys. Rev. **D67**, 014001.

Chung, S. U., *et al.*, 1995, Annalen Phys. **4**, 404.

Cinabro, D., *et al.* (CLEO), 1994, Phys. Rev. Lett. **72**, 1406.

Coan, T. E., *et al.* (CLEO), 1998, Phys. Rev. Lett. **80**, 1150.

Collaboration, B. (BESIII), 2009, Nucl. Instrum. Meth. **A598**, 7.

Cronin-Hennessy, D., *et al.* (CLEO), 2009, Phys. Rev. **D80**, 072001.

Csorna, S. E., *et al.* (CLEO), 2002, Phys. Rev. **D65**, 092001.

Dai, Y.-S., D.-S. Du, X.-Q. Li, Z.-T. Wei, and B.-S. Zou, 1999, Phys. Rev. **D60**, 014014.

Dalitz, R. H., 1953, Phil. Mag. **44**, 1068.

Decamp, D., *et al.* (ALEPH), 1991, Phys. Lett. **B266**, 218.

Dobbs, S., *et al.* (CLEO), 2007, Phys. Rev. **D76**, 112001.

Donoghue, J. F., 1986, Phys. Rev. **D33**, 1516.

Donoghue, J. F., and B. R. Holstein, 1980, Phys. Rev. **D21**, 1334.

Dunietz, I., J. Hauser, and J. L. Rosner, 1987, Phys. Rev. **D35**, 2166.

Dytman, S. A., *et al.* (CLEO), 2001, Phys. Rev. **D64**, 111101.

Dytman, S. A., *et al.* (CLEO), 2006, Phys. Rev. **D74**, 071102, erratum ibid. **D**74, 079904 (2006).

Edera, L. (FOCUS), 2004, prepared for DAFNE 2004: Workshop on Physics at Meson Factories, Rome, Frascati, Italy, 7-11 Jun 2004.

Eeg, J. O., S. Fajfer, and J. Zupan, 2001, Phys. Rev. **D64**, 034010.

Fajfer, S., A. Prapotnik, P. Singer, and J. Zupan, 2003, Phys. Rev. **D68**, 094012.

Falk, A. F., Y. Nir, and A. A. Petrov, 1999, JHEP **12**, 019.

Falk, A. F., and A. A. Petrov, 2000, Phys. Rev. Lett. **85**, 252.

Frabetti, P. L., *et al.* (E687), 1992, Phys. Lett. **B286**, 195.

Frabetti, P. L., *et al.* (E687), 1993, Phys. Lett. **B313**, 253.

Frabetti, P. L., *et al.* (E687), 1994a, Phys. Lett. **B321**, 295.

Frabetti, P. L., *et al.* (E687), 1994b, Phys. Lett. **B331**, 217.

Frabetti, P. L., *et al.* (E687), 1994c, Phys. Lett. **B340**, 254.

Frabetti, P. L., *et al.* (E687), 1995a, Phys. Lett. **B351**, 591.

Frabetti, P. L., *et al.* (E687), 1995b, Phys. Lett. **B359**, 403.

Frabetti, P. L., *et al.* (E687), 1995c, Phys. Lett. **B354**, 486.

Frabetti, P. L., *et al.* (E687), 1997, Phys. Lett. **B407**, 79.

Gabbiani, F., A. I. Onishchenko, and A. A. Petrov, 2004, Phys. Rev. **D70**, 094031.

Gaillard, M. K., and B. W. Lee, 1974, Phys. Rev. **D10**, 897.

Gaillard, M. K., B. W. Lee, and J. L. Rosner, 1975, Rev. Mod. Phys. **47**, 277.

Gao, D.-N., 2007, Phys. Lett. **B645**, 59.

Ge, J. Y., *et al.* (CLEO), 2009a, Phys. Rev. **D80**, 051102.

Ge, J. Y., *et al.* (CLEO), 2009b, Phys. Rev. **D79**, 052010.

Gedalia, O., and G. Perez, 2010, eprint 1005.3106.

Gell-Mann, M., 1964, Phys. Lett. **8**, 214.

Glashow, S. L., J. Iliopoulos, and L. Maiani, 1970, Phys. Rev. **D2**, 1285.

Goldhaber, G., *et al.*, 1976, Phys. Rev. Lett. **37**, 255.

Golowich, E., J. Hewett, S. Pakvasa, and A. A. Petrov, 2007, Phys. Rev. **D76**, 095009.

Golowich, E., and A. A. Petrov, 1998, Phys. Lett. **B427**, 172.

Gronau, M., Y. Grossman, and J. L. Rosner, 2001, Phys. Lett. **B508**, 37.

Gronau, M., O. F. Hernandez, D. London, and J. L. Rosner, 1994, Phys. Rev. **D50**, 4529.

Gronau, M., and J. L. Rosner, 2009, Phys. Rev. **D79**, 074006.

Grossman, Y., A. L. Kagan, and Y. Nir, 2007, Phys. Rev. **D75**, 036008.

Harrison, e., P. F., and e. Quinn, Helen R. (BABAR), 1998, papers from Workshop on Physics at an Asymmetric B Factory (BaBar Collaboration Meeting), Rome, Italy, 11-14 Nov 1996, Princeton, NJ, 17-20 Mar 1997, Orsay, France, 16-19 Jun 1997 and Pasadena, CA, 22-24 Sep 1997.

He, Q., *et al.* (CLEO Collaboration), 2005, Phys. Rev. Lett. **95**, 121801, erratum ibid. **D**96, 199903 (2006).

He, Q., *et al.* (CLEO), 2008, Phys. Rev. Lett. **100**, 091801.

Hinchliffe, I., and T. A. Kaeding, 1996, Phys. Rev. **D54**, 914.

Hoshino, K., *et al.*, 1975, Prog. Theor. Phys. **53**, 1859.

Iizuka, J., 1966, Prog. Theor. Phys. Suppl. **37**, 21.

Kamal, A. N., and R. C. Verma, 1987, Phys. Rev. **D35**, 3515.

Kölbig, K. S., and H. Lipps, 1990, CERN Program Library E211.

Kopp, S., *et al.* (CLEO), 2001, Phys. Rev. **D63**, 092001.

Kubota, Y., *et al.* (CLEO), 1992, Nucl. Instrum. Meth. **A320**, 66.

Lange, D. J., 2001, Nucl. Instrum. Meth. **A462**, 152.

Link, J. M., *et al.* (FOCUS), 2002a, Nucl. Instrum. Meth. **A484**, 270.

Link, J. M., *et al.* (FOCUS), 2002b, Phys. Lett. **B541**, 227.

Link, J. M., *et al.* (FOCUS), 2002c, Phys. Lett. **B537**, 192.

Link, J. M., *et al.* (FOCUS), 2002d, Nucl. Instrum. Meth. **A484**, 174.

Link, J. M., *et al.* (FOCUS), 2003, Phys. Lett. **B555**, 167.

Link, J. M., *et al.* (FOCUS), 2004a, Phys. Lett. **B585**, 200.

Link, J. M., *et al.* (FOCUS), 2004b, Phys. Lett. **B601**, 10.

Link, J. M., *et al.* (FOCUS), 2004c, Nucl. Instrum. Meth. **A516**, 364.

Link, J. M., *et al.* (FOCUS), 2005a, Phys. Rev. Lett. **95**, 052003.

Link, J. M., *et al.* (FOCUS), 2005b, Phys. Lett. **B607**, 59.

Link, J. M., *et al.* (FOCUS), 2005c, Phys. Lett. **B624**, 166.

Link, J. M., *et al.* (FOCUS), 2005d, Phys. Lett. **B622**, 239.

Link, J. M., *et al.* (FOCUS), 2005e, Phys. Lett. **B610**, 225.

Link, J. M., *et al.* (FOCUS), 2007, Phys. Rev. **D75**, 052003.

Link, J. M., *et al.* (FOCUS), 2008, Phys. Lett. **B660**, 147.

Link, J. M., *et al.* (FOCUS), 2009, Phys. Lett. **B681**, 14.

Lipkin, H. J., 1968, Phys. Rev. **176**, 1715.

Lipkin, H. J., 1980, Phys. Rev. Lett. **44**, 710.

Lipkin, H. J., 1987, Nucl. Phys. **B291**, 720.

Malvezzi, S., 2002, AIP Conf. Proc. **549**, 569.

Mitchell, R. E., *et al.* (CLEO), 2009, Phys. Rev. **D79**, 072008.

Muramatsu, H., *et al.* (CLEO), 2002, Phys. Rev. Lett. **89**, 251802, erratum ibid. 90, 059901 (2003).

Niu, K., E. Mikumo, and Y. Maeda, 1971, Prog. Theor. Phys. **46**, 1644.

Okubo, S., 1977, Phys. Rev. **D16**, 2336.

Peruzzi, I., *et al.*, 1976, Phys. Rev. Lett. **37**, 569.

Peruzzi, I., *et al.*, 1977, Phys. Rev. Lett. **39**, 1301.

Peterson, D., *et al.*, 2002, Nucl. Instrum. Meth. **A478**, 142.

Petrov, A. A., 2004, Phys. Rev. **D69**, 111901.

Pham, X. Y., 1980a, Phys. Rev. Lett. **45**, 1663.

Pham, X.-Y., 1980b, Phys. Lett. **B94**, 231.

Pham, X.-Y., 1987, Phys. Lett. **B193**, 331.

Poluektov, A., *et al.* (Belle), 2006, Phys. Rev. **D73**, 112009.

Richman, J. D., and P. R. Burchat, 1995, Rev. Mod. Phys. **67**, 893.

Richter-Was, E., 1993, Phys. Lett. **B303**, 163.

Rosner, J. L., 1999, Phys. Rev. **D60**, 114026.

Rubin, P., *et al.* (CLEO), 2004, Phys. Rev. Lett. **93**, 111801.

Rubin, P., *et al.* (CLEO), 2006, Phys. Rev. Lett. **96**, 081802.

Rubin, P., *et al.* (CLEO), 2008, Phys. Rev. **D78**, 072003.

Sanda, A. I., 1980, Phys. Rev. **D22**, 2814.

Savage, M. J., 1991, Phys. Lett. **B257**, 414.
Schindler, R. H., *et al.*, 1981, Phys. Rev. **D24**, 78.
Selen, M., *et al.* (CLEO), 1993, Phys. Rev. Lett. **71**, 1973.
Summers, D. J., *et al.*, 1984, Phys. Rev. Lett. **52**, 410.
Sun, W. M., 2006, Nucl. Instrum. Meth. **A556**, 325.
Swanson, E. S., 2006, Phys. Rept. **429**, 243.
Tian, X. C., *et al.* (Belle), 2005, Phys. Rev. Lett. **95**, 231801.
Voloshin, M. B., 1999, Phys. Rept. **320**, 275.
Voloshin, M. B., 2008, Prog. Part. Nucl. Phys. **61**, 455.
Zemach, C., 1965, Phys. Rev. **140**, B109.
Zhang, L. M., *et al.* (Belle), 2006, Phys. Rev. Lett. **96**, 151801.
Zweig, G., 1964, CERN-TH-412.